JANUARY 2019 M.Sc. in Electrical and Electronics Engineering AHMED MAJEED HACHIM

REPUBLIC OF TURKEY

GAZİANTEP UNIVERSITY

GRADUATE SCHOOL OF NATURAL & APPLIED SCIENCES

DESIGN AND SIMULATION OF A WIND ENERGY CONVERSION SYSTEM BASED ON DOUBLY FED INDUCTION GENERATOR AND BACK-TO-BACK MODULAR MULTILEVEL CONVERTERS

M.Sc. THESIS

IN

ELECTRICAL AND ELECTRONICS ENGINEERING

BY

AHMED MAJEED HACHIM

January 2019

Design and Simulation of A Wind Energy Conversion System Based On Doubly Fed Induction Generator and Back-To-Back Modular Multilevel Converters

M.Sc. Thesis

in

Electrical and Electronics Engineering

Gaziantep University

Supervisor

Assoc.Prof.Dr. Ahmet Mete VURAL

by

Ahmed Majeed HACHIM

January 2019

REPUBLIC OF TURKEY
UNIVERSITY OF GAZIANTEP
GRADUATE SCHOOL OF NATURAL & APPLIED SCIENCES
ELECTRICAL AND ELECTRONICS ENGINEERING

Name of the thesis: Design and Simulation of A Wind Energy Conversion System Based On Doubly Fed Induction Generator and Back-To-Back Modular Multilevel Converters
Name of the student: Ahmed Majeed HACHIM
Exam Date: 28 / 1 / 2019
Approval of Graduate School of Natural and Applied Sciences

Prof. Dr. A. Necmeddin YAZICI
Director

I certify that this thesis satisfies all the requirements as a thesis for the degree of Master of Science.

Prof. Dr. Ergun ERÇELEBİ
Head of Department

This is to certify that we have read this thesis and that in our consensus; it is fully adequate, in scope and quality, as a thesis for the degree of Master of Science.

Assoc. Prof. Dr. Ahmet Mete VURAL
Supervisor

Examining Committee Members:	Signature
Assoc. Prof. Dr. Ahmet Mete VURAL	…….
Assist. Prof. Dr. Serkan ÖZBAY	…….
Assist. Prof. Dr. Tahsin KÖROĞLU	.....

I now declare that all information in this document has been obtained and presented in agreement with academic rules and ethical conduct. I also declare that, as required by these rules and conduct, I have fully cited and referenced all material and results that are not original to this work.

Ahmed Majeed HACHIM

ABSTRACT

DESIGN AND SIMULATION OF A WIND ENERGY CONVERSION SYSTEM BASED ON DOUBLY FED INDUCTION GENERATOR AND BACK-TO-BACK MODULAR MULTILEVEL CONVERTERS

HACHIM, Ahmed Majeed

M. Sc. in Electrical and Electronics Engineering

Supervisor: Assoc.Prof.Dr. Ahmet Mete VURAL

Jnauary 2019

94 Pages

Wind energy is one of the most growing renewable energy types in the world. Doubly fed induction generator (DFIG) based wind turbines have been used for more than two decades. Modular multilevel converters (MMC), on the other hand, have been initially proposed for high voltage direct current transmission for the purpose of long distance huge power transmission. Voltage levels even up to 100 or more at the output can be obtained using many cascaded power semiconductor bridges in each phase. The major benefits of MMC are well-dropped harmonic distortion at the output and significant voltage rating reduction of power semiconductors. In this thesis, the potential benefits of utilizing a back-to-back MMC system for a DFIG based wind energy conversion system connected to main grid has been investigated by simulation studies. The dynamic performance of the current vector control scheme has been tested by applying unit step-changes which applied to the reference signals of the controllers. Many simulation studies have been designed to verify the simulation model of back-to-back MMC based DFIG wind energy conversion system.

Key Words: Wind Energy; Doubly Fed Induction Generator; Modular Multilevel Converter; Back-to-Back connected converter.

ÖZET

DOUBLE FED İNDÜKSİYON JENERATÖRÜ VE GERİ DÖNÜŞÜM MODÜLER ÇOKLU KONVEYÖRLER ÜZERİNE TABELEN RÜZGAR ENERJİ DÖNÜŞÜM SİSTEMİNİN TASARIMI VE SİMÜLASYONU

HACHIM, Ahmed Majeed

Yuksek Lisans Tezi, Elektrik ve Elektronik Mühendisliği

Danışman: Doç.Dr. AHMET METE VURAL

Ocak 2019

94 Sayfa

Rüzgar enerjisi dünyada en hızlı büyüyen yenilenebilir enerji türlerinden biridir. Çift beslemeli endüksiyon jeneratör (ÇBEJ) tabanlı rüzgar türbinleri iki on yıldan fazla süredir kullanılmaktadır. Modüler çok seviyeli çevirgeçler (MÇSÇ), diğer taraftan, ilk olarak uzun mesafe büyük güç iletimi amacıyla yüksek gerilim doğru akım iletim sistemleri için düşünülmüştür. Çıkışta, her fazdaki kaskat güç yarı-ilekten köprüleri kullanılarak 100 veya daha fazla gerilim seviyesi elde edilebilir. MÇSÇ'lerin ana avantajı çıkışta iyi düşürülmüş harmonik bozulumu ve güç yarı-iletkenlerinin belirgin olarak gerilim ratinglerinin azalımıdır. Bu tezde, ana şebekeye bağlı ÇBEJ tabanlı rüzgar enerjisi dönüşüm sistemleri için sırt-sırta bağlı MÇSÇ'lerin kullanımlarının potansiyel avantajları benzetim çalışmalarıyla araştırılmıştır. Akım vektör denetim şemasının dinamik başarımı denetleyicilerin referans sinyallerine birim adım-değişimleri uygulanarak test edilmiştir. Sırt-sırta bağlı MÇSÇ tabanlı ÇBEJ rüzgar enerjisi dönüşüm sisteminin benzetim modelini doğrulamak için birçok benzetim çalışması tasarlanmıştır.

Anahtar Kelimeler: Rüzgar Enerjisi; Çift Beslemeli Endüksiyon Jeneratör; Modüler Çokseviyeli Dönüştürücü; Sırt-Sırta Dönüştürücü Bağlantısı

“Dedicated To My Country And Beloved Parents and my wife”

ACKNOWLEDGEMENTS

First and foremost I would like to acknowledge Almighty God who granted me wisdom, health and strength to overcome life's difficulties and actualizing my settargets and academic achievement.

I would like to express my heartfelt thanks and deep gratitude to my supervisor, Assoc. Prof. Dr. Ahmet Mete VURAL, for the support of my MSc, study and research.

I would like to show my gratitude and my love to my family for their support andlove through my life. They have given me an endless enthusiasm and encouragement.

Finally, thanks to everyone who has helped me in one way, even in one gesture**.**

Table of Contents

LIST OF FIGURES

Page

LIST OF TABLES

Page

LIST OF SYMBOLS / ABBREVIATIONS

AC	Alternative Current
CCC	Capacitor Commutated Converters
CSC	Current Source Converters
DC	Direct Current
DFIG	Doubly Fed Induction Generate
HVAC	High Voltage Alternating Current
HVDC	High Voltage Direct Current
HV	High Voltage
FSWT	Fixed Speed Wind Turbine Generators
FC	Fixed Capacitor
FCC	Flying Capacitor Converter
FACTS	Flexible Alternating Current Transmission Systems
FFM	Fundamental FrequencyModulation
G	Generator
GSC	Grid Side Converter
GTO	Gate Turn-Off Thyristor
HAWT	Horizontal Axis Wind Turbines
IG	Induction Generator
IGBT	Insulated Gate Bipolar Transistor
GSC	Grid Side Converter
I	Current
LS	Level Sheft
MMC	Modular Multilevel Converter
PD-PWM	Phase Disposition Pulse Width Modulation
PV	PhotoVoltaic
PD	Phase Disposition
POD	Phase Opposition Disposition
PCC	Point Of Common Coupling
PLL	Phase-Locked Loop
PU	Per Unit
PMSG	Permanent Magnet Synchronous Generator
PWM	Pluse Width Modulation
RSC	Rotor Side Converter
VC	Voltage Capacitor
VSC	Voltage Source Converter
SVM	Space Vector Modulation

CHAPTER 1
INTRODUCTION

1.1 Introduction

Power generation has been developed extensively in terms of the use of wind power in the last few years. This is due to the need for the use of renewable, clean energy and because the increase in carbon dioxide emissions has also triggered searches for new sources of sustainable electricity generation; wind power has several advantages in this respect, such as its safety and feasibility [1-3]. The integration of wind energy into electrical grids initially caused concern in terms of its impact on the power quality and the availability of energy system documentation, since these generators are very dynamic and the industry has limited experience in this area [4-6]. Electrical distribution systems are structurally designed to transfer energy to loads from power sources. Wind generators work in distribution networks in an inverted way, providing power to the network from sources in the distribution network, and are thus closer to the loads [7]. Wind generators can improve and enhance reliability and performance due to their configuration and dynamic nature. This includes their primary power and frequency, their initial voltage and the remote control of individual turbines [5]. There are several types of wind generators that vary in terms of their mechanical nature, such as limited variable-speed, variable-speed and fixed-speed wind generators [4]. Power generation systems based on a variable-speed, constant-frequency wind generator are better than fixed-speed systems due to the minimal mechanical stress, lower power fluctuations and preferable rates of power capture. There are three main types of wind generator: directly driven synchronous generators, squirrel cage induction generators (SCIGs), and doubly fed induction generators (DFIGs) [8]. DFIG wind generators currently dominate the market [9] due to their ability to offer constant frequency AC power and flexible control. They also have superior energy transfer efficiency, low investment and its prime mover could

1.2 Wind Energy: An Overview

Today, wind power is considered to be one of the most highly developed sources in the renewable energy sector, and is expected to be used in future power generation. The general engineering approach to wind energy use involves high efficiency and complete control, and the grid integration mechanism requires the most cutting-edge research and development. Figure 1.1 shows the design of a wind turbine, which typically consists of an alternator, gearbox, shaft and blades, with several other connecting components. These are situated in a nacelle, and the electrical control devices are either located on the turbine tower or on the ground.

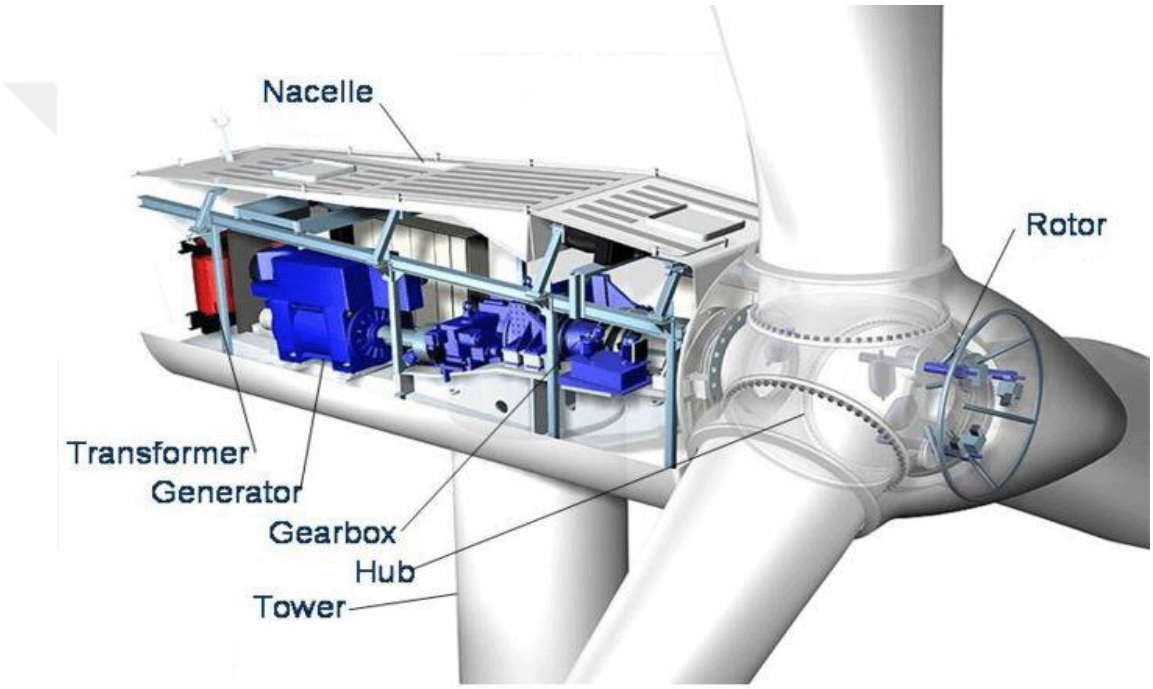

Figure 1.1 General layout of a wind turbine [12]

The rotor blades are designed to extract energy from air currents, and are designed with an aerofoil cross-section to interact with the air via a force arising from the pressure difference between the two sides of the blade. The efficiency of power generation can be improved by pitch and stall control. In addition, the choice of the number of blades has been a long-debated issue in wind turbine design. The three-blade wind generator system is the most widely used, as it is dynamically efficient and suitable for wind farm conditions [13]. In practice, wind turbine blades are equipped with wind protection devices and a recording system to monitor the occurrence of

lightning strikes [14]. As shown in Figure 1.2, a shaft connects the turbine to the electrical generator, either via a gearbox inside the nacelle or directly.

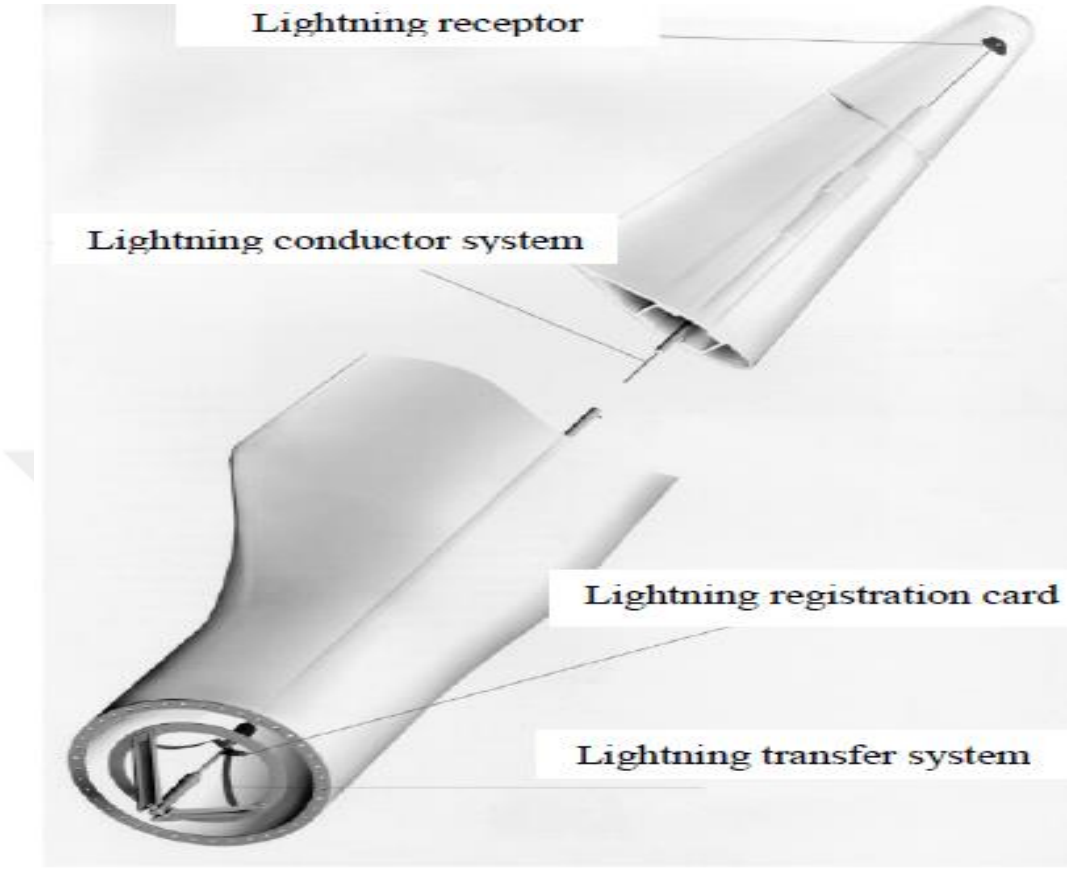

Figure 1.2 Lightning protection for a wind turbine blade [12]

The blades are connected with the shaft via a hub with flanges, and the pitch angle is designed to allow for changes. The generator used in wind turbines converts mechanical energy from wind to electrical energy. Generators used in air turbines are of either the induction or synchronous type, and both of these have many possible modifications and expansions. The primary difference between induction generators and synchronous generators is that the induction generator works on the principle of slip and is driven at an asynchronous speed, while a synchronous generator is driven at a specified synchronous speed that is controlled by the frequency of the supply required. Types of induction generators include the wound rotor type, which will be explored in detail later, or a squirrel cage generator, which is simple and robust. The latter is the preferred type for many industrial systems, and is implemented as shown in Figure 1.3. Synchronous generators are generally used in direct-drive wind turbine applications, as shown in Figure 1.4. The main factor in the wind power calculations

depends on the cube of the wind velocity. The required power rating for a generator can be roughly determined using a special implementation environment [13,15].

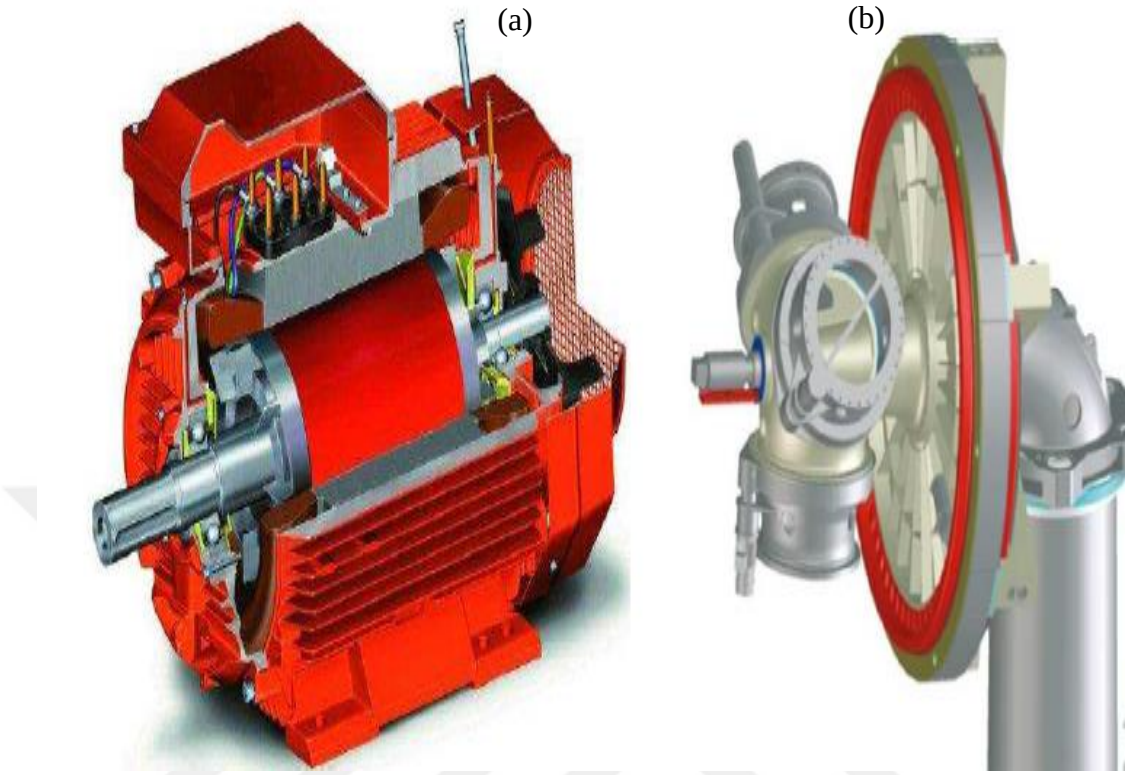

Figure 1.3 (a) An induction generator; (b) a direct-drive synchronous generator[12]

In addition, a wind turbine contains other components that are important for normal operation, such as control systems, a tower, brakes and a yaw mechanism [15,16]. Wind turbines contain a braking system that is used for maintenance and is also required in emergency situations. The yaw mechanism is necessary to align the rotor axis with the wind direction, so that the wind energy can be efficiently used. The tower can be built in either a flexible or a rigid way. The main function of the tower in a wind power system is to reach a higher position, where wind speeds are faster. Flexible towers are cheaper, but they undergo more movement and therefore cannot sustain high levels of pressure, while the solid type of tower has a natural frequency that falls on a frequency pass blade [14] wind power system general power system configuration. The system is connected to the power grid using a converter, as shown in the figure below.

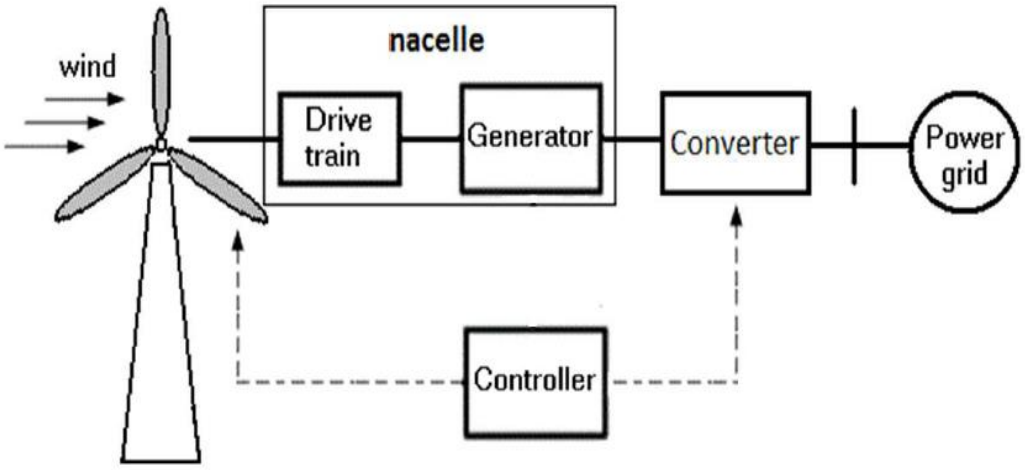

Figure 1.4 Basic configuration of a wind power system [12]

Wind power systems can be categorized into three main types, based on the type of generator used: (i) the permanent magnet synchronous generator (PMSG); (ii) the DFIG; and (iii) the SCIG. There are alternative types of generators, such as the direct-drive synchronous generator system [19,20], the brushless doubly-fed induction generator [17,18], and the multiple-stage geared system [22]. The most common types are the direct-drive synchronous generator system and brushless DFIG. Although the direct-drive mechanism has a simpler and more reliable drive train, it has a higher cost due to its lower rotor speed, and in order to obtain a sufficiently large torque, we need a larger diameter, more poles and higher volume. Wind power systems can be categorized, based on the speed of operation, into variable-speed and fixed-speed systems. The following table shows a comparison of the wind power obtained from these two types of system and the most important advantages and disadvantages of each [23-28].

The drive train uses a multiple stage gearbox, and is directly connected to the grid via a transformer. To help the network, external reactive power reparations and a soft starter are necessary. The fixed-speed system has been successfully used in off-network applications. The system in [17,18] uses a wound rotor induction generator and a stator that is directly connected to the network; the rotor winding has variable resistance, and an electronic power converter is needed to control it. The slip of the generator is adjusted via control over the rotor resistance. The variable velocity system is widespread conception in big power classification enforcement. Partial or ideal converters would lead to variable-velocity operation systems. This type of wind power

generation system currently predominates in the market due to its high efficiency and ride-through capacity during faults. The control system controls the currents and a voltage generator in order to maintain the optimal rotor speed, to give the optimal output power.

Table 1.1 Comparison between types of wind power system

Wind turbine	Advantages	Disadvantages
Fixed-speed system	- Simple and strong structure - Minimum running and servicing costs - Simple to control	- Low efficiency - Power variation due to wind speed and lower pressure - A major drawback is reactive power consumption - Requires a switch to prevent motor working at low wind speeds
Variable-speed system	- Wide range of speeds - Full control enables the optimum process for maximum power production - Can feed into the grid with no need for external energy compensation - Suitable for and commonly utilized in large-scale wind farms	- Complex control of the system - High cost of converters and control - Needs a gearbox multi-stage and slip ring for the DFIG system - The direct drive requires a large diameter and thus has a high cost

Figure 1.5 shows the topology of a practical variable-speed system. Since the low request on the transforming power classification of nearly 30% of the gross power classification, the DFIG with partial converter (shown in Figure 1.5(a)) is the main topology used for wind power generation systems. Due to the use of a rotor-side converter, power is fed back to the network even without squandering the resistor. In

the state of a partially transformer, the PMSG or SCIG systems are associated with a full classification transformer, as shown in Figure 1.5 (b) below. This topology has better network fault ride-through (FRT) capability, since the generator-side converter is fully separate from the network side. However, the transformer rating and losses are high. As shown in Figure 1.5 (c), the use of a direct-drive system removes the gearbox and related losses [25]. The PMSG rotor is connected directly to the turbine shaft and turns at a very slow speed, meaning that a high torque and a large machine radius are required to transfer the same quantity of energy. The use of fewer elements means fewer losses and thus a more effective performance for this kind of system. In addition, the lower cost of the permanent magnet makes this system cheaper. To settlement among machine dimension and spinning velocity, the single-stage gearbox shown in Figure 1.5(d) is used to increase the velocity [24]. Figure 1.5(e) shows the rotor-side converter supplying DC excitation; however the stator is associated to perfect converter such as the condition. Figure 1.5(c) shows an electrical excited synchronous generator (EESG). Although there is an increase in the cost due to the additional winding for excitation, and extra maintenance is also required, the EESG can reduce these losses by controlling the flow using a rotor transformer [19,22,23].

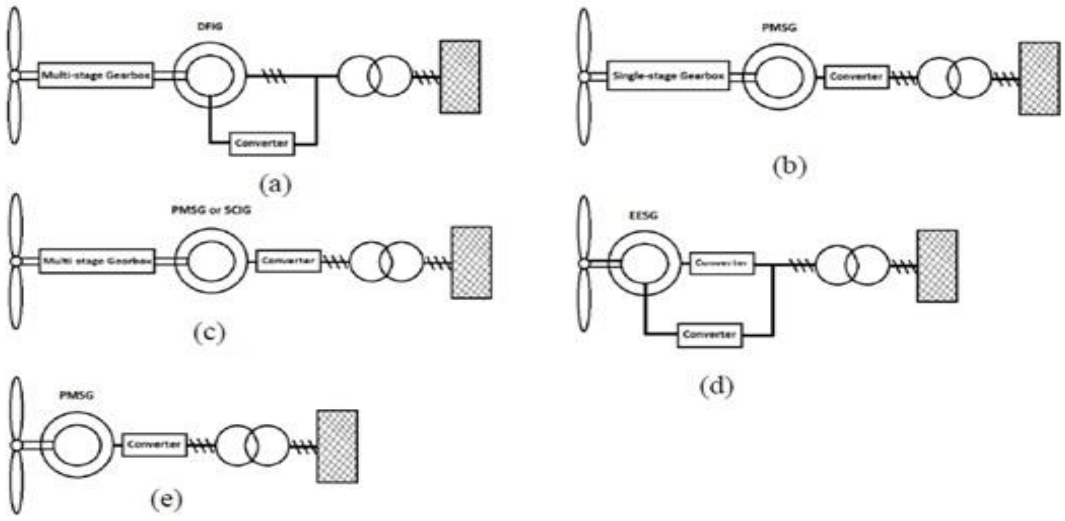

Figure 1.5 The most commonly used topologies for wind power systems: (a) DFIG with partial/matrix converter; (b) PMSG with full converter and lower-stage gearbox; (c) PMSG/SCIG with full converter; (d) EESG direct drive; (e) PMSG direct drive [12]

1.3 Types of Wind Turbines

Wind turbine systems can be categorized into the two main types of vertical and horizontal axis wind turbines, as shown in Figure 1.7 [29]. At first, vertical axis designs (without a yaw system) were thought to be superior, and the position of their gears and apparatus generating at the tower ground. However, several disadvantages mean that vertical axis wind turbines are less commonly used, and are not widespread in the commercial market, for example:

• It is not possible to use a large gearbox with a vertical axis wind turbine, since the housing is typically at ground level, which will cause a heaviness, and the costs due to the transmission shaft will be high.

• In this type, much of the surface of the blade is close to the axis, meaning that the aerodynamic effect is low.

In horizontal axis wind turbines, the blades revolve parallel to the ground and the wind inflow axis. Most of the large turbines used in modern wind farms are horizontal axis turbines, due to their ability to harness a larger amount of wind energy. However, horizontal axis wind turbines are loaded with reverse gravitational loads (the structural load is inverted when the blade moves from the upper to the lower position), and this can impose a limit on the volume of these turbines [30, 31]. The modern wind turbine has two forms: variable or fixed-speed. Wind turbines can also have variable or fixed pitch, which means that the positions of the blades are fixed or variable.

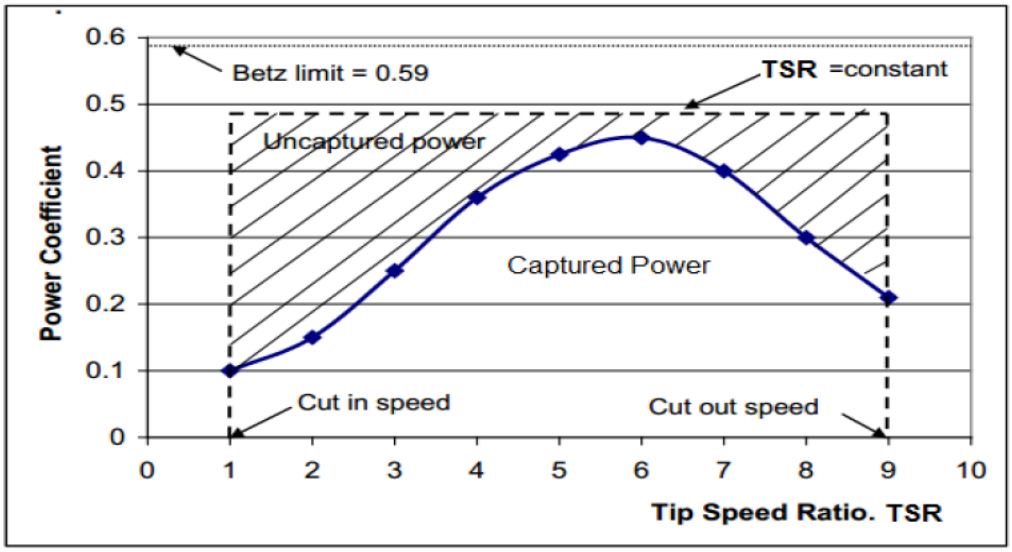

Figure 1.6 Tip speed ratio versus power coefficient [32]

The rotor of the fixed turbine revolves at a fixed angular velocity, and is coupled to a traditional SCIG that has the same frequency as the network to which it is connected, regardless of the variation in the wind velocity. Fixed-velocity wind turbines have the advantages of being robust, low cost and simple.

Their disadvantages include:

- A lack of ability to extract the maximum power from wind (not ideal)
- Additional mechanical stress exerted on the gearbox due to variable wind velocity
- A lack of ability to separate the control of active and reactive transferred power to the network due to the generator type (traditional induction generator)

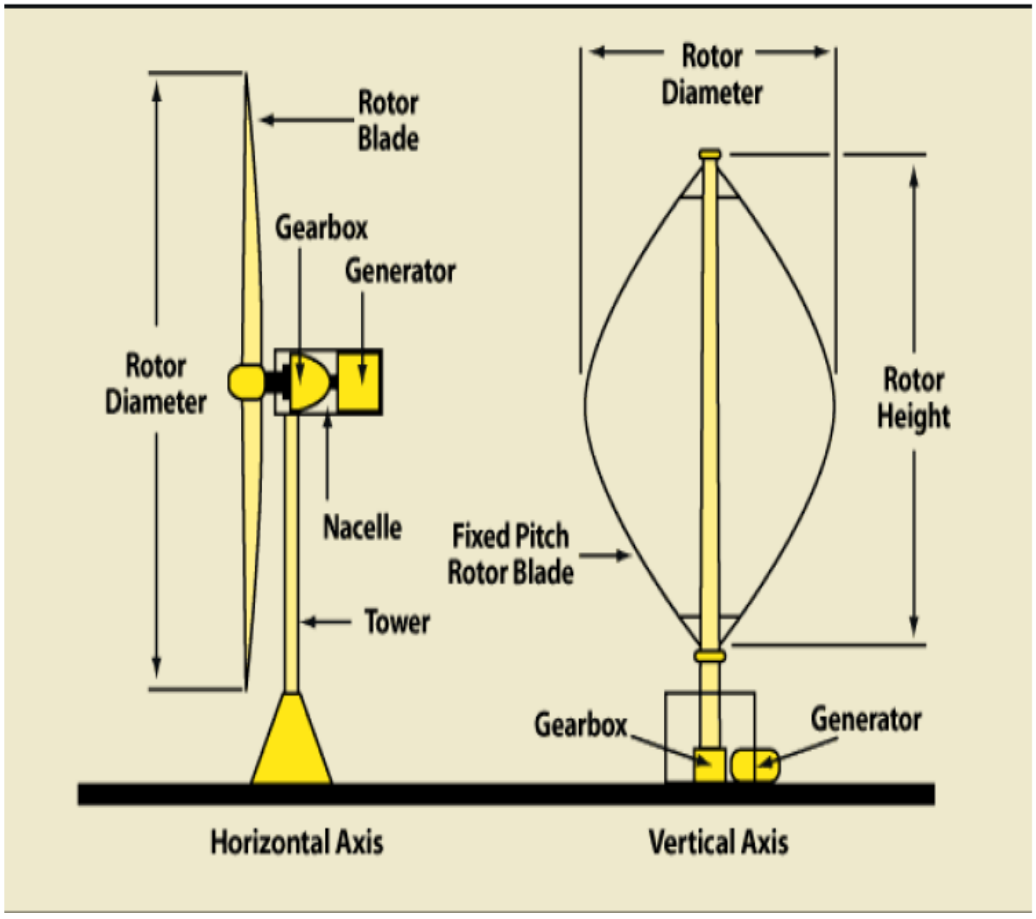

Figure 1.7 Vertical axis and horizontal axis wind turbines [32]

The advantages of variable-speed wind turbines include:

- Highly efficient, ideal tip-velocity ratios over a wider range of wind velocities, allowing them to achieve maximum power
- A type of generator and power converter that can supply DC power while the speed of the wind turbine is variable
- The operator can control the active and reactive power supplied to the network.

The disadvantages of variable-speed wind turbines include:

- Generation of variable frequency
- Complex control of the entire unit
- Dependence of the output voltage on the speed of the rotor and stator

Wind turbine manufacturers have now shifted toward variable-velocity wind turbines, due to their better overall performance. They can take full advantage of variations in the wind velocity, and have the advantage of fewer power fluctuations, lower mechanical stress and an energy output that is 10%–15% higher that that of fixed-speed turbines [33,34].

1.4 Introduction to Wind Energy Conversion Systems

A wind energy conversion system converts the kinetic energy of the wind into mechanical and then electrical energy. A wind energy conversion system can be used with an SCIG generator, a wound rotor induction generator, or a DFIG. The main components of a wind energy conversion system are: (i) a gearbox with a turbine rotor and connected control; (ii) a generator i.e. a power converter with connected control, as shown in the diagram below.

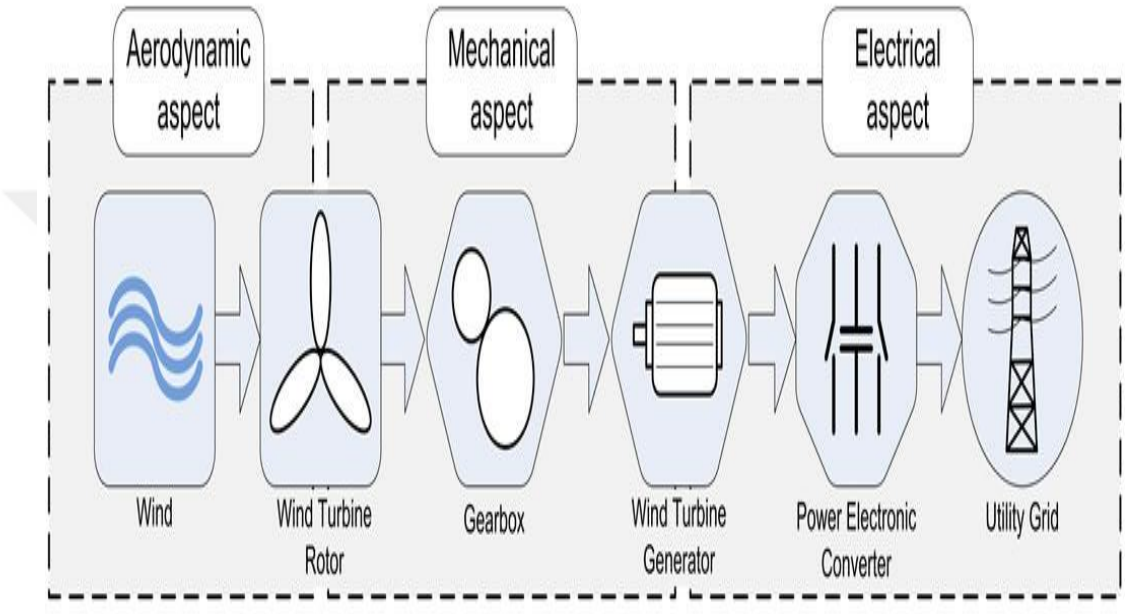

Figure1.8 The components of a wind energy conversion system connected to the grid [32]

1.4.1 Aerodynamic Components

A wind turbine is a structure that extracts kinetic energy from the wind and transforms it into electrical energy. The aspects of the performance of the turbine, such as the power output, wind speed, and torque, are determined by the aerodynamic forces generated by the wind. Several parameters can be chosen to represent the aerodynamic operation of wind turbines, such as the tip speed ratio (TSR) and the power coefficient (PC). The TSR of a wind turbine is the ratio between the linear velocity of the side of the blade and the real speed of the wind.

$$TSR(\lambda) = \frac{\omega R}{v} \tag{1.1}$$

where λ is the the TSR; ω is the rotor angular velocity; v is the wind speed; and r is the rotor radius.

When wind turbines are designed, attention must be paid to wind speed. When the wind turbines rotate very slowly, most wind should pass without hindrance through the blades, meaning that the energy extracted is low; however, when the wind turbines rotate very quickly, the rotating blades should block the flow of wind. For energy extraction, it is therefore necessary when designing a turbine to obtain the highest angular speed efficiency to correspond to the wind speed or the optimal TSR.

When the TSR is very low, wind turbines will tend to be slow, and when the TSR is too high, the blades will rotate very quickly through the air, meaning that energy will not be extracted with optimal efficiency.

The maximum power coefficient of a wind turbine is almost 59%, and this is called the "Betz limit" [30]. In modern-day wind turbines, the power coefficient is in the range 35%–40% [35]. This value is lower than the theoretical Betz limit due to shortcomings and losses from various configurational aspects such as the features of the rotor blades and limitations due tos the friction in the turbines.

Figure 1.6 shows that the most efficient power extraction takes place at an optimized value of TSR [36], for which a low variance is visible between the real TSR curve (blue curve) and the fixed TSR line (discontinuous line). This variance represents the unsaturated power from the wind turbine. Losses due to wind friction, limitations on size and turbine design wastages account for part of this unsaturated wind power, and the remainder is due to the fact that the wind turbine is not working at the best TSR for its working range of wind speeds [30,36]. However, the rotor speed enables the blades to be controlled (major strategy) to give the best TSR at varying wind speeds to extract highest possible energy from the wind (higher PC).

1.5 Importance and Development of Wind Power Systems

Wind energy is currently the fastest growing renewable energy source in the world, according to a report by the Global Wind Energy Council (GWEC) [20] issued on 25 April in Delhi. This report contains annual updates for wind energy markets, and states that by 2016, about 54 GW of clean renewable wind energy systems had been installed across the world. These wind turbines are in more than 90 countries, nine of which have installed more than 10,000 MW and 29 of which have passed the 1,000 MW threshold. The cumulative capacity has grown by 12.6%, to reach a total of 486.8 GW. The penetration levels of wind energy continue to increase. Denmark leads this increase, producing 40% of its power from wind turbines, followed by Portugal, Ireland, Spain, Cyprus and Uruguay, with more than 20%. Germany, Canada and USA obtain 16%, 6% and 5.5% of their energy requirements from wind, respectively. Finally, the Chinese energy market obtains 4% from wind. This flagship publication from GWEC states that 60 GW of new wind installations will be introduced in 2017 and that the installed capacity is expected to be more than 800 GW by the end of 2021. It is clear that the wind market will continue to increase steadily, and thus continue driving wind power generation technology to ever more advanced levels.

1.6 Motivation For The Current Research

The implementation of renewable energy has garnered an enormous amount of interest in recent years, and is now considered an integral part of the larger overall picture of energy generation, due to its ecological friendly features and limited dependence on fossil fuels. At the present time, wind farms (wind power stations) are being built and used around the world in large numbers, and the amount of power from wind turbines is increasing, both from individual turbines and farms. DFIG turbines are invariably the best option for multi-megawatt generation, since a alternate-speed variable-pitch DFIG wind turbine can provide energy transformation at minimal cost with the lowest mechanical stress due to its various advantages. A partial size rate rotor energy transformer is needed for full control of the generator at variable wind speeds. Typically, DFIG wind turbines are constructed hundreds of miles away from the load station, where the electric power network is weak, and are characterized by low short-circuit proportions and a voltage regulation problem.

In this thesis, the option of utilizing a modular multilevel converter (MMC) system in conjunction with a DFIG-based wind energy conversion system will be investigated through simulation studies. A back-to-back half-bridge MMC-based wind energy conversion system with a DFIG that is connected to a three-phase utility grid will be designed, modeled, and simulated under different operating conditions. The capacitor voltage problem in MMCs will be solved using one of the available existing techniques. The capability of the wind energy conversion system to control real and reactive power, the effects of changes in wind speed and other related parameters will be analyzed in depth. Vector control is a well-accepted standard, and hence the control system for the DFIG will be a vector control scheme. In this way, we will test the dynamic performance of the current vector control scheme and apply unit step-changes to the reference signals of the controllers. Several simulation studies will be designed to verify the simulation model of our back-to-back MMC-based DFIG wind energy conversion system.

CHAPTER 2
LITERATURE SURVEY

2.1 Introduction

In this section, a literature review is carried out of DFIG-based wind energy systems and back-to-back MMCs. In the last decade, numerous researchers have carried out studies of models and control strategies for DFIG-based wind turbine-generator systems, and topologies have been designed for the converter.

2.2 Related Works

In [37], Petersson showed that DFIG can be classified into four types: standard, cascaded, brushless, and single-frame cascaded DFIGs. In wind turbine generator systems, only standard and brushless types are used.

Protsenko and Xu used two cascaded induction machines to develop a brushless DFIG [38]. They obtained active and reactive power control by using a closed-loop stator-flux-oriented control scheme.

In [39], Zhang proposed a cascaded brushless DFIG (CBDFIG) that used a direct power control (DPC) strategy featuring rapid, dynamic responses and efficient steady state operation.

Shewarega showed that a DFIG can generally be simulated via miniature request models which can produce a third request display by disregarding the subsidiary expression of the stator transition initial system model demonstrate via ignoring whoever the derivative whence of the stator transition and rotor [40]

In [41], Istvan Erlich suggested an improved third-order model. The stator currents in this model have DC components. In this work, a comparison is made between the suggested model and the full model of wind and slope conditions.

Luna constructed a new reduced third-order model [42] . The stator impedance and inductances are disregarded in this model by stratify the Laplace transform. The author compared this full order model with the safest model for transient analyses.

In [43], a method is presented for power generation using wind turbines located at sea, using a variable frequency in the classification. The volt/Hertz process is applied to type 3 induction in a DFIG that transmits energy from the generation station to the load center inland using high-voltage direct current (HVDC) transmission energy. When the operation of shoreline kinetic wind energy takes advantage, it will provide HVDC-VSC to change the voltage and frequency at the collector system. Also, it will investigate type 3 (WTG-DFIG) with underrated voltage and frequency.

The authors of [44] suggest a control technique for a wind farm module multilevel converter (WFMMC) that is able to automatically absorb wind power and to remove fluctuations in the o/p current by using a method involving closed-loop control of rotor current suggested by a DFIG coating method.

Simulation, field and waveforms because the test results are offered the effective performances the MMC-HVDC can be utilized at larger scales, allowing for successful incorporation into wind farms.

In [45], the effects of a reactive power control strategy were studied by Weng. The paper studied this strategy using the effects of the rotor reactive power Q_r and the stator reactive power Q_s on a DFIG for a wind farm. The rotor current I_{dr} affected the reactive power. Investigate the effect of I_{dr} on the stator reactive power Q_s and rotor reactive power Q_r, the DFIG is operated under different operation.

Patel showed that power is generated from a wind energy conversion system utilizing an MMC topology [46]. A PWM-based MMC topology is utilized to design a multilevel inverter having FACTS. MMCs have lower losses, better voltage quality, growing and redundancy. The suggested system uses a PWM control strategy to inhibit the reactive power and boost the active power. In this grid-connected system, an inverter with FACTS capability is used in a single unit without any extra cost. Hence,

this design can avoid the need for external STATCOM devices to regulate the power factor of the network.

Minyuan Guan analyzed the power transport in the MMC, the power in the storage capacitors and the variable voltage in the sub-modules [47]. A DC voltage ripple caused a circulating current in each phase unit. The author used PSCAD/EMTDC to verify time-domain simulations for an accurate model using a simplified formula. This simplified formula could be used to calculate the DC voltage ripples in phase units in the MMC. The voltage fluctuations in the storage capacitors in the simulated sub-modules were caused by the variation components of active power conveyor to the leg. The fluctuations in the capacitor voltages and the active power in the lower and upper converter legs of each phase unit were not synchronous.

Heigweger suggested an an algorithm to achieve voltage-balancing control for circuit configurations [48]. PWM-MNCs were used to accomplish voltage balancing without an external circuit by combining the average and balancing control with respect to the per phase capacitors. Control was achieved by inserting a balancing element into the modulation pointer for each sub-unit.

In [49], the author suggested estimating the power of the arm by measuring the AC and DC currents without feedback controllers. By reducing the current, an open loop was used to assess the power of the arm, giving better stability.

The thesis in [50] offers several PWM strategies based on a phase- and level-based carrier PWM with respect to the conversion of pulse patterns and waveforms generated by the (2N + 1) and (N + 1) output phase voltages. A carrier-based PWM switch is combined with control technology for an MMC machine. This MMC control approach was analyzed based on PWM, and the performance of various control approaches was tested, including the efficiency, circulating AC component, ripple capacitor voltage SM, and other aspects of the same transformation.

In [51], a PD-PWM was used to improve MMC gating pulse generation. The controllers communicated using PI to control the current active power. The focus was on the determination of suitable carrier-based PWM switching and control methods

for network-connected MMCs. A test of the controller demonstrated that it was able to track step changes in the reference value using a 0.2 ms time delay.

Haddioui suggested solutions for minimizing the switching frequency and the switching losses in power semiconductors [52]. Improving capacitor voltage balancing control optimized.

2.3 Positioning of this Work in The Literature

In this thesis, a back-to-back MMC and DFIG system is designed and simulated to achieve balanced operation with a three-phase MMC. The DFIG feeds the network, and a back-to-back MMC is positioned between the DFIG and separate generation centers. The model also involves loads and conventional medium-voltage AC lines. Time-based simulations of the modelled DFIG with the back-to-back MMC system are carried out in a simulation environment. The stages of this work can be summarized as follows.

Initially, we design the topology for a DFIG with a back-to-back MMC system. This type of power stage was designed using switching modulation strategies based on those available from the literature. A design for a wind energy conversion system based on DFIG and a back-to-back MMC system was developed by investigating their controllers for guidance when connected to the grid. The MMC was designed with a suitable number of levels and DC link voltages, and was coupled to a three-phase balanced bus in an example power system via series reactors to test its internal and external control algorithms using standard proportional integral controllers. The four-quadrant operation provides independent active and reactive power injection to and from the power system. This technique was tested and verified. Following this, the MMC was connected between a wind farm and a separate source.

We chose the location of the MMC in the overall power system design in order to achieve two-way real power flow control at the AC terminals of both. The dynamic responses of the controller for the DFIG and MMC were obtained from the results of a time-domain simulation. An efficient modulation strategy was selected and tested for the switching process. We also modelled a long transmission line that was suitable for the time-domain simulations. Finally, conclusions were drawn and evaluated.

CHAPTER 3

THEORY, MODELING AND CONTROL OF A DOUBLY FED INDUCTION GENERATOR

3.1 Introduction

Over the last few decades, power generation has been enhanced by the adoption of wind energy. The power generated by wind turbines has increased from smaller machines of a few kilowatts to large machines with an output capacity of over 4,500 kilowatts. Based on the capacity of wind power generators, they are classified into three categories: (a) utility scale, which corresponds to large wind turbines (850000 W–3.5000 kW); (b) manufacturing scale, which corresponds to medium-sized turbines (50–600 kW), which are generally used in industry for remote grid generation to meet local power demand; and (c) standard, which is used on a local scale and requires turbines (both one- and three-phase) (400 W–50 kW) with limited capacity, which are mainly used for battery charging and light home loads.

Wind turbines have increased system reliability (wind farms) because they are part of the grid, resulting in lower costs when modern machines are used. Much progress has been made in aspects such as network integration, electrical machines, power transformers and methods for control. However, there are still many challenges and unresolved questions. Following this period of evolution, it is now possible to control the real and reactive power of the generator under variable speed operation. This area of control strategy has become a very complex subject of research, and technology that is expected to provide higher capacity in the future is being developed.

An understanding is required of the possible power systems, system integration techniques, and applications of electronic power transformers and control schematics using a common platform.DFIG-based energy systems are more widely used around the world than other wind turbines that use fixed-speed induction generators, as they have several advantages such as variable-speed operation and four-quadrant reactive

And active power capability. This also results in the minimizing of converter costs and power losses. A DFIG system costs much less than other machines with similar rating, due to minimization of the power rating of the rotor converter, which is the primary cost, as compared with a full-rated converter and a system based on a fully fed synchronous generator with a full-rated converter.

3.2 Components of the Doubly Fed Induction Generator

In the standard conversion system in DFIG-based wind turbines, the stator of the DFIG is connected directly to the grid using a transformer, and the rotor windings of the DFIG are connected with a back-to-back converter via slip rings. The rotor converter system consists of two converters connected by a DC link: a rotor-side converter (RSC) and a grid-side converter (GSC). Figure 3.1 shows a schematic diagram of a DFIG-based wind energy generation system.

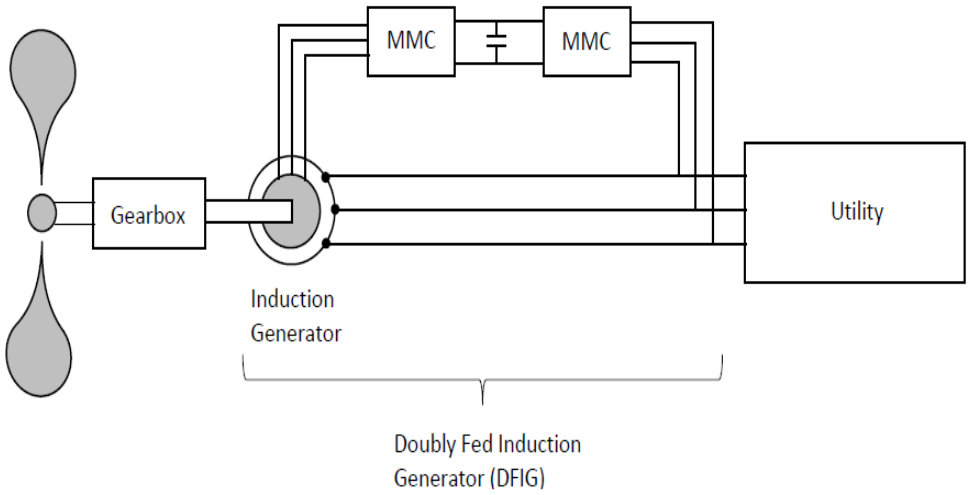

Figure 3.1 Schematic diagram of a DFIG-based wind energy generation system [53]

The generator is called a “doubly fed induction” generator due to its ability to supply the network with energy from both the stator and rotor. The rotor side has approximately 25% to 30% of the rated power of the the generator; this proportion allows the DFIG to have an operational speed range of around 30% of the synchronous speed and to minimize the cost and rating of the rotor converter. The purpose of the GSC is to reduce the variation in the DC link voltage. It is possible to control the torque, the speed of the DFIG and its active and reactive power at the stator terminals [54, 55]. The total power of the generator is not linked to the size of the converter but

to the specified speed range and the power ‘slip’, meaning that the converter costs increase when the speed range becomes wider. Thus, the economic considerations of investment costs and the required efficiency determine the choice of speed. When the DFIG is connected to the network, high transient currents can cause network disturbances, destroying the electronic components of the rotor adapter. A protection system called Kruppars is therefore used, which can be rotor winding short during the fault period by small resistance and released when the error is cleared.

3.3 Principle of Operation of the Doubly Fed Induction Generator

Even though the principle of operation of doubly fed electric machines has been known for decades, a wide range of applications has only recently emerged, and this is almost exclusively due to the development of wind power technologies. The mode of operation specifies the speed range of the DFIG, as it can operate in super-synchronous or sub-synchronous modes in which the speed range may change by ±30%. The mode of operation also specifies the power direction on the rotor side, as it feeds the network with active power via the back-to-back converter at super-synchronous speeds, but consumes power from the grid in sub-synchronous speed mode. This is an advantage of DFIG that is exploited in wind turbines, as it has the ability to output an almost constant voltage to the grid without relying on the rotor speed or wind power. It can also be directly connected to the AC power grid and remain synchronized at all times. The other feature includes the capability to control the reactive power from the rotor circuits to the network, which enables the DFIG to control the voltage stability and power factor rectification at the point of common coupling (PCC). Controlling the rotor speed to compensate for the differences in wind speed is achieved by adjusting the frequency of the AC voltages and the current feed to the rotor windings, and can be understood in terms of the sub-synchronous and super-synchronous modes of operation explained below.

3.3.1 Sub-synchronous Mode of Operation

When the DFIG starts sub-synchronous operation, the wind speed is almost 7 m/s. The rotor speed of the generator (n) fewer the synchronous speed (sn) the rotor frequency (f) of the voltage induced raise as accordingly and positive polarity. This positive polarity means that the AC currents injected into the rotor windings of the generator due to the magnetic field rotate in the same direction as the generator rotor. As a result of controlling the phase sequence of this injected current, the rotor "receives" power from the network via the rotor converters (GSC and RSC). This can be explained in terms of the control over the power flow in the rotor winding of DFIG in the sub-synchronous mode using the equations of an induction machine,as explained below [56, 57].

$$P_g = P_m + P_r = (1-s)P_g + sP_g \tag{3.1}$$

where:

P_g: air gap power

P_m: mechanical power between the rotor and the shaft,

P_r: slip power

sP_g: power between the rotor converters and the electrical grid.

The slip S is defined by:

$$S = \frac{n_s - n_{rotor}}{n} \tag{3.2}$$

When the induction motor operates with short-circuited rotor windings at less than the synchronous speed, the mechanical energy is positive when transported from the rotor to the shaft and is then used to drive a mechanical load (such as a pump or fan). In this situation, the slip is positive ($0 < S < 1$), and the air gap power transported from the stator to the rotor will also be positive. If the influx direction for both P_g and P_m is reversed (i.e. P_g and P_m have negative values) then the machine will work in generator mode (i.e the DFIG is in sub-synchronous mode). The slip power P_r will also be negative and will be provided by the converters (RSC and GSC) to the rotor, where the RSC works as an inverter and the GSC as a rectifier. When we want to reverse the energy of the revolving circuit, we reverse the sequence of the AC voltage stages or the current injected into the rotor winding in the DFIG. The following figure shows the direction of the flow of energy in the DIFG in both synchronous (from network to rotor) and super-synchronous (from rotor to network) networks.

3.3.2 Super-synchronous Mode of Operation

Similarly, when the rotation speed of the rotor generator increases above the synchronized velocity, the rotor frequency of the AC current that needs to be fed to the rotor coil generator is thus increased from a negative polarity.

A negative polarity of the rotor frequency indicates that the phase sequence of the three-phase alternating currents that feed the rotary files will make the rotary magnetic field rotate in the opposite direction to the alternator. This implies that the over-synchronous rapidity slip (S) is negative (S < 0), and the DFIG then works in a super-synchronous mode, where the slip energy P_r is controlled by controlling the phase sequence of the currents injected into the rotor coils of the DFIG. In this mode, the slip energy is positive and is transported from the generator rotor to the network via the rotor converters of the DFIG, where the RSC works as a rectifier and the GSC as an inverter.

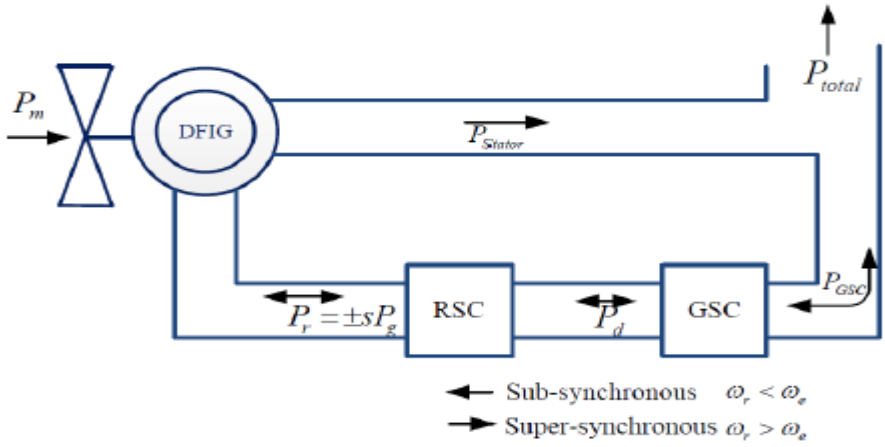

Figure 3.2 Power flow in a DFIG system [53]

3.4 General Control Scheme for a Doubly Fed Induction Generator

The DFIG is widely utilized in many variable-speed wind energy implementations and makes up close to 50% of the wind power systems currently manufactured [58]. Due to the suitability of DFIGs for wind energy generation, numerous control systems

appropriate for this implementation have been developed. Figure 3.2 shows a sketch of a model control for a DFIG that is available on the market. The control models can be classified into three major types depending on their connection with the grid. As wind generation becomes more popular and the number of wind turbines is increasing, grid operators have to include that consumer power, finesse is not compromised. To enable a larger contribution from wind energy without affecting the stability of the power system, most turbines remain connected and contribute to the network even if there is a fault such as an unbalanced three-phase voltage. Wind farms typically operate such traditional power plants for local loads, offering active and reactive power for frequency and voltage retrieval immediately after a fault has occurred. Hence, some of the primary variables that should be controlled are the network frequency, voltage, and power factor, classified in the third control level in Figure 3.2. These preferentially values make wind turbines required appointed quantities of the active and reactive power from wind turbine control, and this is classified as the second level of control in Figure 3.2. The inputs at this level of control are the wind speed v_{wind} (from an anemometer), the pitch angle β and the rotor shaft speed ω. The pitch angle is the linear axis of the blades of the wind turbine, which can be controlled to alter their aerodynamic advantage. Using these inputs, the pitch angle is adjusted to obtain the required wind power. For a particular wind turbine, material structure and wind velocity, the second control level can reveal the maximum power point (MPP), which should be processed by a DFIG as a load. To obtain this as the first control level as shown in Figure 3.2. This level plays the role of controlling the RSC and GSC. The RSC regulates the advanced torque T_{em-}, the active power P_{ref} and the reactive power Q_{ref}, while the GSC supplies a fixed DC link voltage. This is known as RSC and GSC control. The circuit breakers (CB1) and (CB 2) are utilized by the start-up operation and when a fault arises to isolate the DFIG from the network and the local loads.

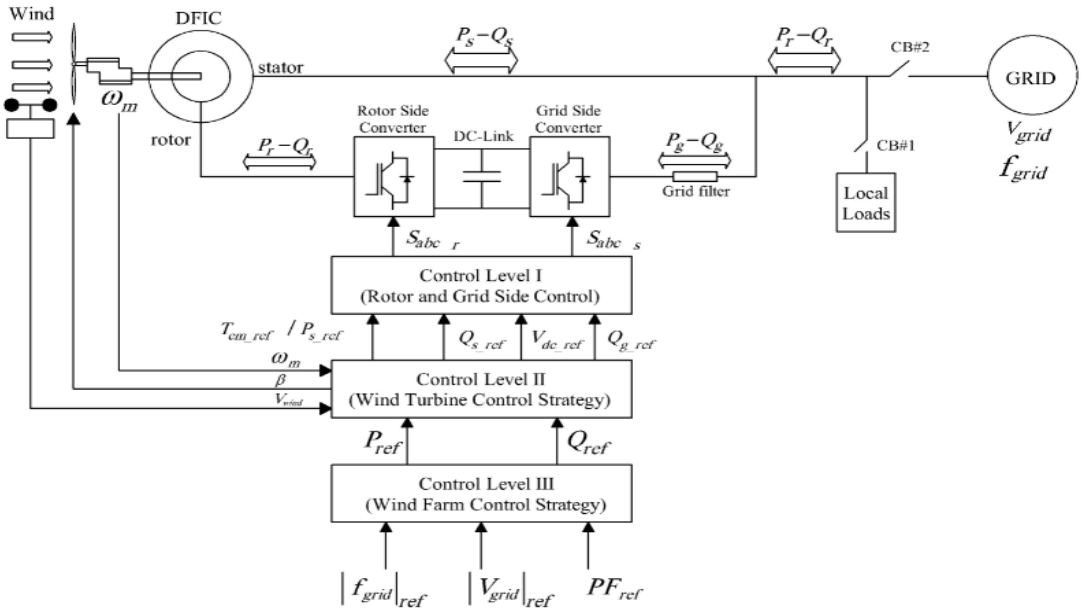

Figure 3.3 Doubly fed induction generator for a wind power system [53]

The model power electronic converter that is used in a DFIG depends on the wind energy system. It is a back-to-back converter that consists of two three-phase voltage source inverters (VSI) participating in the DC link. Figure 3.3 shows the circuit diagram for a three-phase generic back-to-back converter.

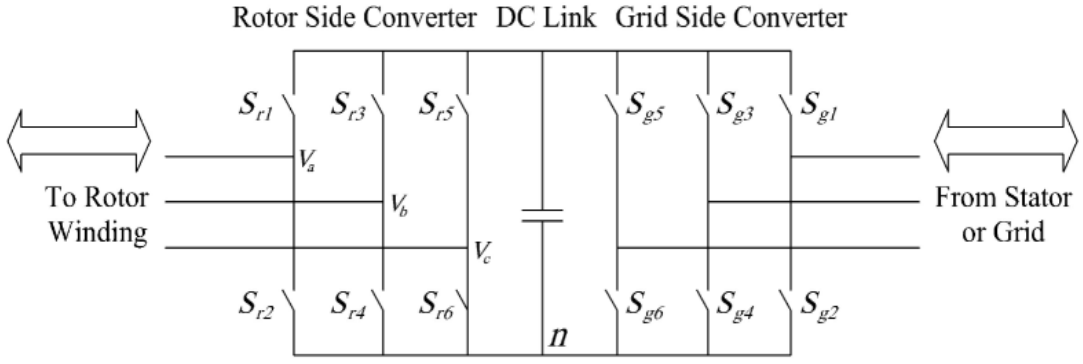

Figure 3.4 General schematic for a back-to-back converter [53]

In Figure 3.3, each converter consists of six switches (SRI to SR6) for the RSC and six (SG1 to SG6) for the GSC. When the converter transforms an AC network voltage with constant magnitude and frequency to a corresponding DC voltage, it is generally known as an active rectifier or pulse width modulation (PWM) rectifier [59], and this is the case for the GSC. When the converter transforms a constant DC voltage into a three-phase AC voltage with variable quantity and frequency for an AC load, it is

typically called an inverter. Whether it is acting as an inverter or a rectifier, the power influx in the converter circuit is bidirectional: the energy can be input from the DC side to the AC side, and vice versa. Hence, the back-to-back converter is known as a bidirectional indirect AC/AC transformer [60-61]. The GSC and the RSC are bidirectional, and the transformer generates a three-phase voltage or current with the required quantity and frequency to be utilized in the rotor windings. The desired voltages or currents are the result of a control process that can vector control and direct power or torque control, which is a major focus of this research work. As shown in Figure 3.2, the outputs of the controllers are leading signals ($S_{abc,r}$ and $S_{abc,s}$) that can be either voltage or current leading. These lead signals determine how the switches in each phase are controlled (ON or OFF) to modulate the voltages or currents that follow up the command reference at the various control levels.

3.5 Evaluation of Control Methods for DFIG

Nearly all control techniques that have been developed for induction motors since 1974 can be used in a DFIG [62]. However, control of the DFIG is more complicated than that of a standard induction motor. Any three-phase magnitude, whether a voltage, current or flux connection, can be expressed as a single revolving vector [63]. Vector control acts to control these space vectors in terms of their magnitude and phase [64-65]. Numerous different combinations can be used, and they each have advantages and disadvantages [66-67]. Figure 3.4 shows the categorization of control strategies for a DFIG, which fall into two main types:

1- Field-oriented control (FOC) [63,66-68];
2- Direct torque control (DTC) / power control (DPC) [69-72].

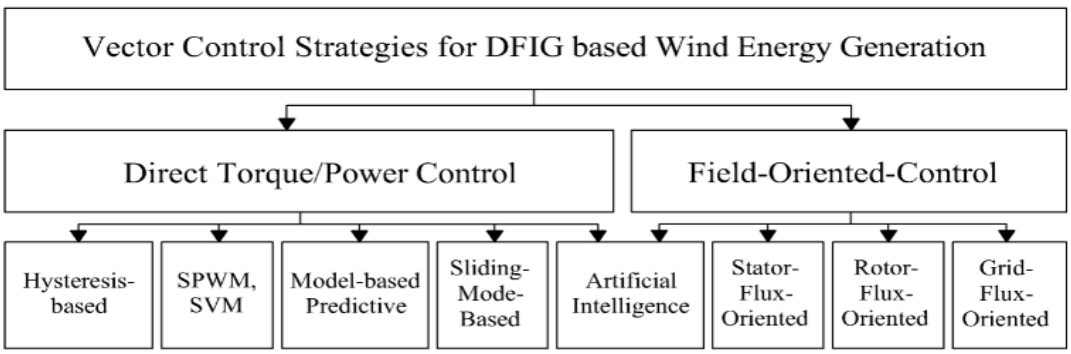

Figure 3.5 Classification of control methods for induction machines [53]

3.5.1 Field-Oriented Control

FOC was invented in 1970 as a control technique for a split excited DC machine. In a DC machine, the field flux generated via the field winding is vertical to the armature field, which is supplied via stator windings. Due to the decoupling between the stator and field flux space vectors, when torque is controlled, the difference in field flux is not influenced by the armature flux. The same comprehended, is extensive for induction machine [66] utilizes a three-phase to two-phase (dq-frame) transformation in which the sinusoidal variables are mapped to DC quantities using a rotating direct axis (d) and a quadrature axis (q). The vector control technique used for a squirrel cage induction motor [63] can be applied to a DFIG [61,73]. In an SCIG, the electronic converter is associated with the stator coils to control the input currents in the dq frame, which is aligned with the rotor influx [63]. This method is shown in Figure 3.5 for a DFIG.

In DFIGs, the RSC is connected to the rotor coils; consequently, this control technique is used on rotor currents that utilize a rotating frame aligned with the stator flux, which is known as stator-flux orientation [61,73,74], or with the orientation of the air gap flux [75,76]. The rotor currents can be divided into two elements, one in line with the direct axis of the stator flux (ird), which is accountable for contributing to it, and the other with (irq) quadrature axis, which is perpendicular to it. The reference rotor current is calculated depending on the active power P_s and the reactive power Q_s. The power can be controlled by changing the volume of (irq) while holding the (ird) and the field flux fixed. For this, the volume and phase angle in relation to the stator flux vector need to be controlled. In this method, there is a linear relationship between the power and the control changing. It can be shown that (irq) can also be regarded in terms of the real power P_s, and (ird) as the reactive power Qs, allowing for decoupled control of these important variables [61]. The difficulty of flux assessment in a stator-flux orientation technique requires researchers to develop orientations that are dependent on network voltage information [77,78]. For network voltage orientation, all variables need to be transferred from a three-phase ABC to a two-phase (dq) synchronous reference framework. For this conversion, the shaft rotating angle θr and stator voltage phase θs are needed; these can be acquired from the encoder and phase lock loop (PLL), respectively.

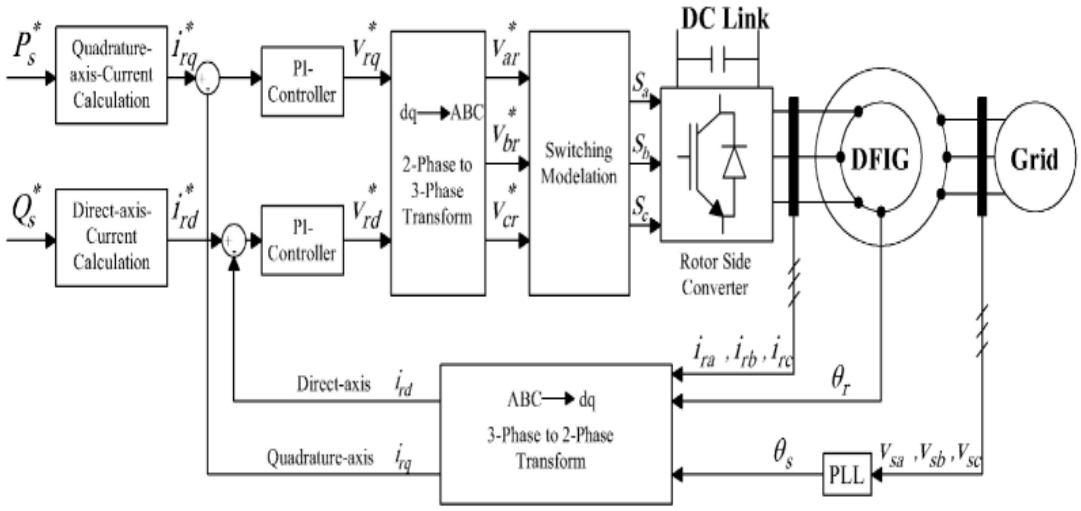

Figure 3.6 Schematic diagram of field-oriented control [53]

Artificial intelligence (AI) controllers have been developed that depend on specialized knowledge (human knowledge) and the implied inaccuracy [79]. A fuzzy logic controller (FLC) and synthetic neural network (SNN) are examples of AI controllers and have been utilized widely in power electronic implementation applications [80,81]. In [82], fuzzy logic controllers are utilized in place of the PI controller to avoid the dependency of the controller on the machine parameters. The pitch angle control for a DFIG wind turbine during neural grid was discussed in [82].

Since FOC is dependent on rotor current vector control, in a stator voltage or flux reference framework, it requires the conversion of the stator voltages, currents and control output variable between a stationary and a synchronous reference framework. FOC also requires accurate information about the DFIG parameters, such as the inductances of the rotor and stator, the resistor, and the mutual inductance. Hence, the control execution may be degraded when the actual values of the parameters vary from those utilized in the FOC control system. The rotor current controllers must be tuned neat to give a good dynamic response [78]. These disadvantages of FOC have motivated researchers to develop a newer control technique with minimal reliance on the machine parameters and requiring minimal effort for compensator tuning. This novel control technique is called DTC [83].

3.5.2 Direct Torque/Power Control

DTC was developed in the 1980s for squirrel cage induction motors in order to reduce the difficulty of control and tuning efforts in FOC [84,85]. This controller was extended to cover the DFIG in 2002 [83]. The DTC technique depends on a space vector representation of the obtainable AC output voltages of the rotor side converter, which is utilized in a two-level voltage source inverter. Figure 3.6 shows a schematic diagram of the DTC method. DTC is mainly composed of three blocks: the estimation block, hysteresis-dependent controllers and the DTC switching table. The torque T_e and the rotor flux amplitude ψ_r is elementary control variance [83,86]. The rotor and stator flow space vectors rotate clockwise (sub-synchronism) or anticlockwise (super-synchronism) at a distance known as the torque angle, which is rated in estimation block utilize rotor and stator currents. The actual torque is also rated utilize stator and rotor currents and voltages measured amount. It is possible to control the torque by modifying the angle between the stator and rotor flow space vectors. In order to affect the rotor flux path and amplitude, various voltage vectors from the DTC are injected into the rotor of the generator. The reference torque and rotor flow are compared to their actual values and proceeds during the three-level and two-level hysteresis controllers, consecutive to supply error signal state for switching table to choose a suitable rotor voltage vector. These voltage vectors are supplied by the two-level voltage source converter, the RSC, which provides energy to the rotor windings.

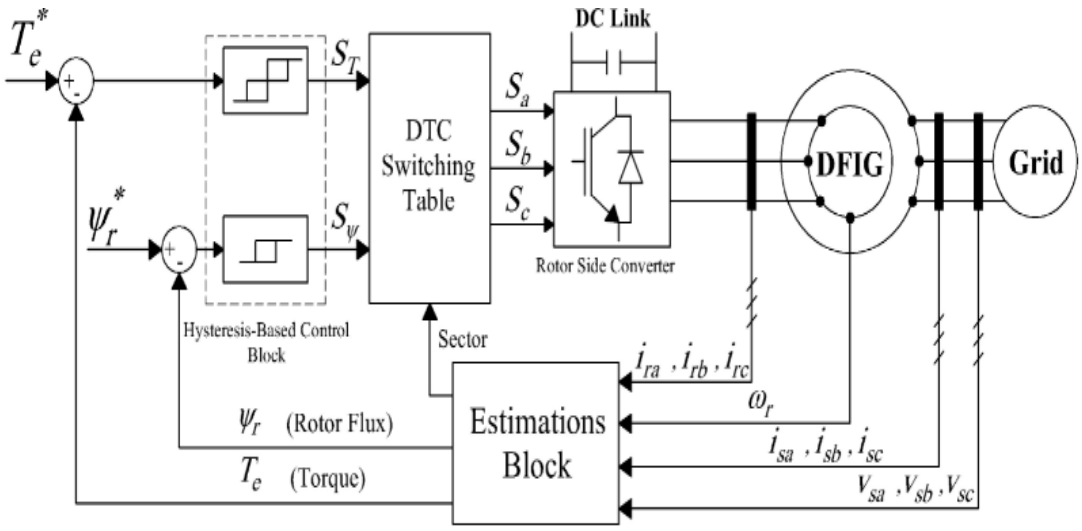

Figure 3.7 Typical block diagram for direct torque control [53]

The direct power control (DPC) mechanism depends on DTC, and was developed more than a decade ago for controlling three-phase rectifiers [87]. In the indirect power control (DPC) process, the elementary variable signals are stator active P_s and reactive power Q_s [88-90]. Also indirect power control (DPC), there is a block and no necessity to appreciation the control variables because the stator active and reactive power can be calculated based on the stator voltages and currents. Figure 3.7 presents a basic diagram of DPC. As shown in the figure, DPC depends on how the inverter switching vectors are chosen for the DPC switching table utilizing the rotor or stator flow stance, and the errors in the active power and reactive powers. Hence, better performance, robustness and lower sensitivity to variance in the system parameters are the major advantages of the DPC technique [89].

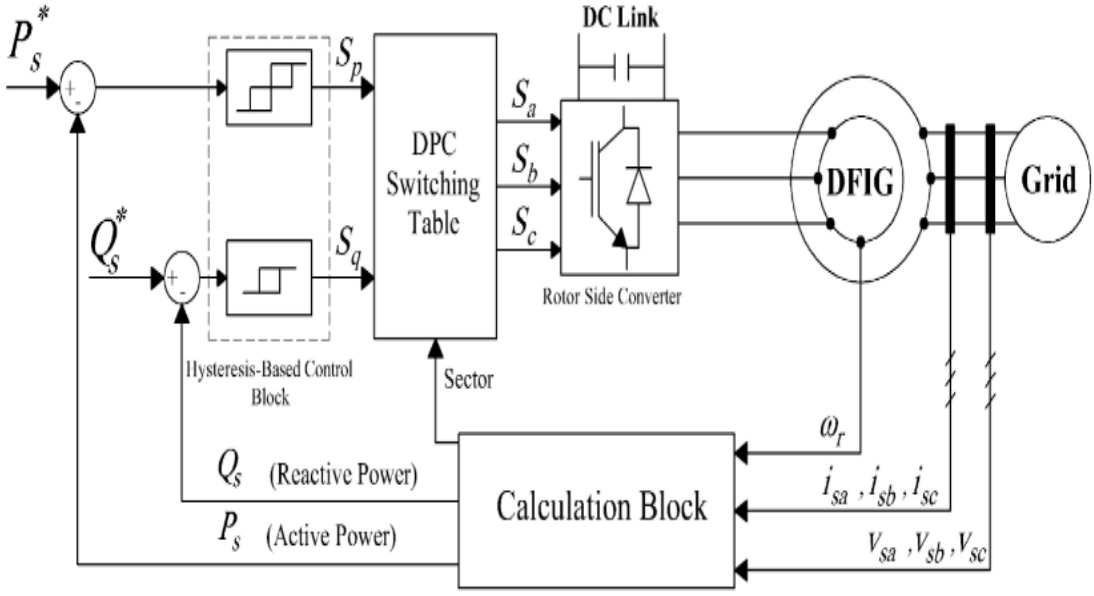

Figure 3.8 Typical block diagram for direct power control [53]

By comparing DTC with DPC, it can be seen that DPC does not require the rotor currents acquaintance and control variable appreciation block. Both of these techniques have high dynamic performance since they use hysteresis-dependent controllers, which have a tolerance for high levels of fluctuation in the sophisticated torque or power and also work at a variable switching frequency, which is a source of nonlinear behavior. The switching frequency of the RSC is strongly affected by the shaft velocity, which is primarily due to the power slope that depends on the rotor velocity. The variable switching frequency may also output larger amounts of acoustic

noise of variable intensity, a non-uniform allocation of switching havoc for each semiconductor switch in the power inverter and currents that have inconsistent harmonic consist [90,91]. The harmonic in stator currents complexly the purpose of an AC filter with ability of suction a large range of frequency components, as well complexly the heat-sink design. Thus, a number of researchers have investigated DPC and DTC techniques for a DFIG to minimize the output ripple and save RSC switching fixed [90-92]. These include the use of space vector modulation (SVM) [90-93], a discrete vector modulation mechanism (DSVM) [94,95], a predictive DPC (PDPC) diagram [96-97], and slip-mode control (SMC) [90]. Fuzzy logic has been used in DPC for a DFIG by replacing the hysteresis-dependent controller and traditional switching table with fuzzy controllers [95,96]. These contributions have given rise to improvements in DPC performance, but at the same time have led to the development of more complicated schemes. In [90], the required rotor voltage vectors are calculated using a fixed period and space vector modulation. This process adds a fixed switching frequency feature to the DPC system, calculating duty ration of each voltage vector in each specimen time raise the mathematical calculations. In the DSVM process [94], the three rotor voltage vectors used in the switching period are chosen based on a modified search table and a five-level hysteresis comparator. In model-dependent PDPC, using a fixed period of time, three series of rotor voltage vectors are injected to the rotor coils. These vectors are selected depending on the reduced cost functions of active and reactive power errors. The major disadvantages of PDPC are difficulties in online calculation from the microprocessor's point of view and the complexity of control.

In [100], the enforcement of an SMC strategy for a DPC drive was suggested. In an SMC strategy, the controller is designed by choosing a suitable quadratic Lyapunov function to supply the RSC output voltage references as an input to SVM.

3.6 Multilevel Converter Topologies

In the late 19th century, Baker and Bannister presented the initial concept of multiple-level converters [101]. Topologies for multi-level converters have been achieved by connecting single-phase inverters in series. Discrete sources (DC) have been utilized in setting up a topology, with a multilevel voltage at the output.

Traditional systems contain a two-level converter topology. In this topology, the converter links the positive or negative DC link voltage in a three-level converter topology. Just an additional neutral voltage has been looking at the result. The signal on the AC side of the two- or three-level converter is a series of pulses comprising the desired frequency and upper harmonic signals, which can be eliminated by suitable filters. Multiple-level converters aggregate the minimal voltage steps using a sine method at the AC terminals of the output, which are acquired either from capacitors or discrete DC sources. As the number of voltage levels is increased on the AC side, the generated voltage waveform starts to resemble a sinusoid. The output voltage harmonic discoloring of the multiple-level converters is lower than that of the two- or the three-level converters, which is the main advantage of multiple-level converters. Further features of multilevel converters include the following:

- A multiple-level topology can readily be expanded to broad power and voltage levels simply by increasing the series associated with the submodule number.
- Due to the forward output waveform, voltage alteration velocity, the mean DV/DT average is small, and this also reduces the problem of electromagnetic compatibility.
- A multiple-level topology has the ability to switch at low frequencies (until the fundamental frequency is reached). In this way, the switching losses per switching device reduction and semiconductor thermal administration are handled more easily.

Multi-level converters in case input deformity and output joint-mode voltage are minimal in comparison with the lower two- or three-level converters.

- The multi-level topology is comparatively separate from the variable state of the appliance art of semiconductor. They can be made up to utilize standard and proven semiconductor devices.
- In a traditional two-level converter topology, a number of semiconductors are connected in series and operate simultaneously. A lateness of operation between

one of them causes failure in the converter. However, in a multilevel converter topology, the voltage classification of semiconductors is restricted via the voltage level stride size, can be used singly semiconductor. Therefore, the failure average of multi-level converters is minimized.

However, there are several disadvantages of multi-level converters, as follows:

- There is a high initial cost, since multi-level converters depend on a larger number of semiconductors and circuit components.
- Multi-level converters have complex structures, meaning that switching and control are more difficult than in a two-level converter topology.

3.7 Classification of Topologies in the Multiple-Level Converter

3.7.1 Diode-Clamped (Neutral-Point-Clamped) Multi-Level Converter

In 1981, a diode-clamped multilevel converter was proposed [102], and in the 1990s, numerous papers were published covering level diode-clamped multiple-level converters for the compensation of static VAR.

A diode-clamped converter incorporates (n-1) capacitors on the DC bus and generates (2n-1) levels of output line voltage and n levels of phase voltage. Additional characteristics include [103, 104]:

- A high voltage classification should be selected for blocking diodes.
- Device classification is difficult due to the different current valuated of devices.
- The output waveform can give a better harmonic content when compared with a two-level converter.
- Problems may arise from an unbalanced capacitor voltage.
- When it is necessary to increase the number of clamping diodes, the situation becomes more complicated.

We used a diode-clamped multilevel converter system (the 36 MW ± 15.9 kV Eagle Pass) back-to-back HVDC light, installed in September 2000, which allows the exchange of power between different stations [105].

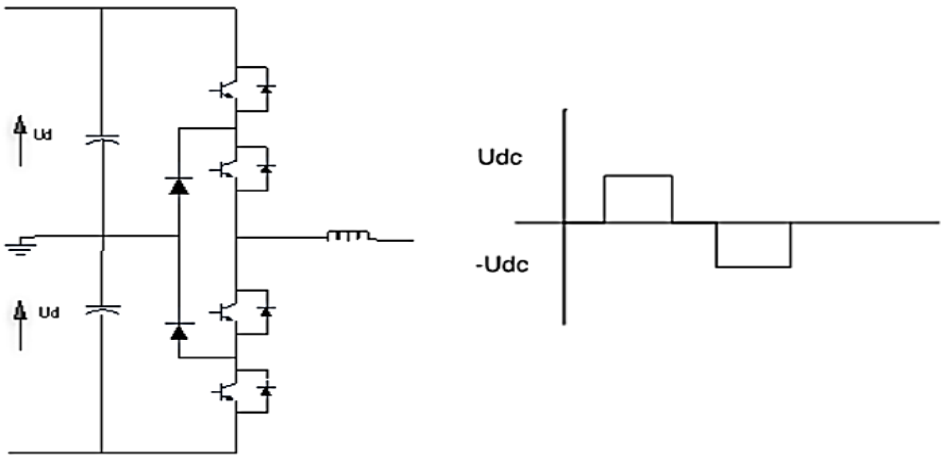

Figure 3. 9 Three-level, three-phase VSC [106]

3.7.2 Flying Capacitor (Capacitor-Clamped) Multi-level Converter

In 1992, Meynard and Foch proposed the flying capacitor multi-level converter [107]. In this topology, capacitors are used for clamping. This topology provides a much more flexible approach in which various switching combinations can result in identical voltage levels. A comparison of the capacitor-clamped converter with the diode-clamped converter shows that the former consists of a large number of 'floating' capacitors; when the number of levels increases, the number of capacitors also increases. The use of high numbers of capacitors provides ride-through capability during outages, but this topology increases the cost and means that control becomes more complex. This topology has been used in many motor drive applications. In a capacitor-clamped converter topology, the voltage synthesis has more flexibility than in a diode-clamped converter, but this topology has a disadvantage due to an irregular duty problem from the switches. Figure 3.5 illustrates a single phase, three-level capacitor-clamped converter [104, 108].

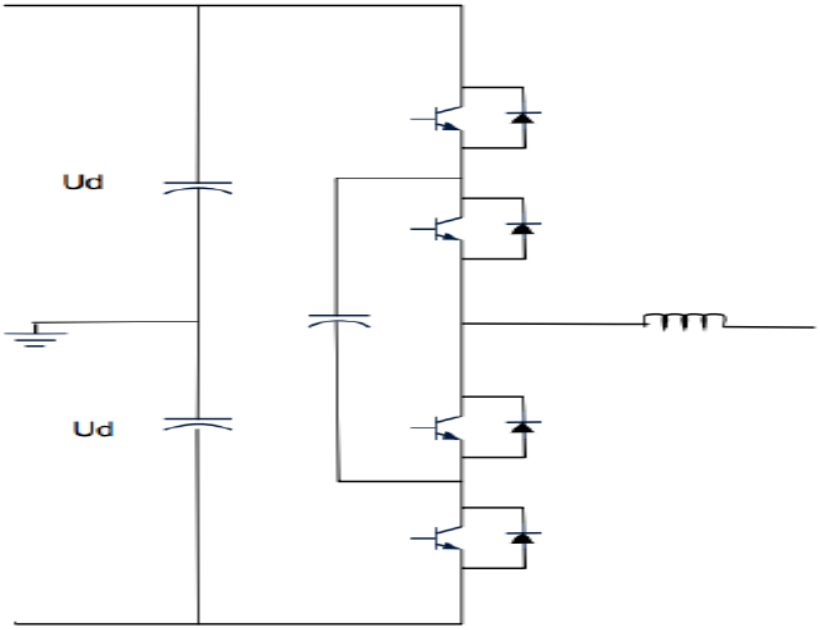

Figure 3.10 The capacitor-clamped or flying capacitor converter [106]

3.7.3 Cascaded Multi-Level Converter

A cascaded H-bridge topology can be implemented in an VSC-based multi-level converter in which each H-bridge module requires a separate DC power supply. A single H-bridge structure can generate three voltage levels: 0, $+U_{dc}$ and $-U_{dc}$. A sequence of these bridges results in a staircase output, a waveform in which each step matches each single bridge. In order to obtain higher levels of the output waveform, more H-bridges should be connected. Generally, this case (for an n-level converter) requires 1/2(n−1) H-bridges per phase. The main advantage of this topology is that it needs a lower number of elements in comparison to other topologies for the same voltage level.

It also has a modularized circuit layout and does not require more clamping capacitors or diodes. The disadvantage of this topology is the need for separate DC sources, which makes the design difficult for higher levels. Figure 3.6 shows a single-phase cascaded H-bridge structure [109].

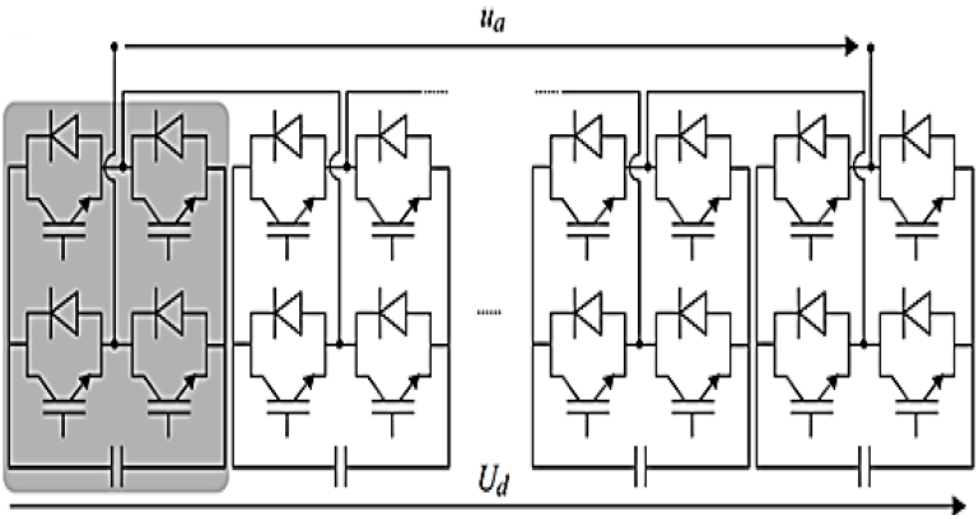

Figure 3.11 Single-phase cascaded H-bridge structure [106]

3.7.4 Modular Multilevel Converter

The MMC topology was first proposed by Lesnicar and Marquardt in 2003 [110]. Numerous researchers have studied multi-level converters, and they have become one of the most attractive topologies, particularly for high-power implementation transmission systems (VSC-HVDC), STATCOM applications, medium-voltage motor drives and renewable energy. The linkage of systems to the network is the typical enforcement areas of MMC. The figure below shows the details (submodule, arm) of a typical converter arrangement for an MMC.

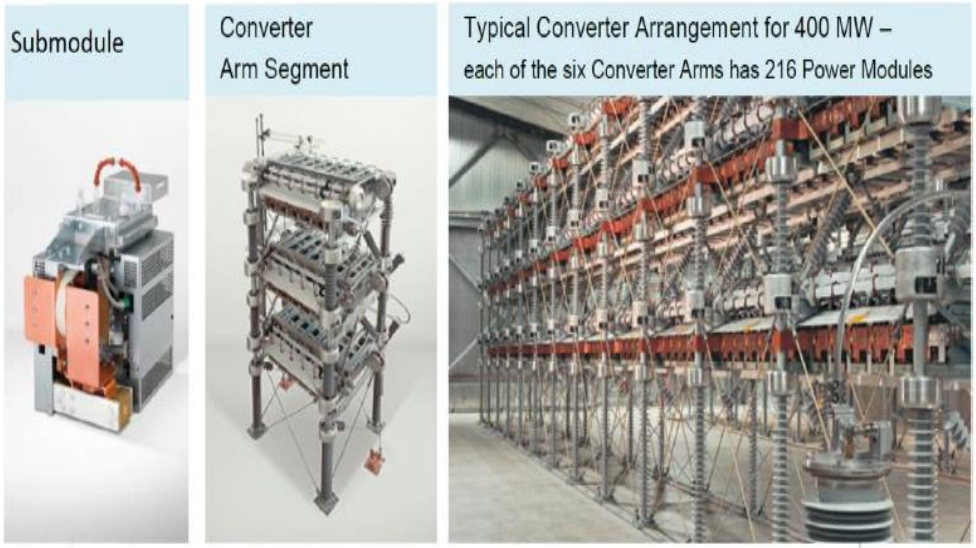

Figure 3.12 Submodule, arm and typical converter arrangement for an MMC by Siemens [106]

This topology is based on VSC and is known as an MMC. It contains a common DC link and does not require DC link capacitors. This topology can be used to directly control the DC link voltage during the switching states of the submodules (SMs), meaning that no separate DC power supply is necessary as in a cascaded H-bridge topology. The main structure of this topology is less complicated than the cascaded H-bridge structure. Each cell consists of two switches: a main and an auxiliary switch. The output voltages are achieved from a single structure. An MMC can generate zero and $+U_{dc}$ voltage levels, but not $-U_{dc}$ as in the cascaded H-bridge.

In the zero level case, the capacitors charge or discharge based upon the trend of the load current, and subsequently a slight imbalance is formed. The capacitor voltages can be controlled during the process of controlling the switching-in of the different cells in all the zero voltage output.

The arm inductances offer a way for the circulating currents during the balancing process straight with lower input currents. In the MMC topology, the modular nature grants, interest as high levels and thus it can obtain higher voltages by during putting cells together. In the case where a high number of SMs are used, the MMC does not require filters, which is a great advantage when compared to other multi-level converters. Figure 3.7 illustrates the structure of an MMC [109, 104].

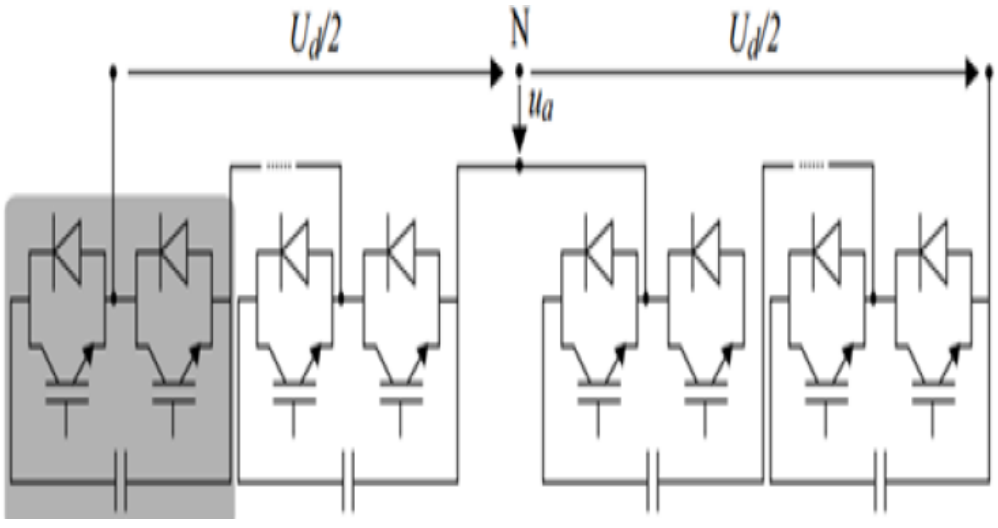

Figure 3.13 Structure of a modular multilevel converter [106]

3.8 Structure of a Modular Multilevel Converter

3.8.1 Introduction

An MMC consists of a set of elements called submodules (SMs). Figure 3.8(a) shows these SMs. The series of linked SMs in each phase is called a leg, and each leg is divided into upper and lower arms; the number of SMs in each arm is the same. The capacitors in the leg are connected to a regular DC link voltage, and it is not necessary to use the large capacitors that are required in two-level or NPC topologies. However, inductors are integrated within the arms to minimize transient currents [107]. Numerous SM topologies can be used. The main reason for this variation in cell structure is that it can lead to many possible voltage levels on the SM station. However, when the number of elements is increased, capacitor balancing becomes more difficult. In experimental studies, losses are due to switching and the capacitor voltage balancing problem. The half-bridge (HB) topology is generally the most appropriate, as it efficiently utilizes the SMs in cases where bidirectional energy conversion is necessary [112]. The SM topology is composed of an HB containing two bi-directional power electronic switches of the IGBT type with a capacitor parallel to the switches, as shown in the figure below.

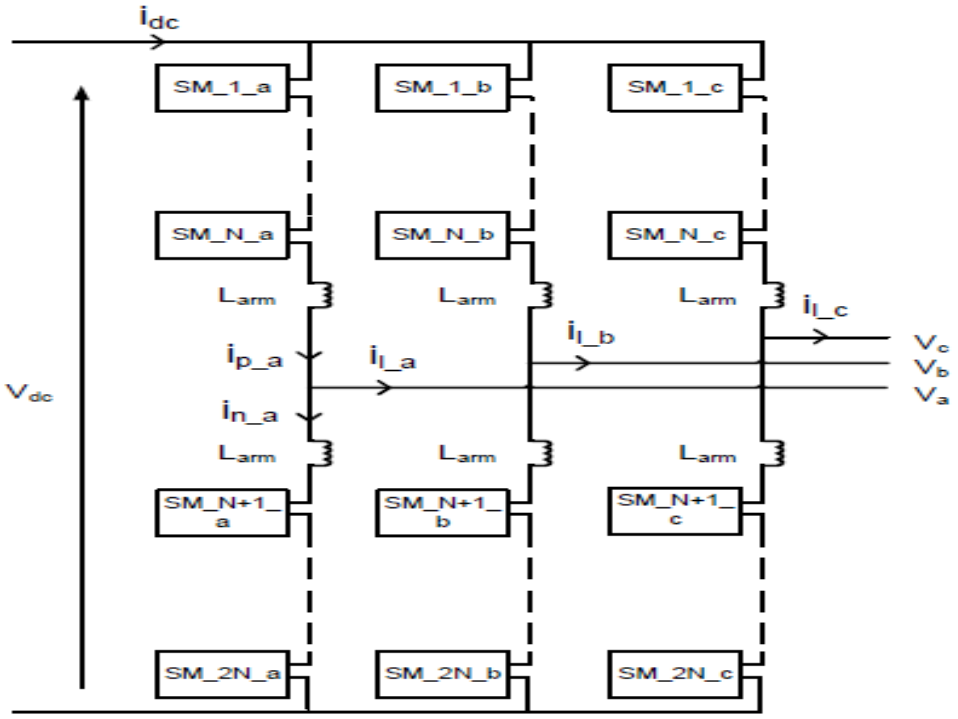

Figure 3.14 The basic components of an MMC [106]

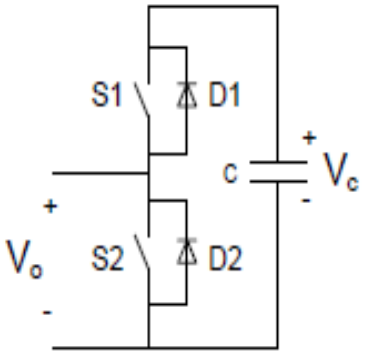

Figure 3.15 A half-bridge sub-module for an MMC [106]

The capacitors act as as voltage sources and power dielectrics. In the case of the SM, the switches include parallel diodes and the arm circuit and ensure that current constantly flows. A possible layout of the current trajectory and a HB SM are shown in Figure 3.9 [113]. In all cases, only one switch in the HB circuit can be in the ON state. If S1 is in the ON state and S2 is OFF, the HB circuit is in the ON state in this case; otherwise, when S2 is ON and S2 is OFF, then we can say that the HB circuit is ON (bypassed) or OFF (switched). The voltage on both sides of the HB circuits is the same as the voltage across the secondary capacitor Vc if switched ON/entrance, or zero if switched OFF/bypassed. If both keys are ON, then the SM capacitor is short-circuited. If both keys are OFF, the voltage on both sides of the SM is unbounded and in the direction of the current, and the voltages on each side vary. Depending on the state of the HB circuit and the direction of the SM current, the secondary capacitor is either charged or discharged. For each combination of switching states discussed above, the voltages on both sides of the HB and the capacitor charge/discharge state are shown in the table below.

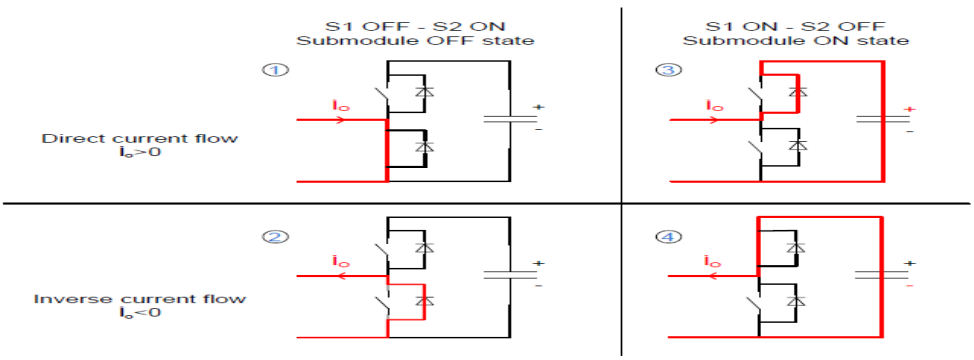

Figure 3.16 States of the half-bridge (chopper) circuit and current paths [106]

Table 3.1 Switching states for a half-bridge circuit

State number in Figure 2.9	S_2	S_1	V_o	Current direction	Current path	Capacitor charge
1	1	0	0	$i_o>0$	S_2	-
2	1	0	0	$i_o<0$	D_2	-
3	0	1	V_c	$i_o>0$	D_1	Charge
4	0	1	V_c	$i_o<0$	S_1	Discharge

In this topology, the MMC of the DC link energy is not stored in a single large capacitor, as in the situation of traditional VCs, but is distributed among the SM capacitors. In order to avoid additional currents within the converter that result from the voltage imbalance, the energy values of the capacitors in the converter should be maintained in a stable state as far as possible. It is assumed here that all the capacitors are uniformly and equally charged. In the fixed state, in the open-loop process of the converter between the 2N SMs in a phase leg, N of these for the input to the current route. Hence, the natural rate voltage of the SM capacitors V_C can be expressed in the following form:

$$V_c = \frac{V_{dc}}{N} \tag{3.3}$$

Modification of the number of entrance SMs in the leg is the reason for an imbalance between the DC exporter and the phase leg, meaning that the internal circulating currents can charge and discharge the capacitors in the SMs. It is therefore important to note that this situation is valid for the open loop process of the converter and is a natural balance poin

3.8.2 Mathematical Model of the MMC

The three-phase MMC consists of a total of 2N series-linked switching cells or SMs that form a phase leg [114], as shown in the figure below.

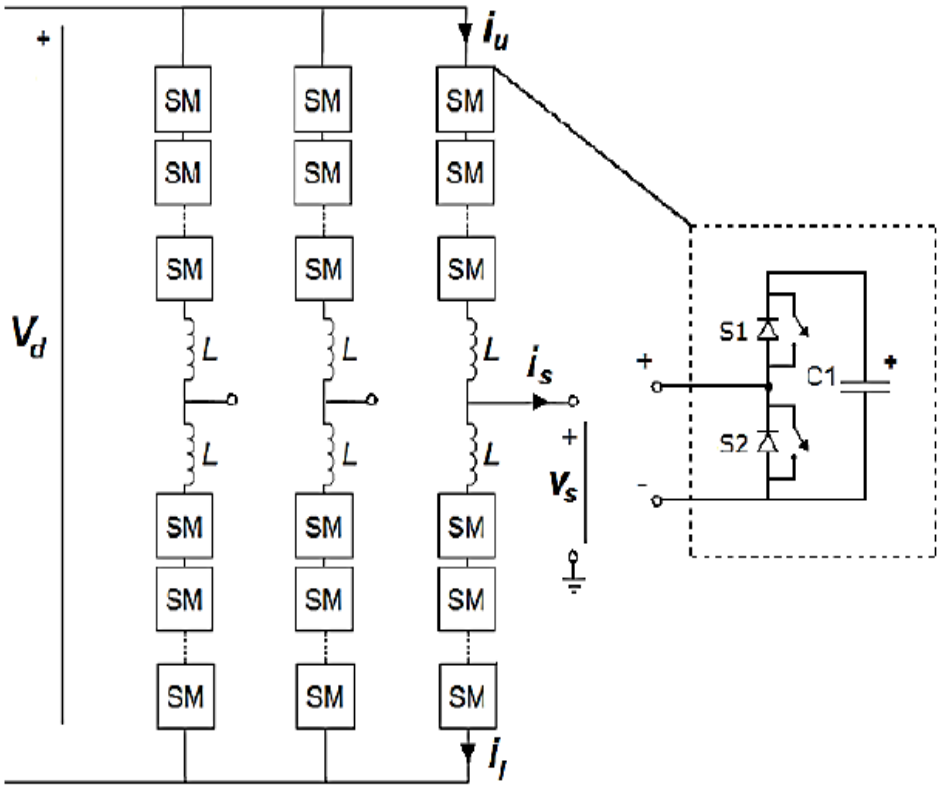

Figure 3.16 Structure of an MMC circuit [106]

In the phase leg, SMs are isolated in the upper and lower arms, with one inductor per arm or each single coupled inductor. The SM switches are controlled using a method in which at any instant, the SM is either linked or bypassed to the arm. Each of the arms in the converter is acting as a controlled voltage exporter with a voltage range varying from zero to V_{dc}. The arm voltage is determined by the switching state of the SM of the arm, which can be calculated by Equation (3.1). The current pass during arm composed of two portions, generality current and the load current everywhere the phase-legs in the converter, as shown in Equations (3.2) and (3.3) [115].

$$V_{rm} = \Sigma_{i=1}^{n} s_{sm} * V_{c,sm} + L_{rm} \frac{di_{rm}}{dt} \qquad (3.4)$$

i: is the upper arm current. : is the lower arm current.

i_{ld}: the current cost of half an output (ac side). I_{rc}: circulating current.

I_{rc} consists of the DC link current and the AC currents that are linked to the V_dc ripple in the phase stick and the voltage variation between phase sticks. Depending on Equations (3.2) and (3.3), the common current and the output current can be represented with regard to the currents in the lower and upper arms as in Equations (3.4) and (3.5) [112]:

$$i_p = \frac{i_{ld}}{2} + I_{rc} \tag{3.5}$$

$$i_o = \frac{i_{ld}}{2} - I_{rc} \tag{3.6}$$

This is an equation for the voltage in the upper and lower arms beside the circulating voltage.

The combined voltages in the arm should be equal to the DC link voltage and the voltage should be regularly distributed between the SMs in the lower and upper arms as well as in the phase leg. Additionally, when the SM is linked inside the arm, the load current passing through from the capacitor produces a ripple in the SM voltage. The active power (P_{ac}) and reactive power (Q_{rc}) of the three-phase system can be calculated using Equations (3.9) and (3.10) as follows [116]:

$$I_{rc} = \frac{i_p = i_o}{2} \tag{3.7}$$

$$i_{ld} = i_p - i_o \tag{3.8}$$

where L1, L2, L3 are the currents in legs 1, 2 and 3, respectively; and V1, V2, V3 are the voltages in legs 1, 2 and 3, respectively.

3.8.3 MMC Switching Modulation

3.8.3.1 Introduction

Switching operation in MMCs is of two types: low-frequency and high frequency switching. In low-frequency switching, the calculated pulse model is used to drive the converter, and a harmonic elimination process can be utilized to make the performance of the converter more effective. These techniques use lower switching materials, but can give high efficiency. However, their strength depends on the dynamic response. Usually, these techniques subject to the low-voltage results and the current waveform harmonic deformation can be a converter, to need smaller and minimize cost, negative filters and with a rapid dynamic response to alterations in the source or load. Although the high-frequency switching process tends to have higher switching computation (which implies higher switching losses) than low-frequency switching, these losses can be reduced with a suitable design, and the main drawback of high-frequency switching can be overcome. A third form of switching, combined switching, can be added to maximize the benefits of the two processes above. This process takes advantage of both high-frequency and low-frequency switching. The figure below shows the switching process for an MMC.

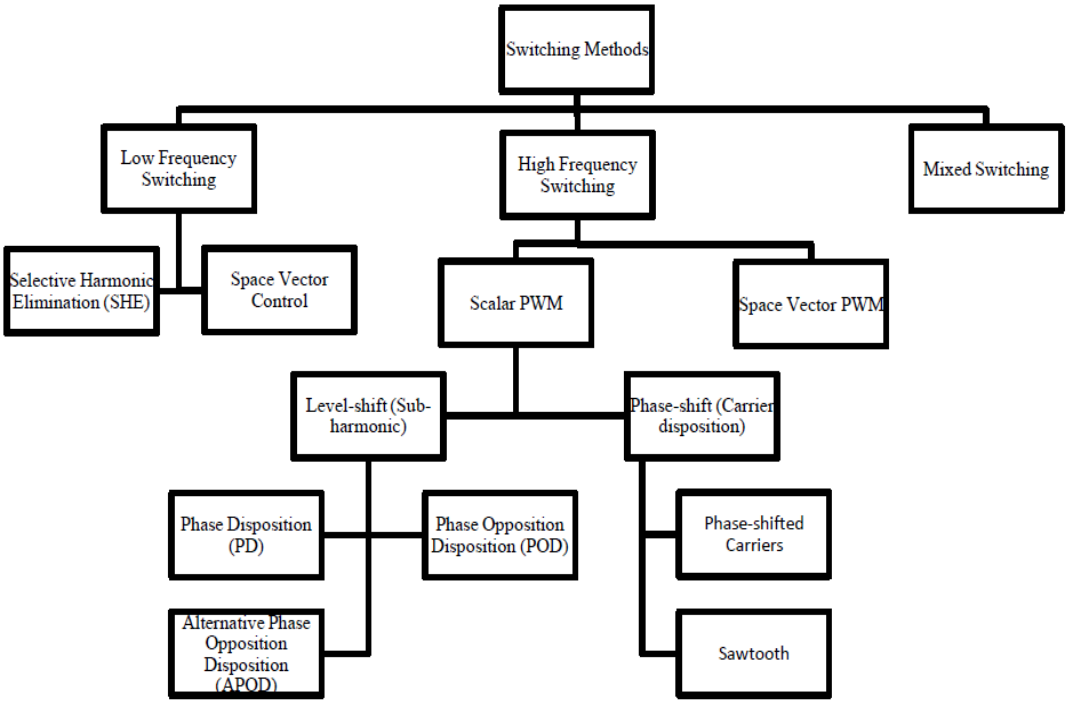

Figure 3.18 Switching methods for modular multilevel converters [106]

3.9 High-Frequency (Carrier-Based) Switching

Designers of MMCs often use the high-frequency switching method, as it is easy and gives satisfactory performance when implemented. The carrier frequency in high-frequency switching is fixed, and in each switching time, output voltage that implies values and reference are made similarly. For this purpose, a standard or space vector technique can be utilized. The standard technique uses a reference (modulation) waveform with the required high-frequency carrier waveform, magnitude of the output voltage and frequency. The carrier and volume of reference are compared and at the moving points, switching takes place. The space vector method, on the other hand, creates a vector graph in space for all switching conditions of the transformer, and the output signal is represented by a vector. In order to obtain the required output voltage, the converter is driven by the related switching pulse pattern created based on the signal vector and the switching case vectors. The implementation of scalar techniques is more straightforward, although both of these techniques can generate an equal switching pulse pattern.

3.9.1 Standard PWM

3.9.1.1 Level-Change (Sub-Harmonic) Methods

These techniques use N similar triangular carriers relayed continuously in V_{dc} (the DC-link voltage). Because supply a balanced exploitation of circuit elements that generate various voltage levels, the peak-to-peak amplitudes of the carriers are set similarly in each one, V_{dc}/N, which is a necessary but insufficient condition. They have a frequency of F_c. Carriers do not ford. Based on the phase-shift of carriers with clings to each other, level-shift techniques can be divided into three sub-methods:

i) Phase disposition (PD)

ii) Phase opposition disposition (POD)

iii) Alternative phase opposition disposition (APOD)

i) Phase Disposition

In the PD technique, all the carriers are in phase. To illustrate this using an MMC with four SMs in each phase arm, the carriers in the PD technique are dislodged in the V_{dc} band. This situation is illustrated in the figure below.

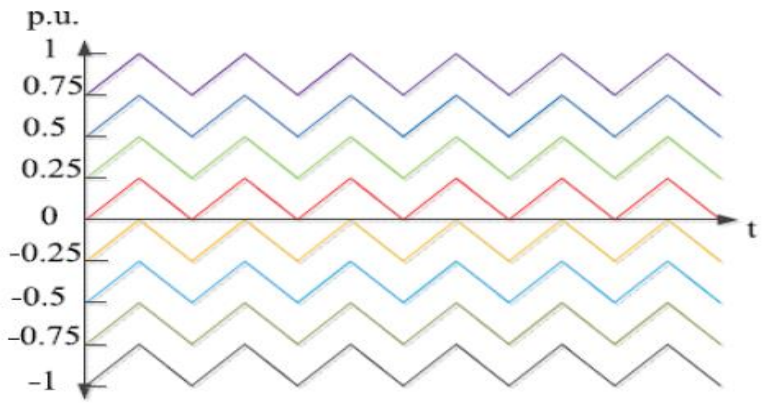

Figure 3.19 The phase disposition method [106]

ii) Phase Opposition Disposition

In the POD technique, the carriers overhead the zero axes, and below the zero axes are 180° out of phase. The MMC has four SMs per phase arm in the POD technique, and these are dislodged in the V_{dc} band. This situation is shown in the figure below.

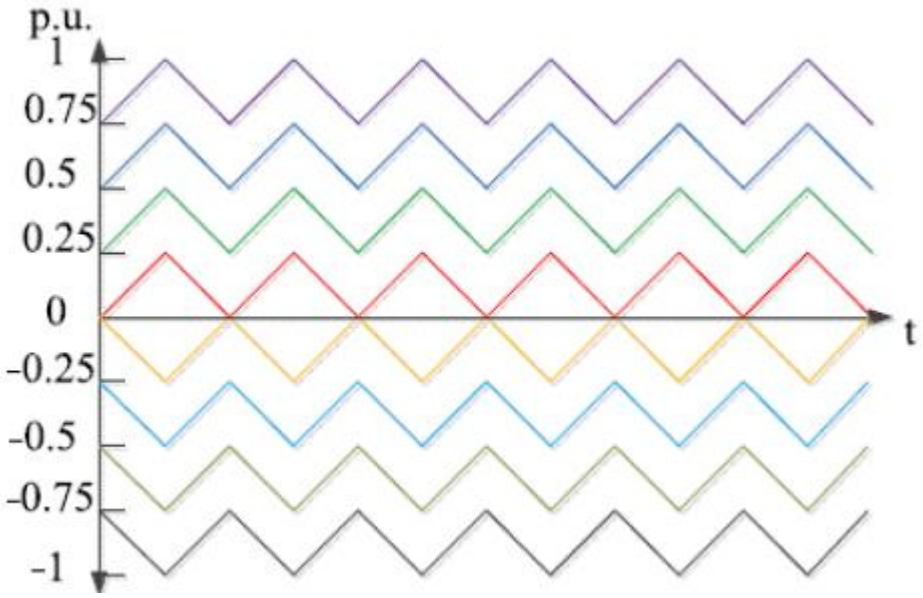

Figure 3.20 The phase opposition disposition method [106]

iii) Alternative Phase Opposition Disposition

In the APOD technique, persistent carriers are 180° out of phase. The MMC has four SMs per phase arm in the APOD technique is dislodged in the V_{dc} band. This situation is illustrated in the figure below.

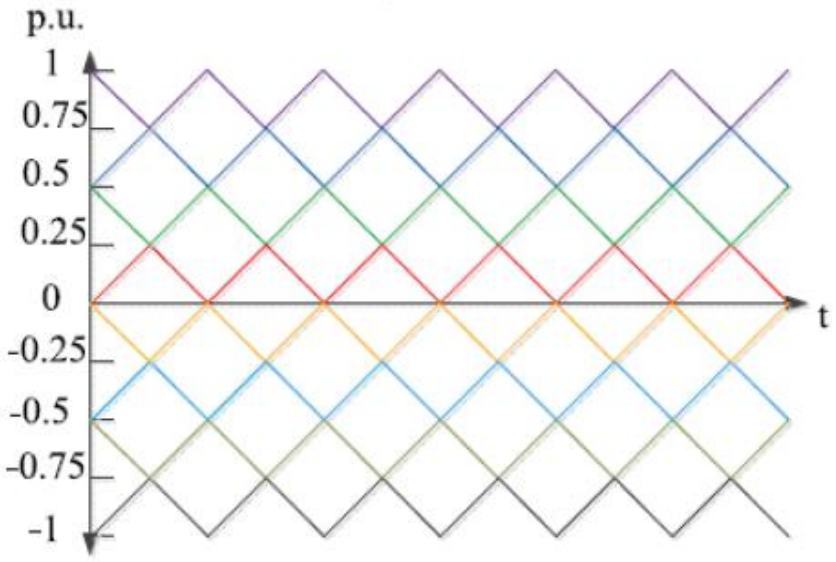

Figure 3.21 The alternative phase opposition disposition method [106]

3.9.1.2 Phase-Shift (Carrier Disposition)

Again, this technique requires N similar triangular carriers being dislodged with a phase shift of 360°/N among each other in the whole DC link voltage (V_{dc}). The carriers have a frequency of F_c and a peak-to-peak amplitude of V_{dc}. Transporters passed one to other. For a MMC with four SMs in each phase arm (N=4), the transporters in the phase-shift technique are dislodged in the V_{dc} band, as shown in the figure below.

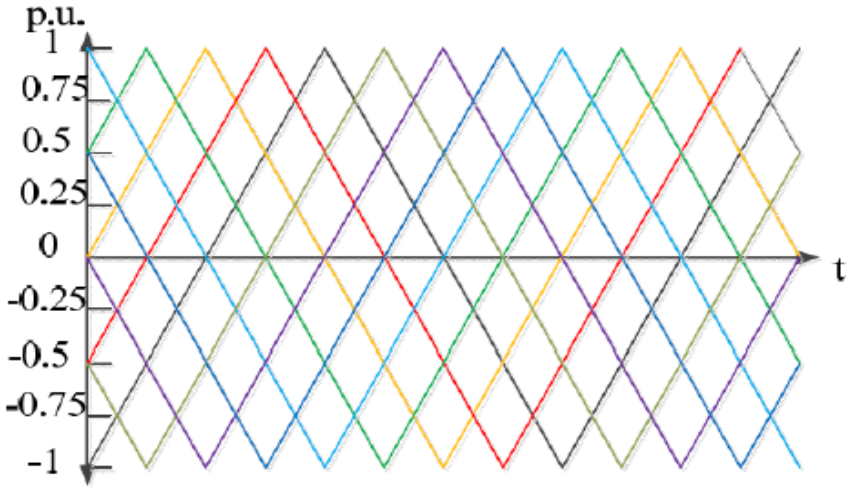

Figure 3.22 The phase-shifted carrier method [106]

In the literature, there are other phase-shift techniques in which the transporters are similar to those shown in Figure 4.5, but these are sawtooth waveforms rather than triangular. This technique is called "sawtooth rotation". For convenience, carriers in

sawtooth rotation technique for a MMC have four SMs per phase arm (N=4) as shown in Figure 4.6 below.

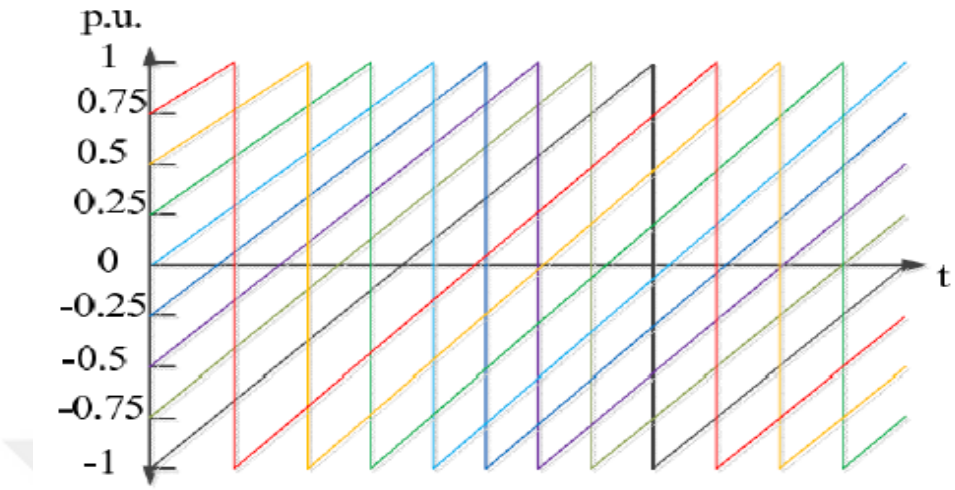

Figure 3.23 The sawtooth rotation method [106]

3.9.2 Space Vector Pulse Width Modulation

In the 1980s, the SVM replacement strategy for classical PWM was proposed [113]. SVM is used to find switching pulse widths, and it has begun to be preferred in recent years, since today's control systems involve digital applications. The SVM strategy creates a vector diagram in space for all converter switching cases and the output signal is represented by a vector. To obtain the required output voltage, the converter is driven during the regarding switching pulse pattern produced depending on the signal vector besides the switching case vectors. For an n-level converter, there is n3 switching collection, which performs eight collections for a two-level converter. Two of these collections are zero states, since they short-circuit the AC side of the converter. The other collections are fixed vectors, meaning that any arbitrary output vector can be produced from the fixed vectors SV-1 to SV-6. Figure 3.19 shows a diagram for two-level modulation. For a three-level converter, the magnitude of the SV is 27 [108].

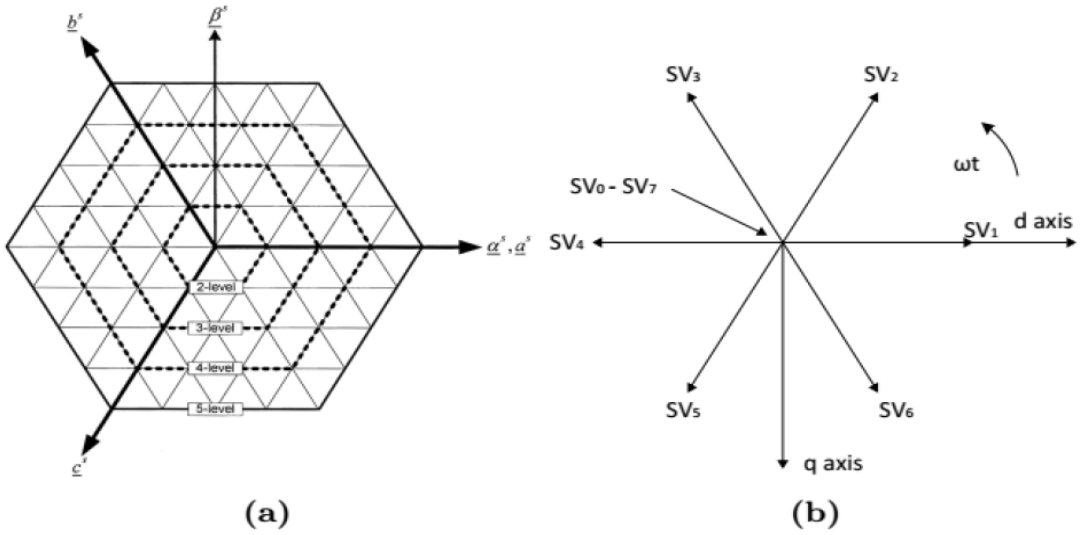

Figure 3.24 The space vector diagram: a) five-level structure; b) two-level SVM [106]

So that each switching state conforms to an SV, the demand output is controlled by the duty turning for each SV. The SVM and carrier-based scalar PWM techniques can create identical switching pulse patterns, although the application of the scalar PWM technique is simpler [118].

3.9.3 Carrier Sets and Numbers of Output Voltage Levels

In a traditional two- or three-level converter, the level of the output voltage is constant. This is not the case for an MMC. An MMC converter with N SMs per arm can give 2N+1 or N+1 output phase-neutral voltage levels. In practice, the case is based on upon the carrier sets used for lower and upper phase arm switching two essential scalars, PWM technique, means phase and level shift are usually used. Each technique uses a total of N carriers to form a carrier set. High and low switching for MMC arms is done either via two varying carrier sets, or using the same carrier set in which there is a definable phase variation between carriers. The switching technique, only utilizing one set or two or most carrier sets for low and high arms leads to N+1 or 2N+1 phase-to-neutral voltage levels at the converter output [108].

3.9.3.1 Level Phase Voltages for (2N+1) (N+1) Level-Shift Methods

i) Phase Disposition Method

The PD technique (with N+1 levels) needs to be carried out using two different carrier sets for the lower and upper arms, which can form the voltage of the phase. In the first, the carrier set is modulated in the same way as shown in the figure below. The second set of carriers has an additional N similar carriers with an amplitude of V_{dc}/N and dislodged contiguously in the V_{dc} band, from zero to V_{dc}. However, this carrier set has a phase difference of π radians relative to the first carrier set. The SMs in the lower and upper arms switch with both the first and second carrier sets. In this case, the output phase voltage has (N+1) levels. Figure 2.20 shows the case of the PD technique for a phase leg with four SMs. The converter equal switching frequency f_{ceq} is equal to the frequency of the level-shifted carriers, as shown in Equation 3.9 below [106]:

$$f_{ceq} = f_c \tag{3.9}$$

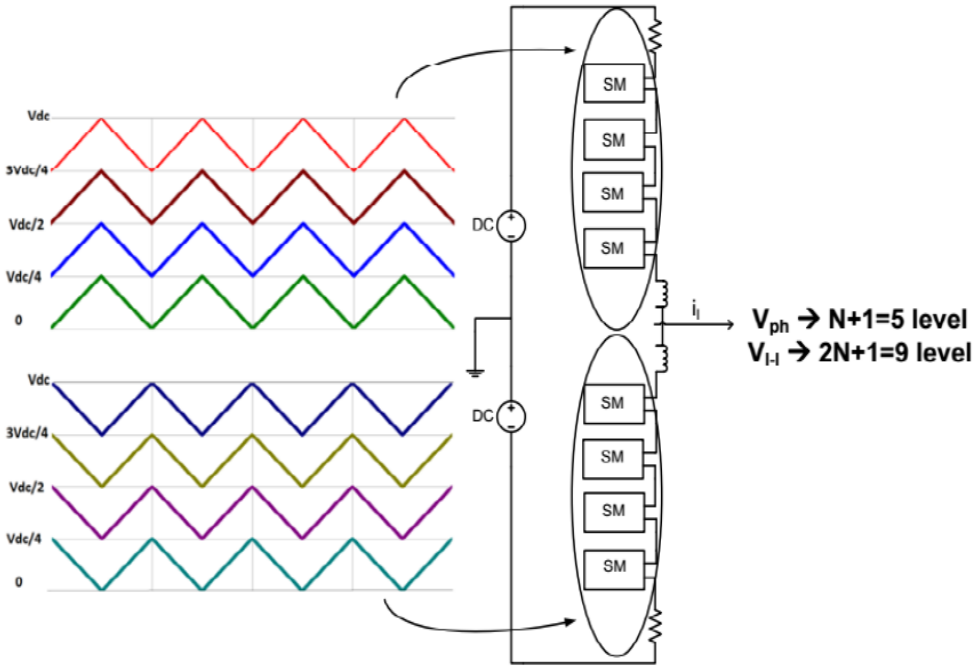

Figure 3.25 Carrier sets for the phase disposition method for the case with (N+1) phase voltage levels [106]

The PD technique with (2N+1) levels requires a single carrier group since the lower and upper arms can form the phase voltage. ON the first, the carrier set is modulated

in an identical way, as shown in the figure below. The SM in the lower and upper arms is transported through this carrier group. In this case, the output phase voltage will have (2N+1) levels. Figure 3.21 shows the case for the PD technique for a phase leg with four SMs. The converter equal switching frequency f_{ceq} is equal to twice the frequency of the level-shifted carriers, as shown in the Base below 3.16 [106]:

$$f_{ceq} = 2 * f_c \tag{3.10}$$

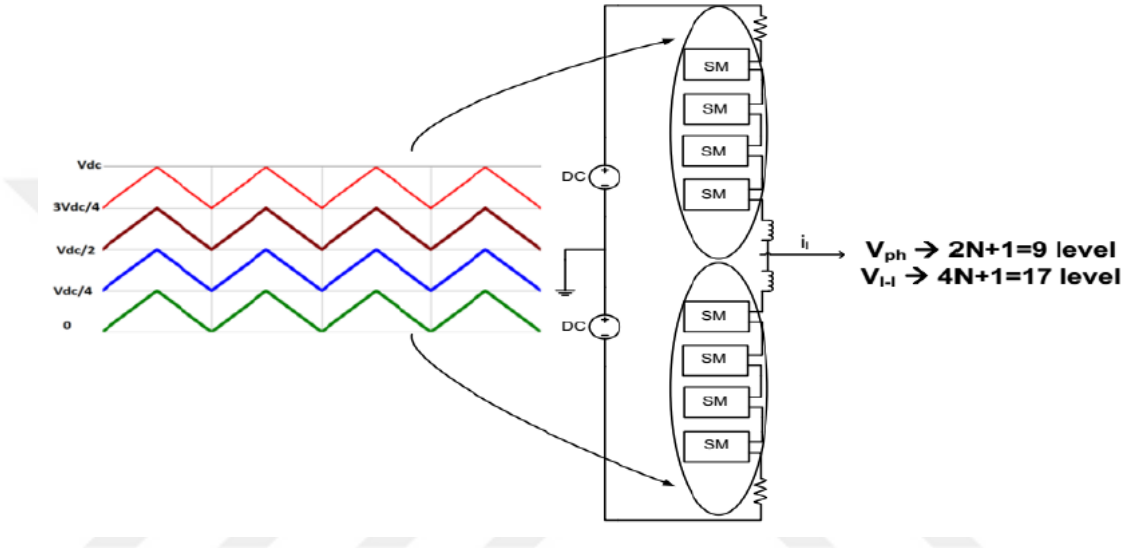

Figure 3.26 Carrier set for the phase disposition method for 2N+1 phase voltage levels [106]

ii) Phase Opposition Disposition Method

In the POD technique (N+1 levels), a single carrier group is used since the lower and upper arms can form the phase voltage. On the first, the carrier group is modulated in the same way as explained in Section 2.4.3.3. The SM in the lower and upper arms is switched with this carrier set. In this situation, the output phase voltage has (N+1) levels. Figure 3.22 illustrates the POD technique for a phase leg with four SMs. The equal switching frequency of the converter, f_{ceq}, is equal to the frequency with the level phase carriers as shown .

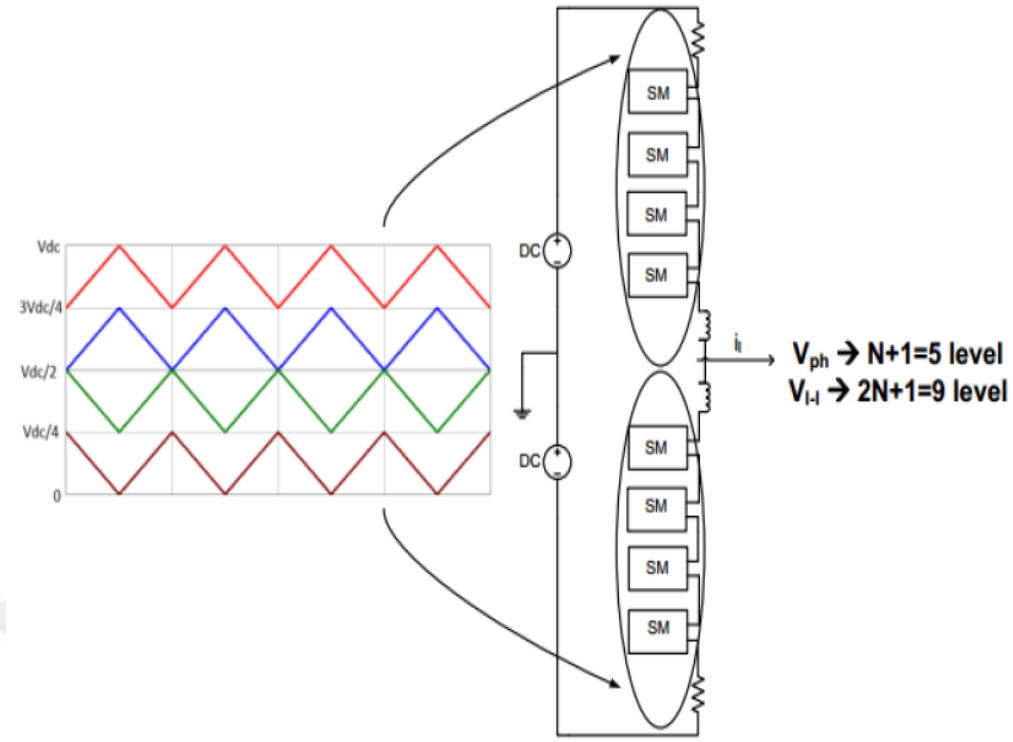

Figure 3.27 Carrier set for the phase opposition disposition method for (N+1) phase voltage levels [106]

In the POD method (2N+1 levels), the needs to be performed through two different carrier groups for lower and upper arms are able to form the phase voltage. The first carrier set is modulated in the same way as described in Section 2.4.3.3. The second set of carriers has an additional N identical carriers with amplitude V_{dc}/N and dislodge contiguously in the V_{dc} band, from zero to V_{dc}; however, this carrier set has a phase difference of π radians relative to the first carrier set. The SMs in the lower and upper arms switch with the first and second carrier sets. In this situation, the output phase voltage has (2N+1) levels. Figure 3.23 shows the PD technique for a phase leg with four SMs. The converter equal switching frequency f_{ceq} is equal to the frequency with the level-shifted carriers, as shown .

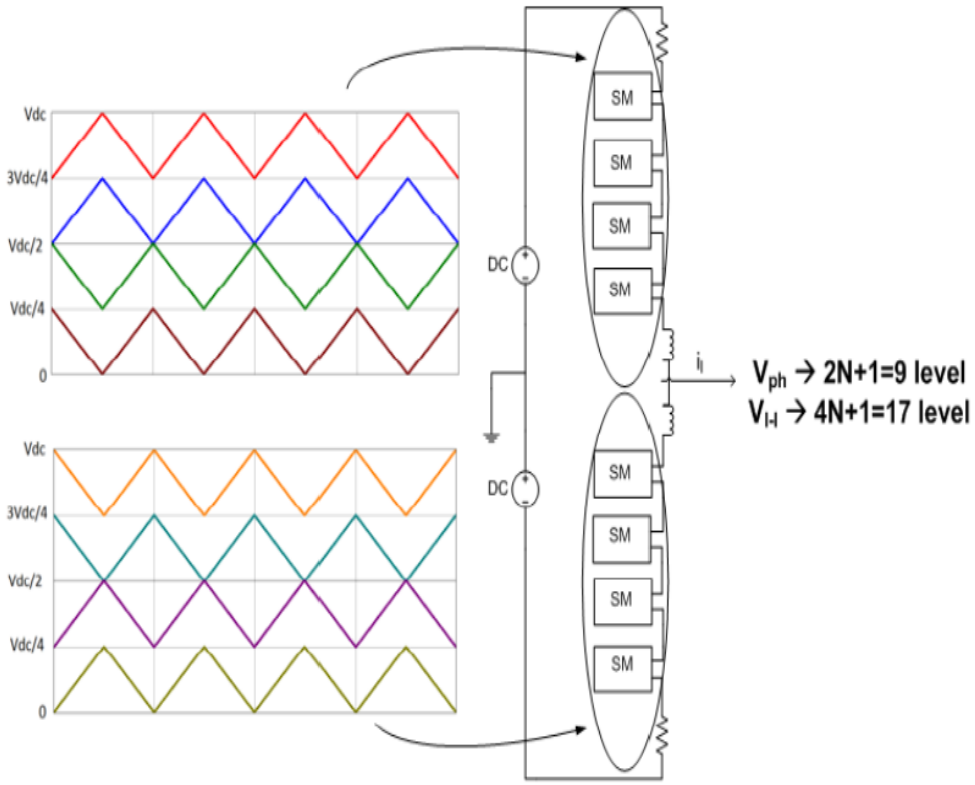

Figure 3.28 Carrier sets for the phase opposition disposition method for 2N+1 levels of phase voltage [106]

iii) Alternative phase Opposition Disposition Method

The APOD technique (N+1 levels) requires a single carrier group for the lower and upper arms to form the phase voltage. The carrier set is modulated in the same way as described in Section 2.4.3.3. The SM in the lower and upper arms is switched with this carrier group. In this situation, there are (N+1) levels of output phase voltage. Figure 3.24 shows the case of the APOD technique for a phase leg with four SMs. The equal switching frequency of the converter f_{ceq} is equal to the frequency with LS carriers as shown .

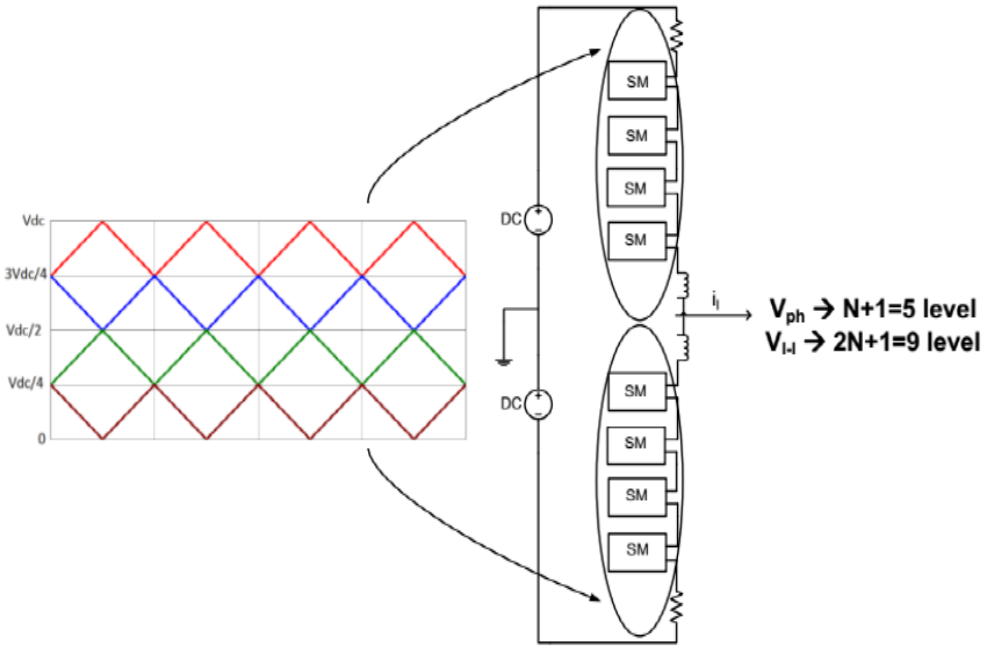

Figure 3.29 Carrier set for N+1 levels of phase voltage in the alternative phase opposition disposition method [106]

The APOD technique (2N+1 levels) requires two different carrier groups for the lower and upper arms to form the phase voltage. The first carrier set is modulated in the same way as described in Section 2.4.3.3. The second set of carriers has once most N similar carriers along with an amplitude of V_{dc}/N and dislodge contiguously in the V_{dc} band, from zero to V_{dc}. However, this carrier group has a phase difference of π radians relative to the first carrier set. The SMs in the lower and upper arms switch with the first and second carrier sets. In this case, the output phase voltage will have (2N+1) levels. Figure 3.25 shows the case for the APOD technique for a phase leg with four SMs. The equal switching frequency of the converter f_{ceq} is equal to the frequency with the level-shifted carriers, as shown [106].

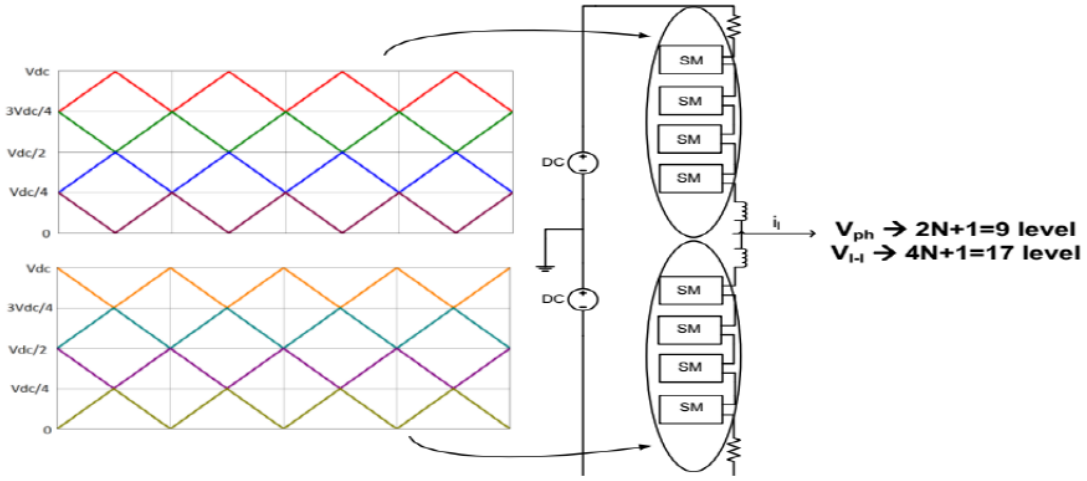

Figure 3.30 Carrier set for the alternative phase opposition disposition method for 2N+1 levels of phase voltage [106]

3.9.3.2 Level Phase Voltages for (N+1) (2N+1) Phase-Shift Methods

i) (N+1) Phase-Shift Methods

In the phase-shift technique, carrier groups are modulated depending on whether N is even or odd. When N is odd, two different carrier sets are used for the lower and upper arms. The first carrier set is organized in the same way as described in Section 2.4.3.3. The second carrier set is modulated using an identical waveform, but with a phase variation of π/N radians relative to the first group. The SMs in the lower and upper arms are switched using the first and second carrier sets. The output phase voltage of this situation is (N+1) levels. Figure 3.26 shows the case of a phase shift when N is odd (the phase leg has N=3) [20, 51]. When N is even, only one set of carriers can be used for the lower and upper arms. This set of carriers is the same as described in Section 2.4.3.3. The SMs in the lower and upper arms are switched using this carrier set. The output phase voltage for this situation has (N+1) levels. Figure 3.27 illustrates the phase-shift technique in the case when the leg has N=4. In these two situations, the equal switching frequency of the converter f_{ceq} is equal to the number of carriers times the frequency of the PS carriers, as shown in Equation (3.11) [106]:

$$f_{ceq} = N * f_c \tag{3.11}$$

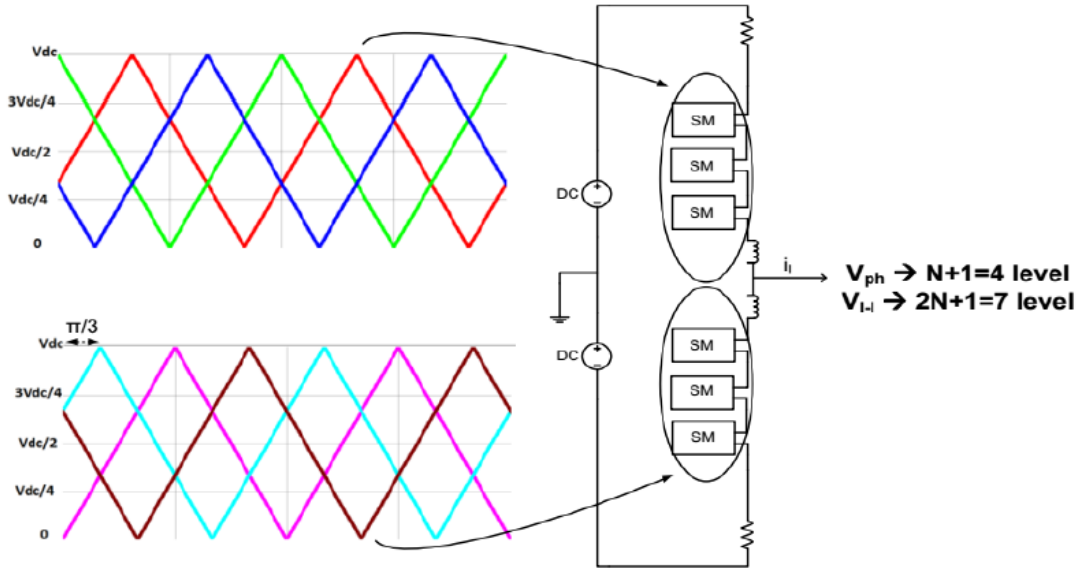

Figure 3.31 Carrier sets for the phase-shift method with (N+1) levels of phase voltage with an odd number of submodules [106]

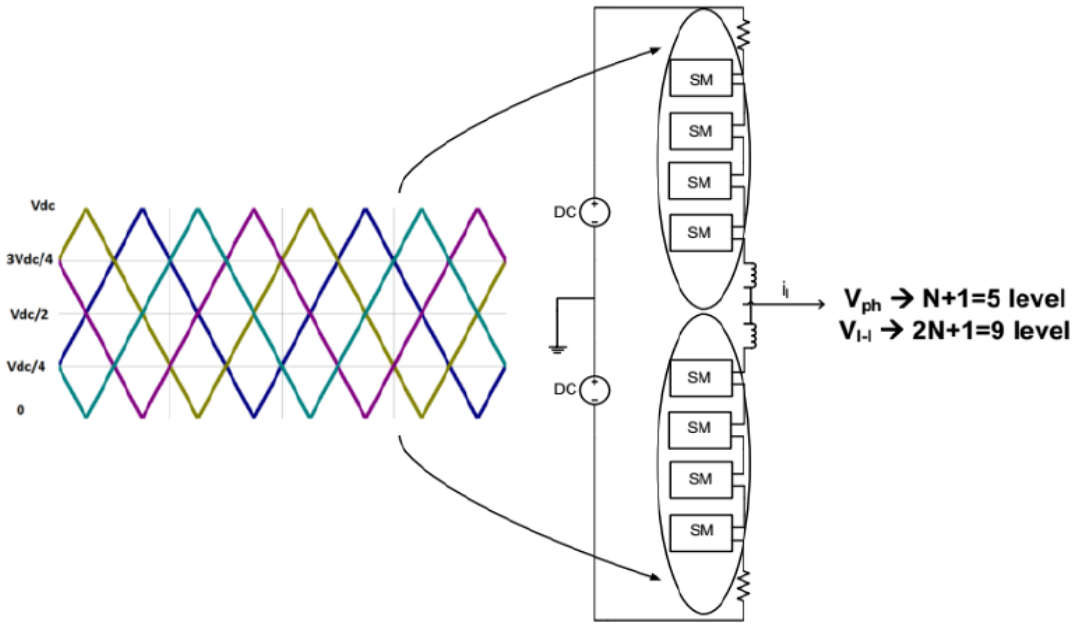

Figure 3.32 Carrier set for the phase-shift method with N+1 levels of phase voltage with an even number of submodules [106]

ii) (2N+1) Phase-Shift Methods

As for the (N+1) phase-shift technique, there are two situations, i.e. odd and even values of N. When N is odd, only one carrier set is used for the lower and upper arms. This carrier set is described in Section 4.2.1.2. The SMs in the lower and upper arms

are switched using this carrier group. The output phase voltage for this situation has (2N+1) levels. Figure 3.27 shows the situation with a phase-shift technique for the situation when the leg has N=3. When N is odd, two different carrier sets are used for the lower and upper arms. The first carrier set is modulated in the same way as described in Section 4.2.1.2. The second carrier set is modulated with an identical waveform, but with a phase difference of π/N radians relative to the first set of SMs in the lower and upper arms, which are switched using the first and second groups of the carrier. The output phase voltage of this situation has (2N+1) levels. Figure 3.29 shows the case of a phase shift when N is even (the phase leg has N=4). For other two situations, the equal switching frequency of the converter $fceq$ is proportional to the number of carriers multiplied by the frequency of the PS carriers, as shown in Equation (3.12) [106].

$$f_{ceq} = 2N * f_c \tag{3.12}$$

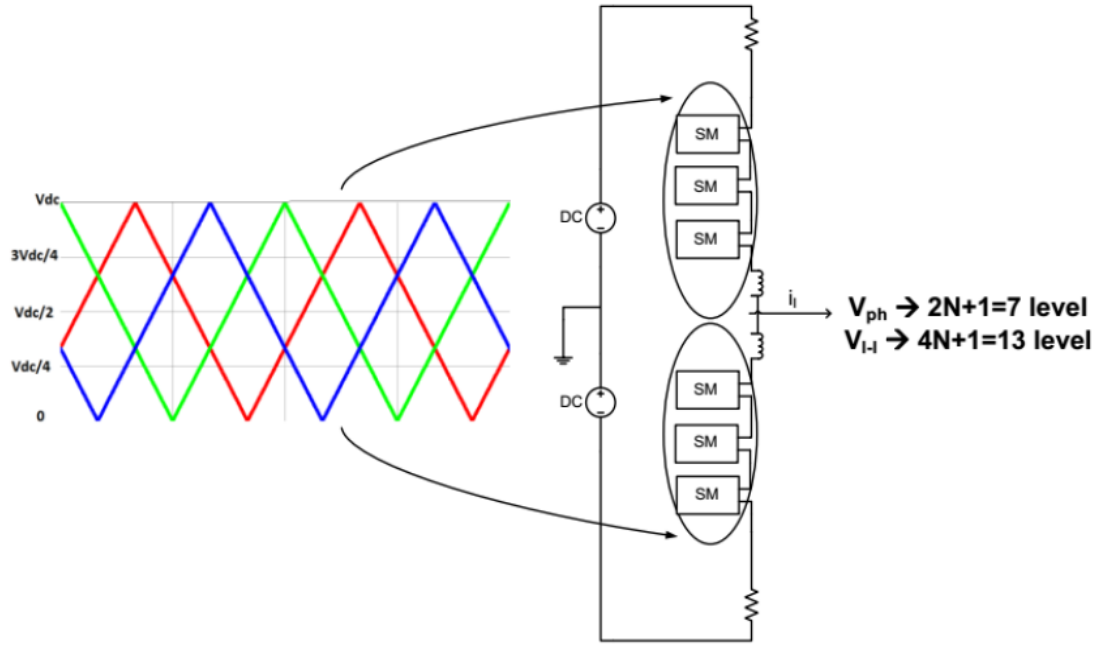

Figure 3.33 Carrier sets for the phase-shift method for 2N+1 levels of phase voltage with an odd number of submodules [106]

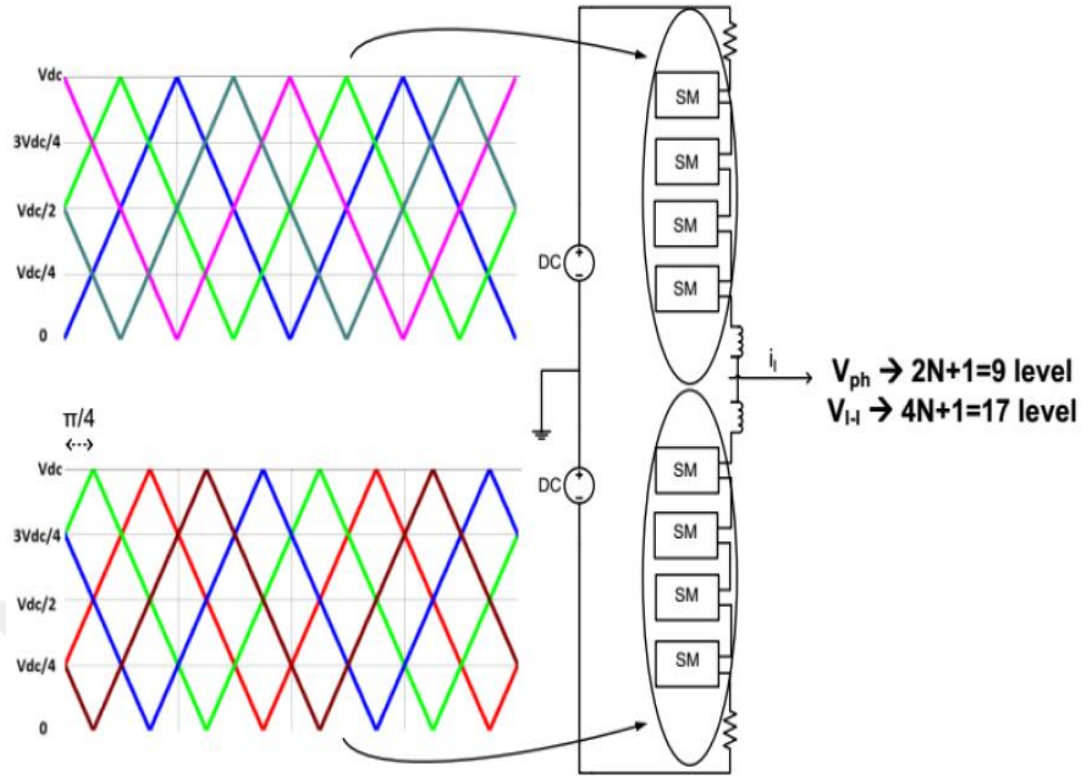

Figure 3.34 Carrier sets for the phase-shift method for 2N+1 levels of phase voltage for an even number of submodules [106]

CHBTER 4
DFIG AND HVDC SIMULATIONS

4.1 Introduction

This chapter offer the process for simulating wind energy conversion system based on doubly fed induction generator and back to back modular multilevel converter Where it offers investigate the performance of grid connected wind farm for high power transmission through the HVDC system.

4.2 System Design Method

The simulation model of the wind energy conversion system based on DFIG and MMC based HVDC transmission system, taken from the literature is utilized as a base model. In this study, the wind farm connected to the grid by a transmission system. This transmission system designed based on the voltage source converter. It contains MMC rectifier at the generator side. It acts an AC/DC converter. The grid side contains another MMaC converter. It acts a DC/AC converter. The function of the MMC in the the DFIG side is to avoid the ripples in the output and the function of the grid's side MMC is to balances the DC at common coupling point.

We used 5 pairs of half MMC for designing the full bridge for each phase. This MMC is a bi-directional VSC his function is the interfacing between the DC and high-voltage AC side in the designd system. For every phase in the system, the MMC contains a posatiive arm, negative arm and a controller producing the pulses for these arms. We use the side d-q controller in the grid side to to achieve a constant DC voltage at the common coupling point and this is the main motive of this work. The d-q controller takes 3ph grid current and voltage into the input along with the controller and coupling DC voltage. The model of DFIG and MMC left-side and MMC right-side connected with gride are illustrated in Figure 4.1 and Figure 4.2, respectively.

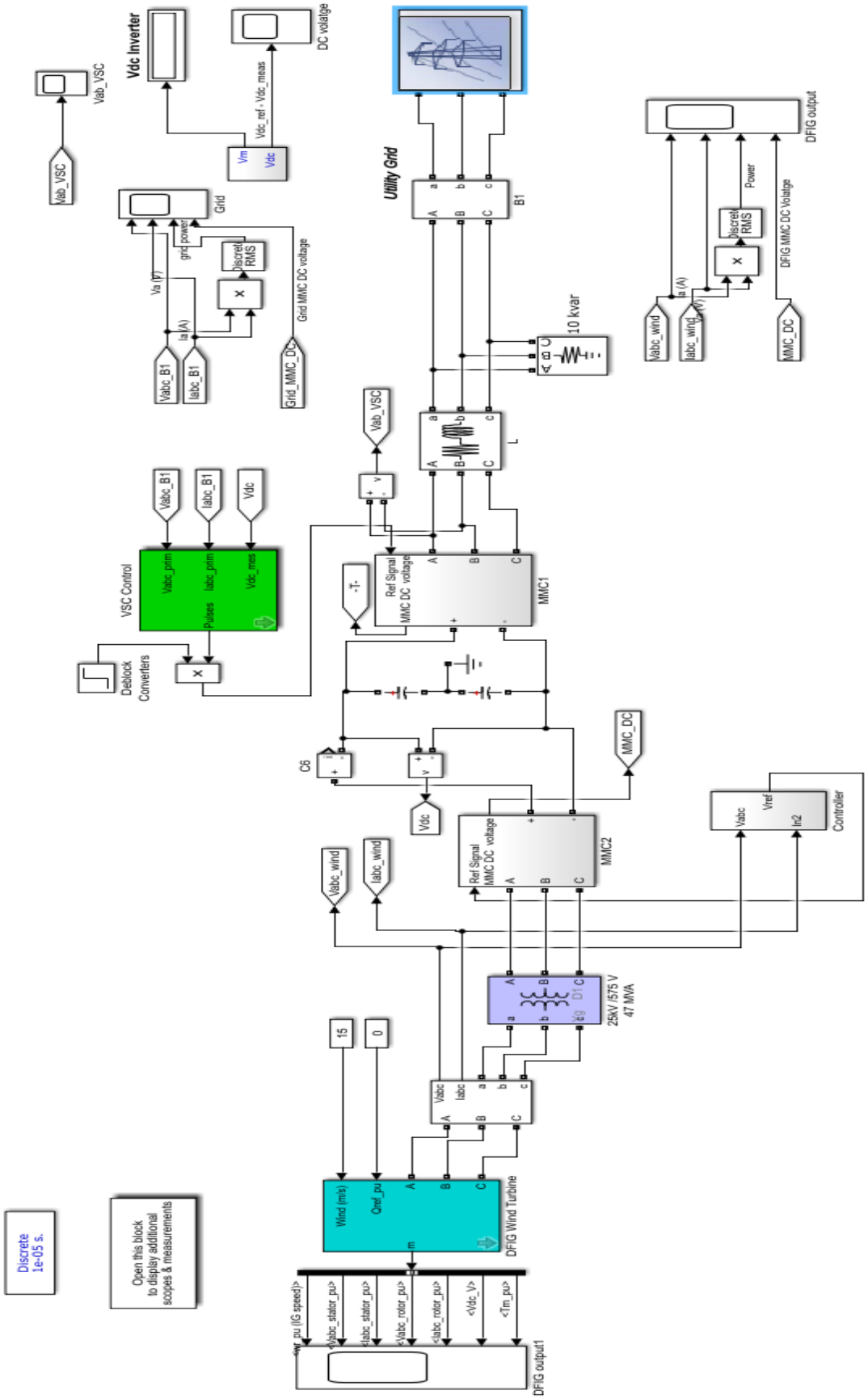

Figure 4.1 The Model of DFIG with MMC

4.3 System Configuration

The DFIG based wind turbine connected with the grid by using a voltage source converter based transmission system. It contains MMC at the DFIG side acts as AC/DC converter and another MMC at grid side acts as DC/AC converter. The function of DFIG side MMC is to prevent the ripples in the output voltage and the function of the grids side is to balance the DC at common coupling point (PCC). Figure 4.2 and 4.3 show the block diagram of the entire system. We have used five pairs of half-MMC for the full bridge for every phase and a controller for applying a gating pulse to them.

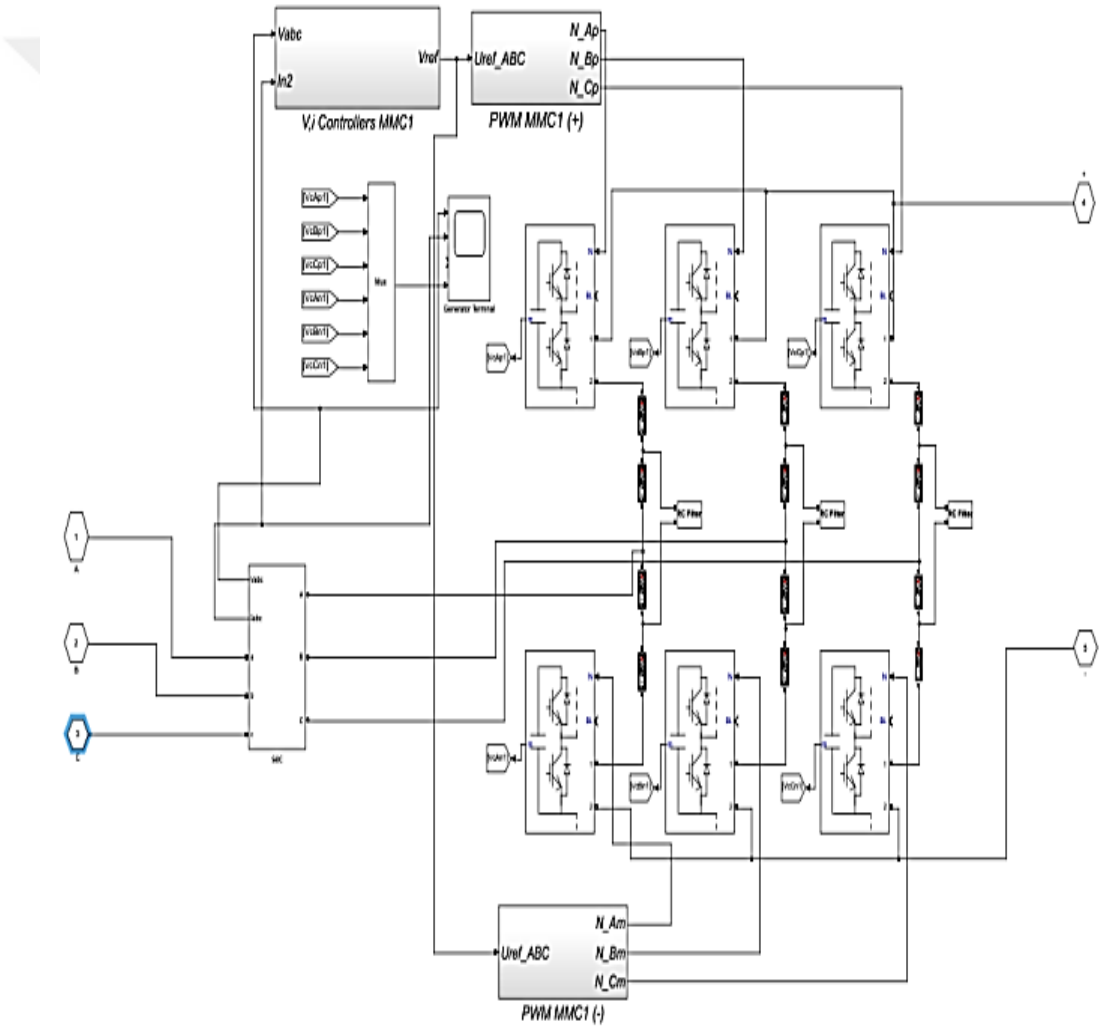

Figure 4.2 The block diagram of MMC rectifier

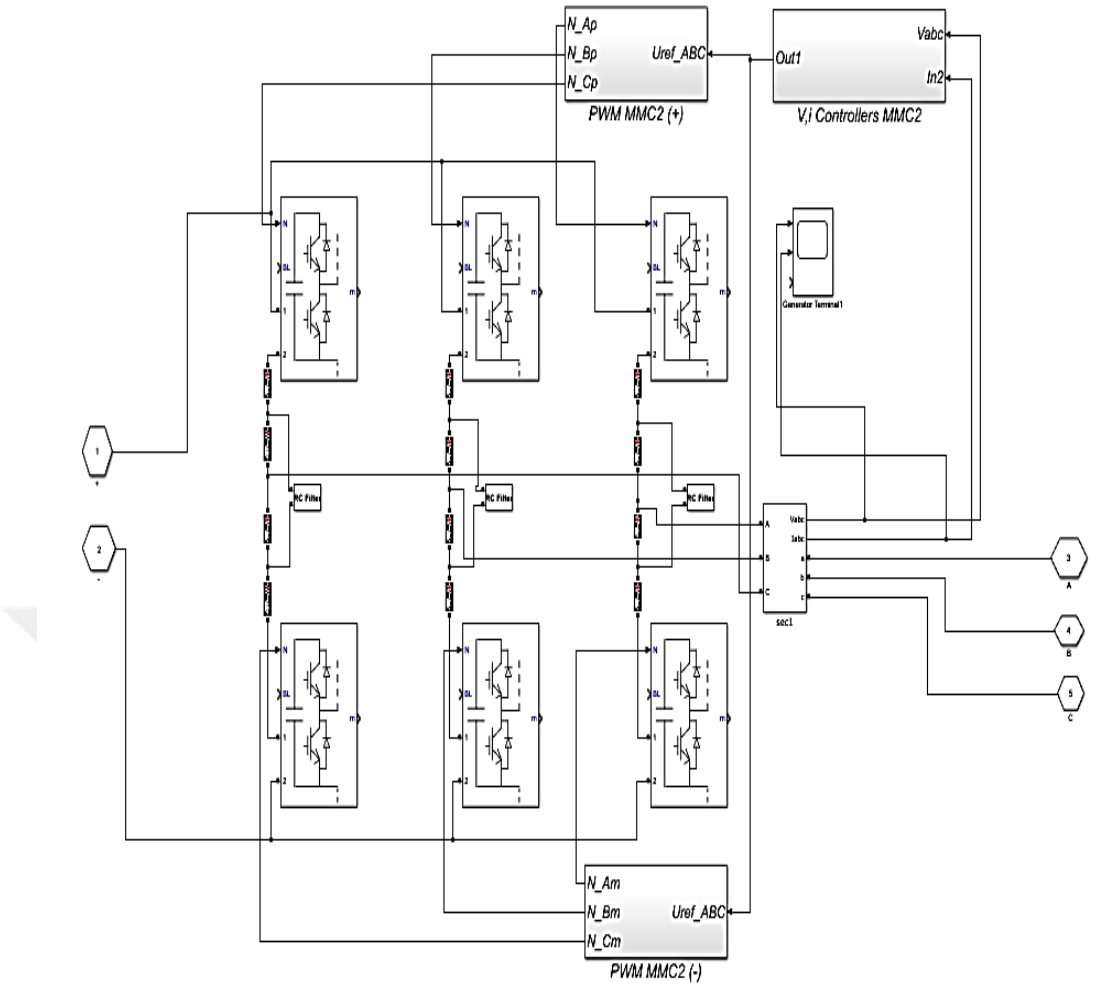

Figure 4.3 The block diagram of MMC inverter

The main purpose of this design is to maintain the stability of the voltages at a specified point. This point is the common point of coupling (PCC) and we can implement this by using the d-q controller. This controller takes the three-phase voltage and current of the grid into the input along with coupling DC voltage and controller.

4.4 Controller Design

We need for two controllers in the system in order to operate the converter in the the grid side and the other for the rectifier in the DFIG side. Luckily, the used d-q controller in the DFIG and grid side could operate the 5 level MMC bridges. We accented here only on the controllers of the MMC and neglected the start controller of the DFIG because there is a lot of work published on it. When the DFIG plant connected to the grid, the main aim is to transfer maximum power and maintain the power in case of load change when these power transferred from DFIG to PCC. On the grid side, the controller of the MMC is responsable for to maintain the DC voltage constant between the rectifier and converter. These two controllers (the converter and rectifier) are not dependent of each other and each of them has its own job where:

- The converter controls Vdc and Q
- The rectifier controls P & Q

The figure below shows the block diagram of the controller

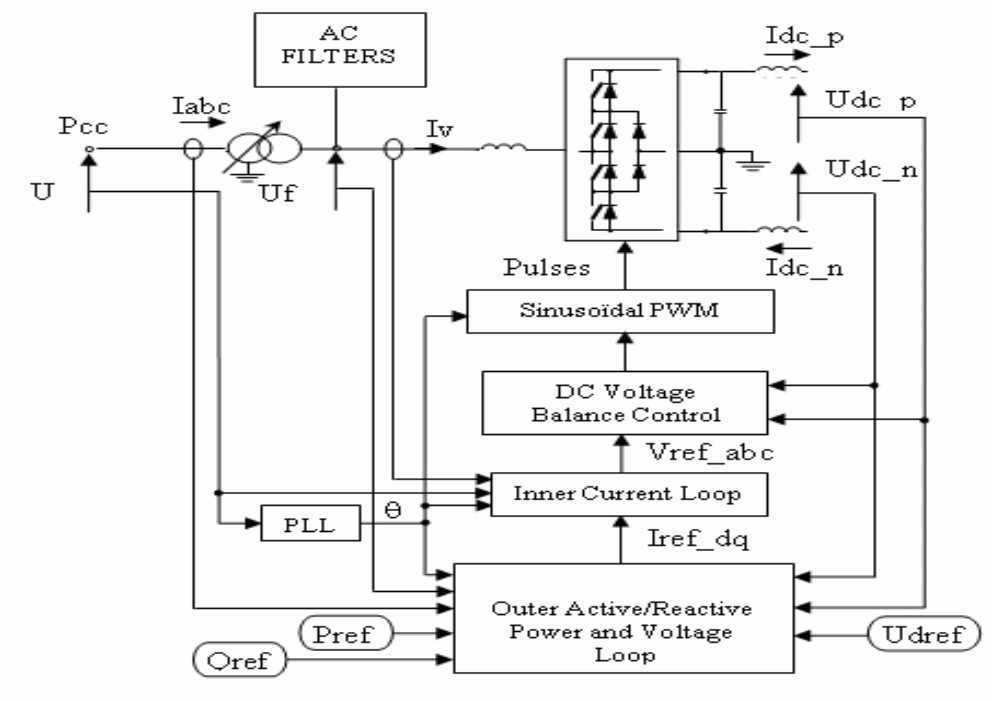

Figure 4.4 Block diagram representation of MMC controller

The sampling time adjusted as 0.3 µs. We have adjusted the sampling time so that it is 10 times more than simulation sample time. Also in order to get the optimal gate pulses, we have adjusted the PWM as 33 times the normal frequency. We used antialiasing filters in the bridge sub-block. Thereference signal is sent by the controller

to PWM with a carrier frequency of 33 times of normal frequency. We chosed the unsynchronized PWM mode for operating the system. The voltage and current are sampled and sent as an input feedback for the controller We used Clark transformation to convert the three phase components into imajinary and real part (space vector quantity). On the transformer's primary side, the signal is rotated into ±pi/6 in order to match the signal orientation due to transformer usage at the wind farm. The calculated components by Clark transformation are applied to compute the quadrature axis 'q' and direct axis 'd' depending on the d-q transformation block. Finally, we used a signal calculation block to calculate the modulation index, reactive power, DC current and voltage Where the controller needs it.

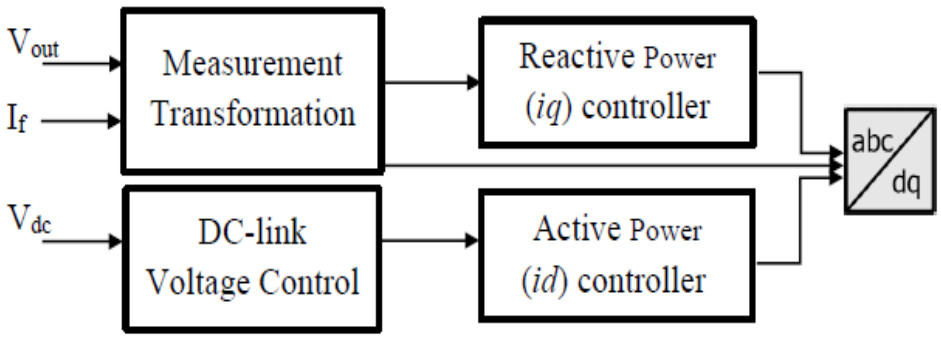

Figure 4.5 Real & Reactive power control System scheme

4.4.1 Phase Locked Loop (PLL)

We have used the phased lock loop block in order to get the phase synchronous angle (sin(Θ), cos(Θ)) for d-q transformation. The fundamental real component of the grid side phase (A) is in-phase with the sin(Θ) in steady state at the coupling point (Uabc). The outer loop of voltage, active and reactive power

The input Iref-dq current is calculated using this loop. This loop could use the flow of active power at the PCC or pole-to-pole DC voltage i.e. it could operate with two controlling modes. The q axis is used for checking the reactive power flow and the d axis is used for checking the active power flow. The figure below descibe the active and reactive power loop.

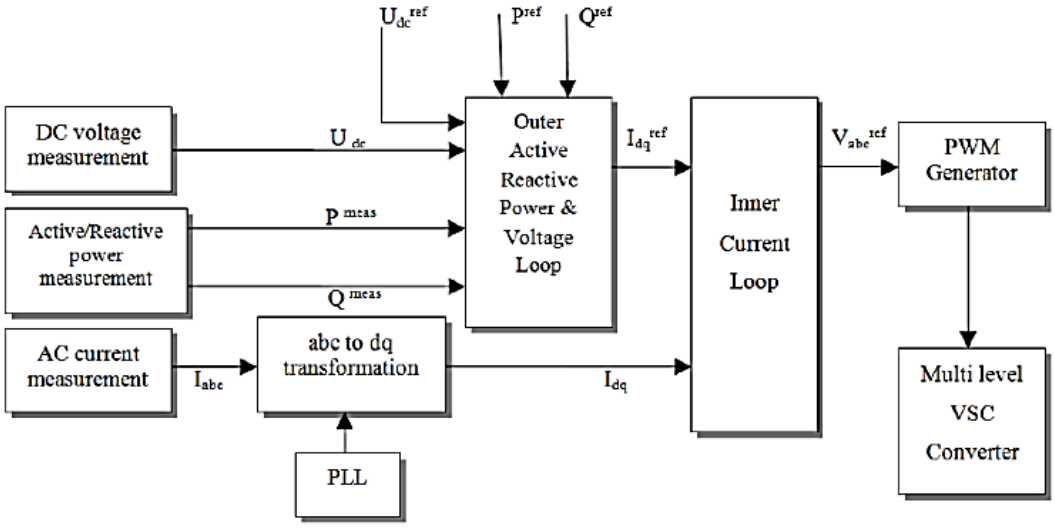

Figure 4.6 Block diagram active and reactive power loop

The speed response increased by using a PI controller in the reactive power controller which is exist in this block. The AC distortion at the output of PI controller may reset the PCC voltage to zero if it is less than a constant value so we used regulator to avoid it. This regulated o/p is sent to the PI with a difference with the reference PCC DC voltage. Two PI controllers used to control the PCC AC voltage that keep the AC grid side in the secure range.

On the other side, the active power controller has a similar function of the reactive power controller, it just uses an extra ramp controller that regulates the power order so that the desired value obtained. When the fluctuation happens in the AC system, the charge is took by the DC controller and override the active-power regulator so that the PCC DC voltage maintaid but we should notice that if the system needs to enable the DC-control block, it should disable the active power block. The block of current reference regulator takes this block's output as a reference value. As the dq reference current is, the input to the inner current loop there for the reactive and active power input to this loop should be changed to current finally. The current reference calculation block converts this reactive and active power into current. The current reference calculation block

Estimates the current reference by dividing the power reference over the voltage. The current limitation , block exerts the limit to scale the reactive and active power equally. When limit is imposed , the block give th priority to the active power in DC voltage control mode.

4.4.2 Inner Current Loop

The figure 4.7 descibes the main functions of Inner Current Loop.

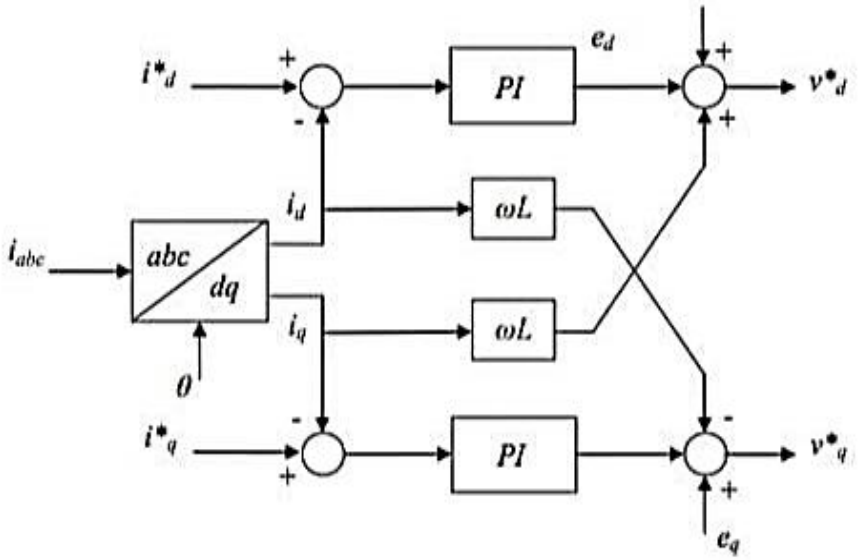

Figure 4.7 Block diagram structure of inner current loop

The block of AC current in the model uses the method of feed-forward to keep track of changing d and q current reference vector. These changes in the current could happens as a result of short circuit faults (SCF). When the voltage drop is detected, the model adds the voltage across the impedance by computing the difference between what should be converter voltage and U_dq voltage.

The dynamics of the VSC currents are represented by the state equations with using an approximation by neglecting the AC-filters and used in the model and so as to obtain two independent first-order plant models we have coupled the q and d components. We have used the PI controller also here in order to control the converter current in this block. In steady state case, this procees wil reduce the error to zero. The AC Current Control block output represents the Vref_dq_tmp (the unlimited reference voltage vector)

The amplitude of the reference voltage vector are limited by the block of Reference Voltage Limitation to 1.0 because over modulation is not desired.

CHAPTER 5
SIMULATION RESULTS

5.1 Introduction

This chapter presents simulation results validating the use of the DFIG with back to back MMC transmission system.

5.2 Simulation Software and Model Parameters

As described in chapter 4, the model has been designed and simulate by used MATLAB Simulink. The test includes two parts one is to test the DFIG generator alone then to test the back to back MMC with using DFIG as a power source.

5.2.1 DFIG Generator Simulation Results with Variable Wind Speed

In this part we tested the power generation from DFIG generator with variable wind speed. The DFIG has been connected to (575 V) AC power source with a frequency of 50 Hz. The wind speed has been taken as sequence with time were there values are (10, 12, 15, 5, 15, 10, 12) for a period of 30 second that changed every 5 second. The other DFIG Parameters are in follows

The main parameters of the system model are listed in Table 5.1.

Table 5.1 DFIG Simulation parameters

Name of Parameter	Value and Unit
Asynchronous Machine Power	4.5 (MW)
Voltage (line-Line)	575 (V)
Frequency	50 (Hz)
Stator Resistance	0.01965 pu
Stator Inductance	0.0397 pu
Rotor Resistance	0.01909 pu
Rotor Inductance	0.397 Pu

5.2.1.1 DFIG System Aspects

To investigated the operation of DFIG system for generating power, we investigated the aspects concern how system works and determine the system accuracy. These aspects are in follows:

5.2.1.2 Induction Generator Speed (IG Speed)

This part simulates the variation of IG speed with wind speed. The simulation results for different wind speed are in Figures 5.1.

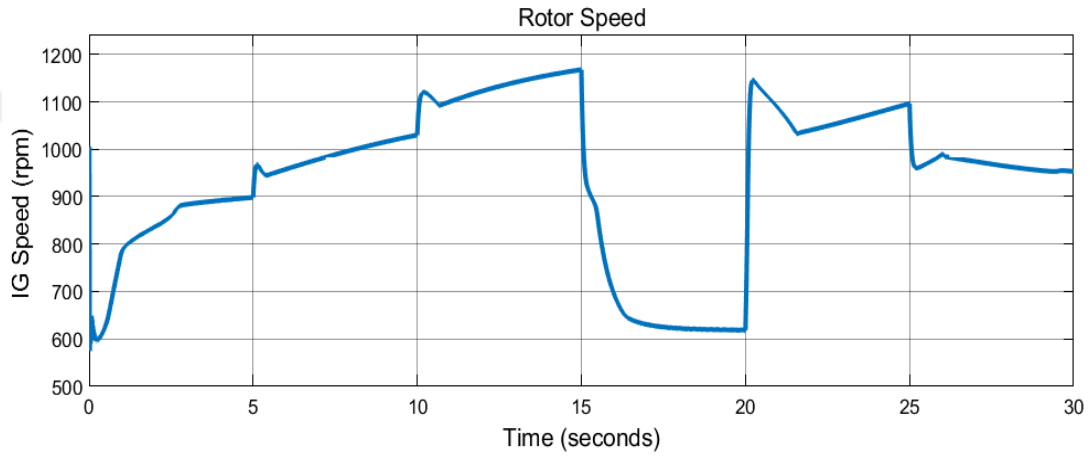

Figure 5.1 IG speed varition wind speed for variable speed of (10, 12, 15, 15, 10) m/sec that changed every 5 second period

5.2.1.3 Torque Mechanical (Tm)

This part simulate the varition of Tm with wind speed. The Simulation results for different wind speed are in Figure 5.2.

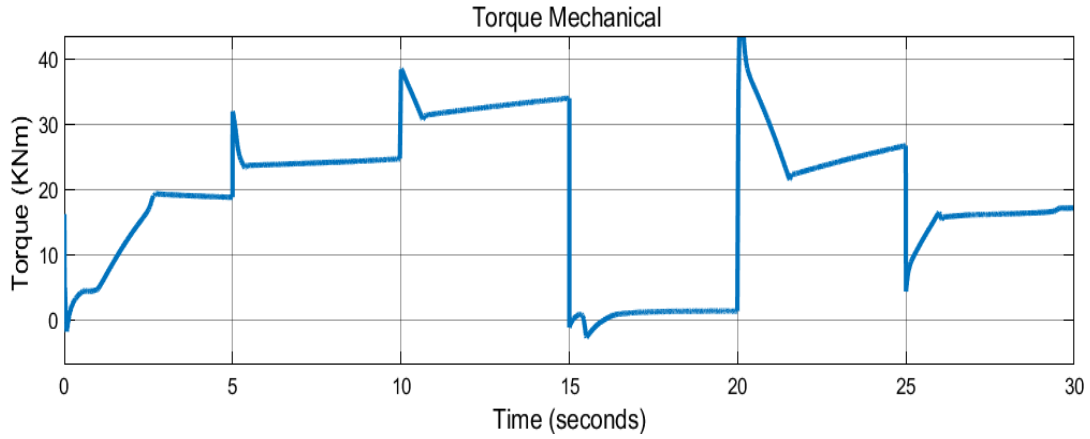

Figure 5.2 Torque Mechanical varition (KNm) with wind speed for variable speed of (10, 12, 15, 15, 10) m/sec that changed every 5 second period

5.2.1.4 AC Voltage, Current and DC link of DFIG

In this part we have been tested the waveforms of regenerating signal for AC voltage and current in addition to DC Link of DFIG to investigate the signal stability and variation with variable wind speed. Figure 5.3 shows the voltage, current and DC link variation with wind speed

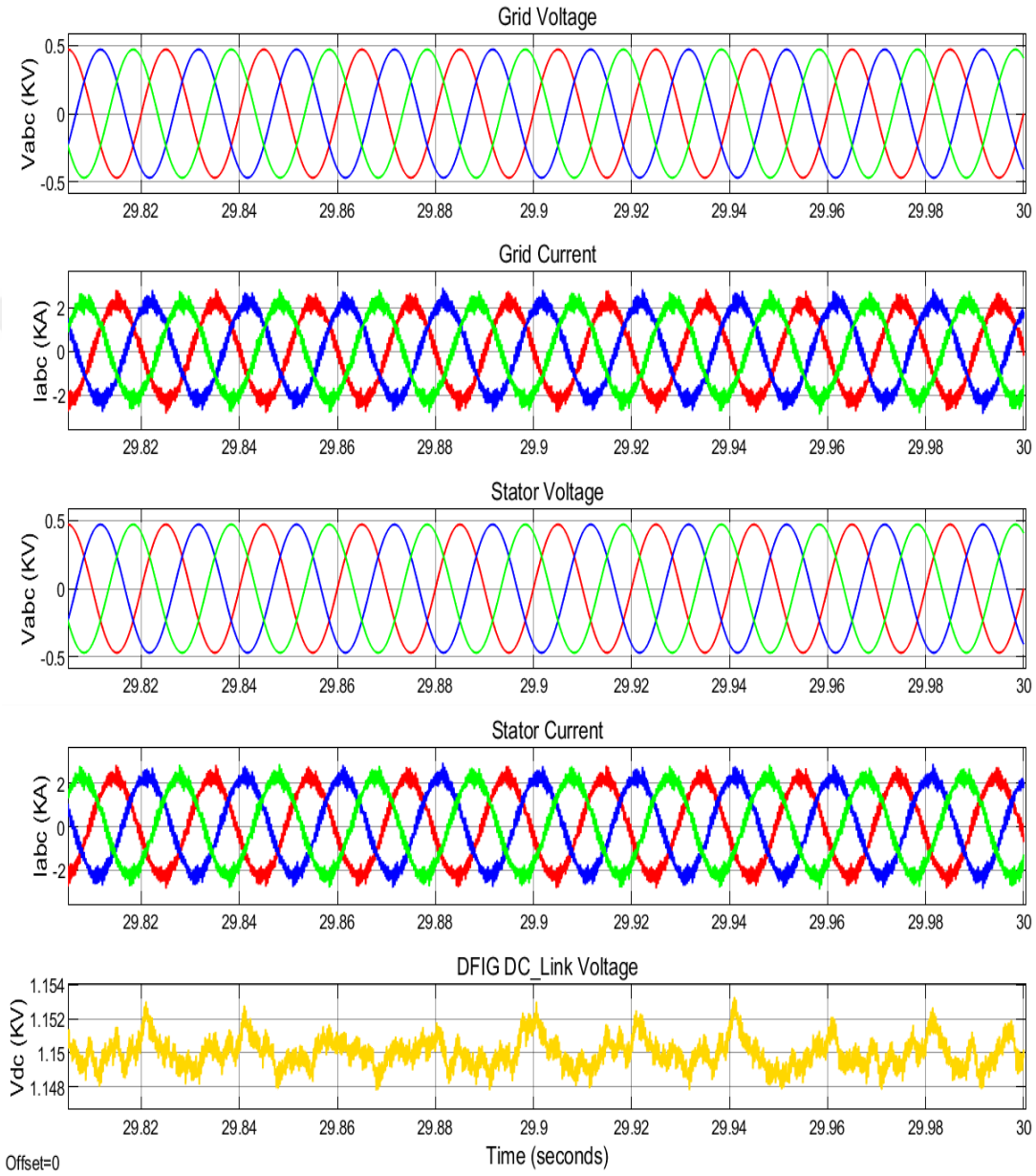

Figure 5.3 The DFIG voltage and current signals (zommed). From up to down, Vabc(Volt), Iabc(Amper), V_Stator(Volt), I_Stator(Amper), Dc link voltage (Volt)

5.2.1.5 Active, Reactive and Apparent Power

In this part we have been tested the active, reactive and apperent power generated to investigate the power vartion with wind speed . Figure 5.4 shows the simulation result for active and reactive power, and Figure 5.5 shows the simulation result of apperent power.

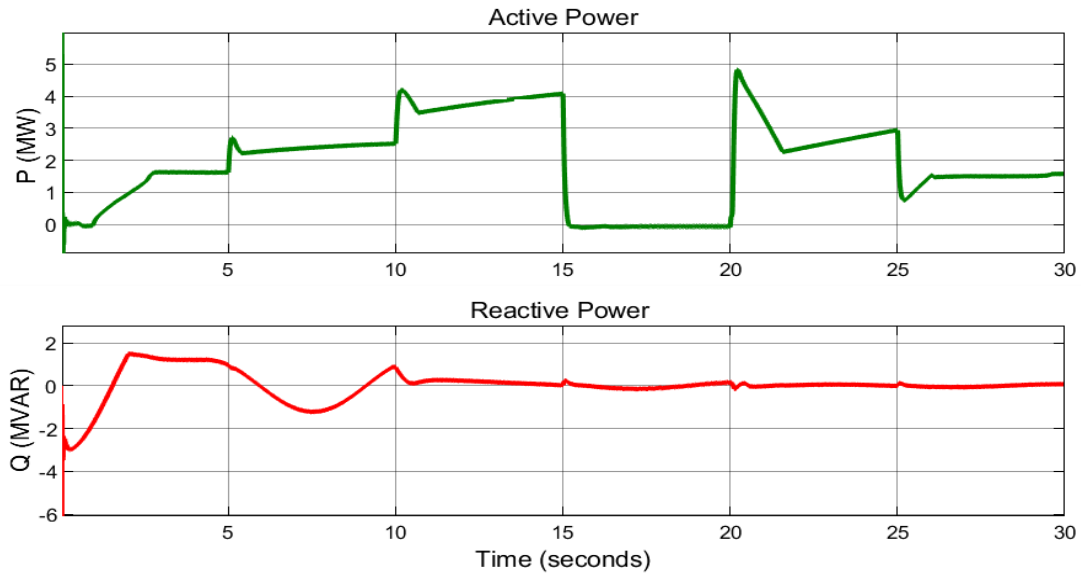

Figure 5.4 DFIG power generation with time for different wind speed values. From up to down. Active Power (MW), Reactive Power (MVAR)

In other hand the apparent power of the system is shown in Figure 5.5

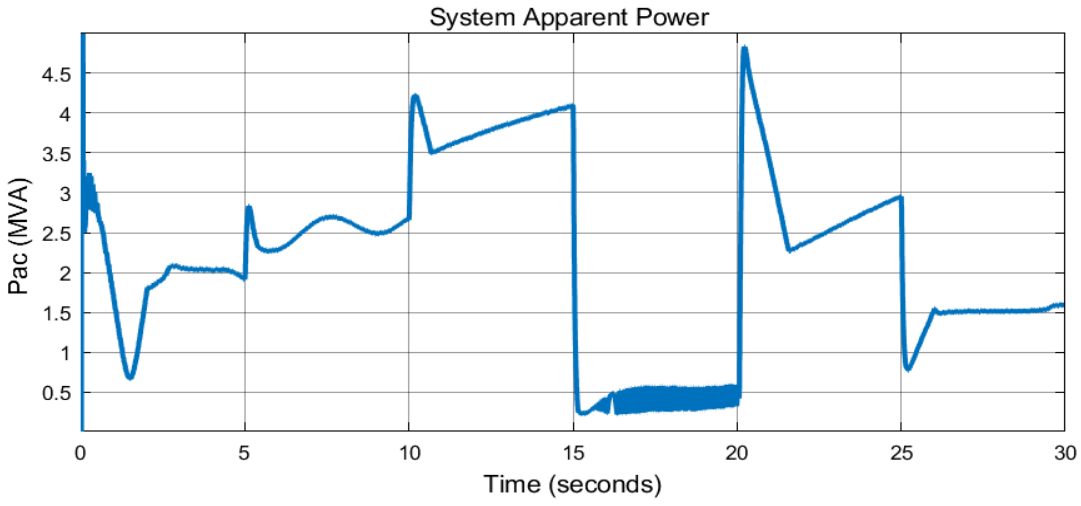

Figure 5.5 System apparent power per time (MVA)

As can noticed from previous results shown in figures 5.1, 5.2, 5.3 and 5.4, its clear that the power of DFIG generator is effected by wind speed, for first period (0 - 5) sec we put the wind speed to be (10), the DFIG IG speed (shown in figure 5.1) raised and it reach steady state at about 4 second and it reach to (~900 rpm), as a result the torque mechanical (figure 5.2), active, reactive and apperent power (figure 5.4 and 5.5) have also changed related to IG speed where power reach to 1.635MW at steady state, in the second period (5-10) sec we put the wind speed to be (12), as in previous the IG speed raised and torque reach steady state at (5.5) second (0.5 second for stability) the active power is also changed where raised to be 2.5MW, in third period (10-15) we put the wind speed to be (15), and also the IG speed raised and both torque mechanical and active power raised too where the active power reach up to 4.1 MW, in fourth period (15-20) we put the wind speed to be (5), the IG speed dropdown to (~618 rpm), the torque mechanical has also dropdown to zero and thus the active power is reach to zero. In fifth period (20-25) we changed the wind speed to be 15, thus the IG speed has been raised again and as a result the both torque mechanical and active power raised too where reach to 2.95 MW (it need more time to reach the exact generation power than 5 second). And finally for last period (25-30) sec the wind speed reduced to (10), and also the IG speed reduced and both torque mechanical and active power reduced too where active power reach nearly 1.58 MW.

From these results, it clear that the DFIG is effective by the wind speed value and power generation is related to wind speed value (raised as wind speed raised), it can also notice that the active power is about zero when wind speed is 5. The voltage and current signals is also uniform and stable and it also changed as result of wind speed changed. The DFIG dc link voltage is also uniform and stable. As a result the DFIG generator is good and can be connected with MMC in next part.

5.2.2 DFIG with Back to Back MMC Simulation Results

In this part we have connected DFIG with back to back MMC. As described in Chapter 4, the back to back MMC is consists of two parts, MMC1 on the left where the DFIG is AC power sources while the second part is MMC2 that connected to AC power grid. The both MMC are connected with each other via DC Link. The number of submodules is selected to be five per arm. Each submodule is consisted from one half-bridge IGBT. Each single-phase arm has two RL and filter between upper and lower arms for filtering. The main parameters of the system model are listed in Table 5.2 (the DFIG Generator parameters are same as in table 5.1).

Table 5.2 BTB MMC Simulation parameters

Name of Parameter	Value and Unit
Grid Phase to Phase Voltage	160 (KV)
Nominal Primary Voltage	25 (KV)
Nominal Primary Voltage	260 (V)
Nominal System Frequency (Fnom)	50 (Hz)
Grid Power	4.5 (MW)
Number of SM/arms (Nb_PM)	5
PWM Carrier's frequency	1685 (Hz)
Power Module Capacitor	37.58 (mF)
Capacitors Initial Voltage	108 (V)
Nominal DC Bus Voltage (V_dc Reference)	5 (KV)
Arm Resistance	0.443 (Ohms)
Arm Inductance	0.141(mH)
Filter Resistance	5.32 (K Ohms)
Filter Capacitance	0.01794 (mF)
DC Link Resistance	0.5 (Ohms)
DC Link Capacitance	12 (mF)
Arm Resistance	0.443 (Ohms)
Arm Inductance	0.141(mH)
Sampling Period (Ts)	5 (µsec)

The total simulation time has been selected to be 30 seconds to test all system conditions and stability as well as determine the time needs for system to reach its steady-state operating point. In this part we have test system works with variable wind

speed. Two case study have been taken, one when no power source (Grid) is conned to DFIG generator in MMC1 and second when power source is connected to DFIG in MMC1. The results are in follows:

5.2.2.1 Case 1 (No power source connected with DFIG)

This case study investigates the results when DFIG connected directly to MMC1 without power source. To investigated the operation of DFIG BTB MMC system for generating power, we investigated. Figure 5.6 shows the system model of case 1.

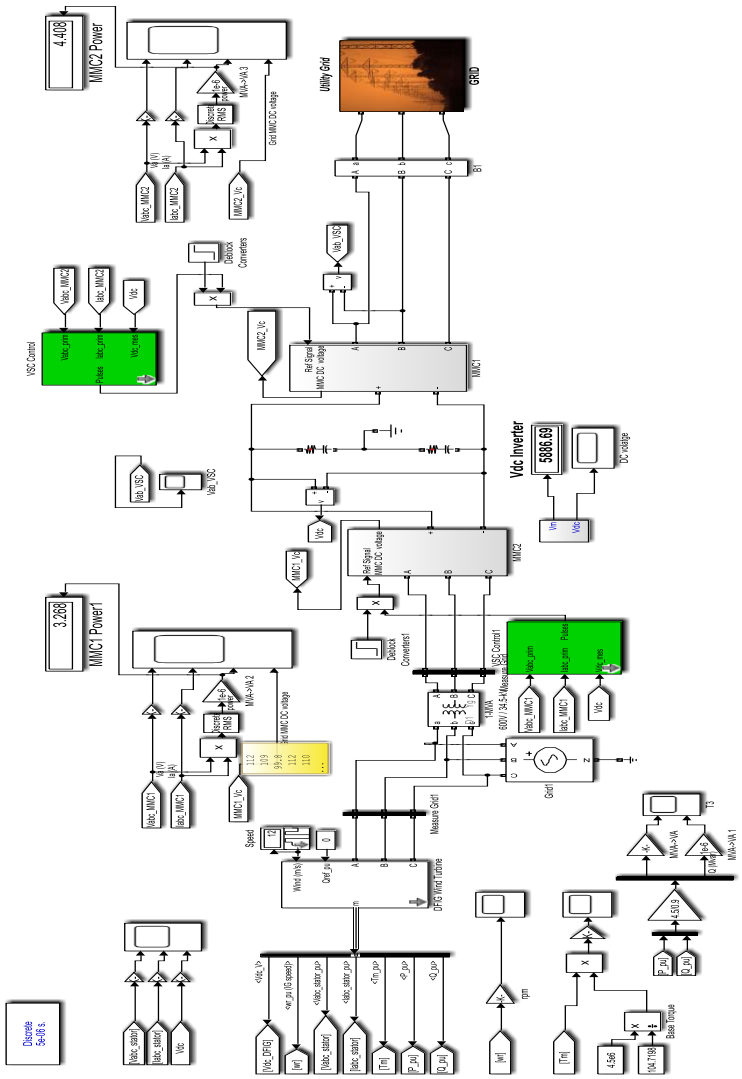

Figure 5.6 DFIG BTB MMC System Model

5.2.2.2 Induction Generator Speed (IG Speed)

This part simulates the variation of IG speed with variable wind speed. The results is shown in Figure 5.7.

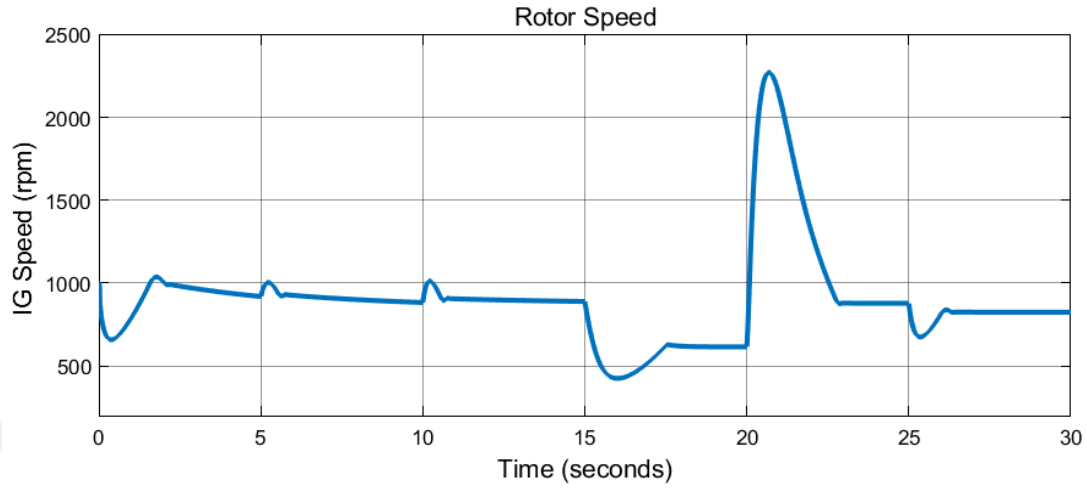

Figure 5.7 IG speed varition with variable wind speed of (10, 12, 15, 15, 10) m/sec that changed every 5 second period

5.2.2.3 Torque Mechanical (Tm)

This part simulate the varition of Tm with wind speed. The Simulation results for different wind speed are in Figure 5.8.

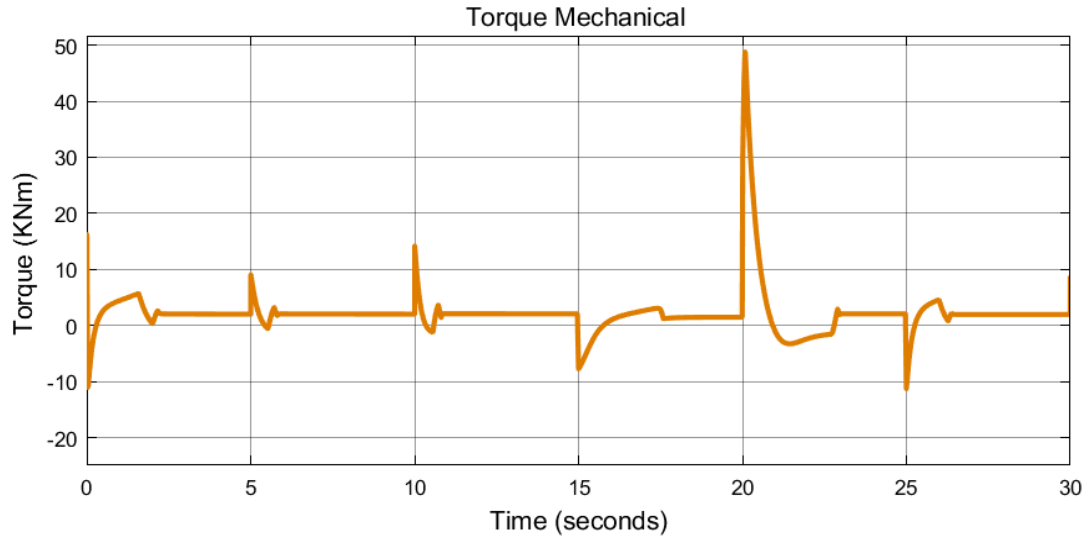

Figure 5.8 Torque Mechanical varition (KNm) with wind speed for variable speed of (10, 12, 15, 15, 10) m/sec that changed every 5 second period

5.2.2.4 Active, Reactive and Apparent Power

In this part we have been tested the active, reactive and apperent power generated to investigate the power vartion with wind speed . Figure 5.9 shows the simulation result for active and reactive power, and Figure 5.10 shows the simulation result of apperent power.

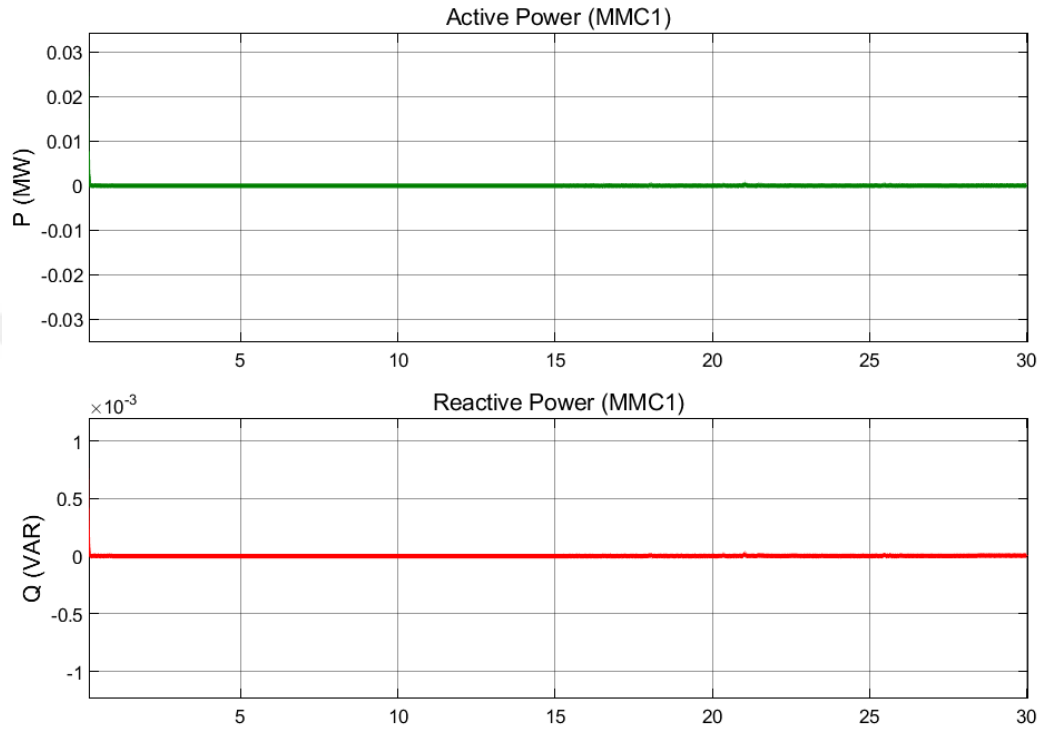

Figure 5.9 DFIG power generation with time for different wind speed values. From up to down. Active Power (MW), Reactive Power (MVAR)

In other hand the apparent power of the system is shown in Figure 5.11

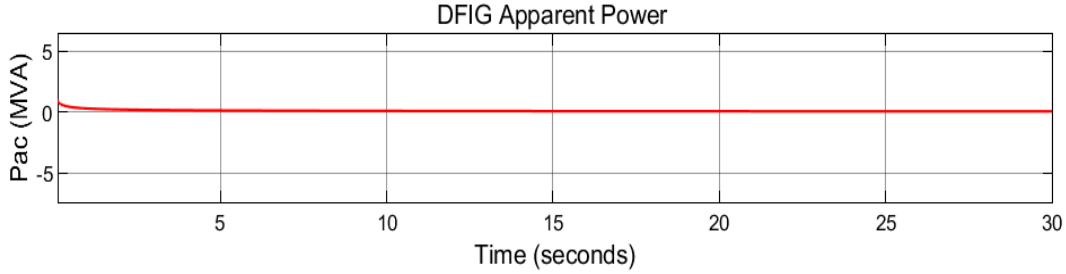

Figure 5.10 MMC1 (DFIG Side) apparent power per time (MVA)

As can see from results when wind speed changed, the IG speed is reltivaly low and torque mechanical very low and as a result the active powe as well as apparent power become zero.

As noticed from DFIG simulation result (without MMC), its appears that the DFIG need to connect with 3 phase grid or sources and need about 1 sec to power start rising and about 4 sec to be stable, Thus we modified this system by added power source in parell to DFIG MMC line. The details are described in case 2.

5.2.2.5 Case 2 (Power Source Connecte with DFIG):

In this model the DFIG connected directly to MMC1 and a 608 V power source has been connected in parallel to DFIG and MMC. Thus, we investigated the operation of DFIG BTB MMC system for generating power in this case.

The aspects concern how system works and determine the system accuracy. These aspects are in follows:

5.2.2.6 IG Speed, Torque Mechanical, Active/Reactive Power

In this part we tested the IG speed and Torque Mechanical, and active/reactive power of DFIG when connected to MMC.

5.2.2.7 Induction Generator Speed (IG Speed)

This part simulates the variation of IG speed with wind speed. The Simulation results for different wind speed are in Figures 5.12.

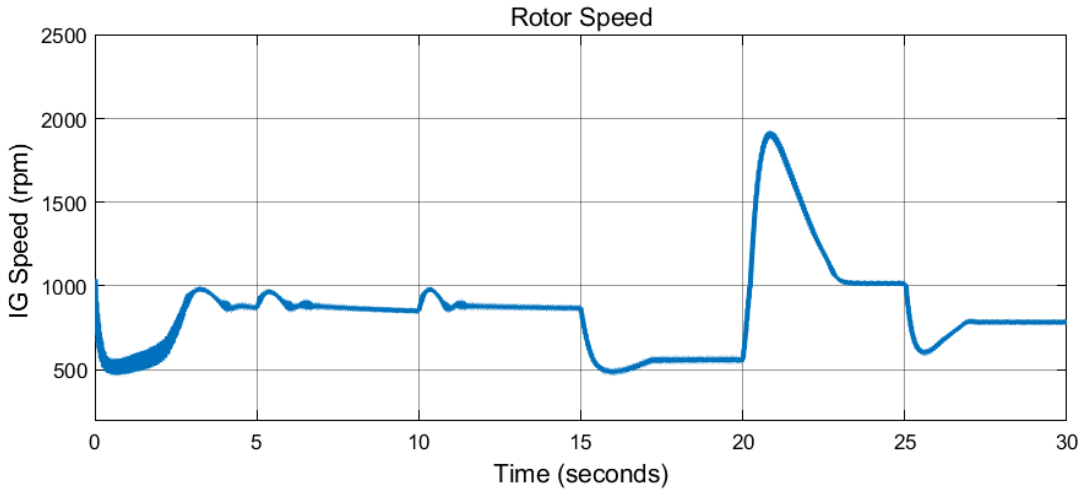

Figure 5.11 IG speed varition wind speed for variable speed of (10, 12, 15, 15, 10) m/sec that changed every 5 second period

5.2.2.8 Torque Mechanical (Tm)

This part simulate the varition of Tm with wind speed. The Simulation results for different wind speed are in Figure 5.13.

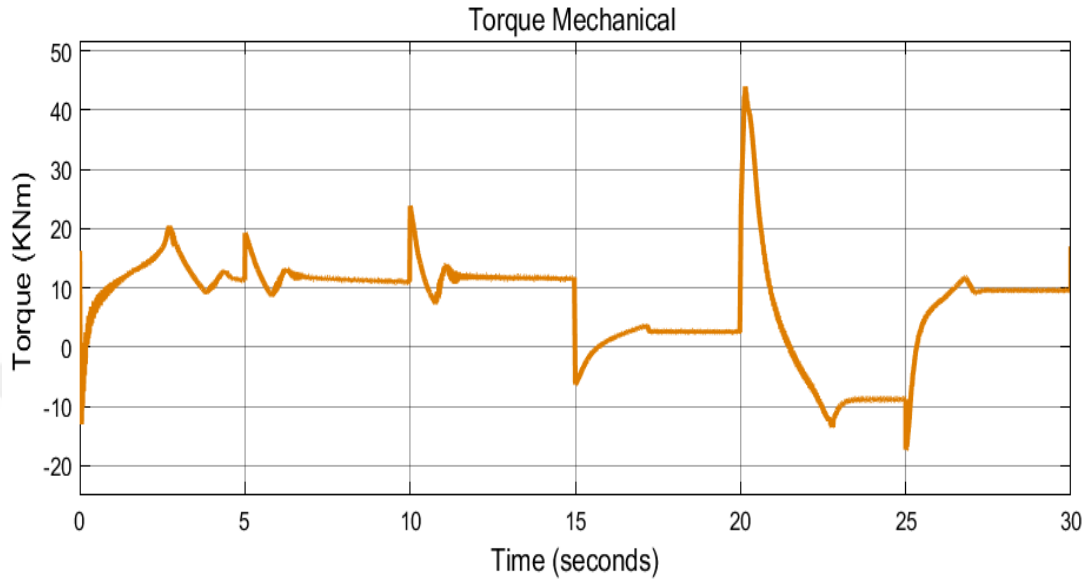

Figure 5.12 Torque Mechanical varition (KNm) with wind speed for variable speed of (10, 12, 15, 15, 10) m/sec that changed every 5 second period

5.2.2.9 AC voltage, current and DC link of DFIG

In this part we have been tested the waveforms of regenerating signal for AC voltage and current in addition to DC Link of DFIG to investigate the signal stability and variation with variable wind speed. Figure 5.14 shows the voltage, current and DC link variation with wind speed .

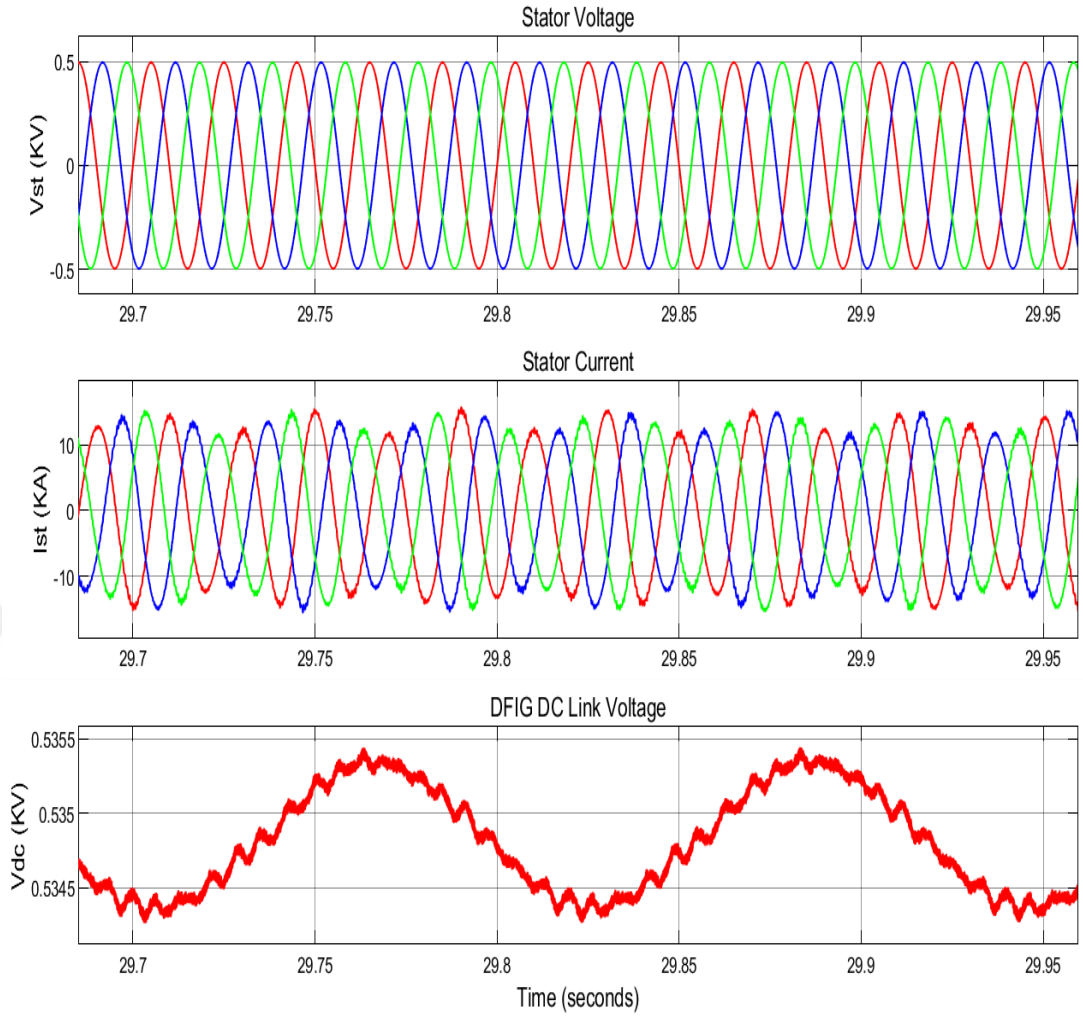

Figure 5.13 The DFIG voltage and current signals. From up to down, V_Stator(Volt), I_Stator(Amper), DFIG Dc link voltage (Volt)

5.2.2.10 Active and Reactive Power

In this part we have been tested the active, reactive power generated to investigate the power vartion with wind speed .

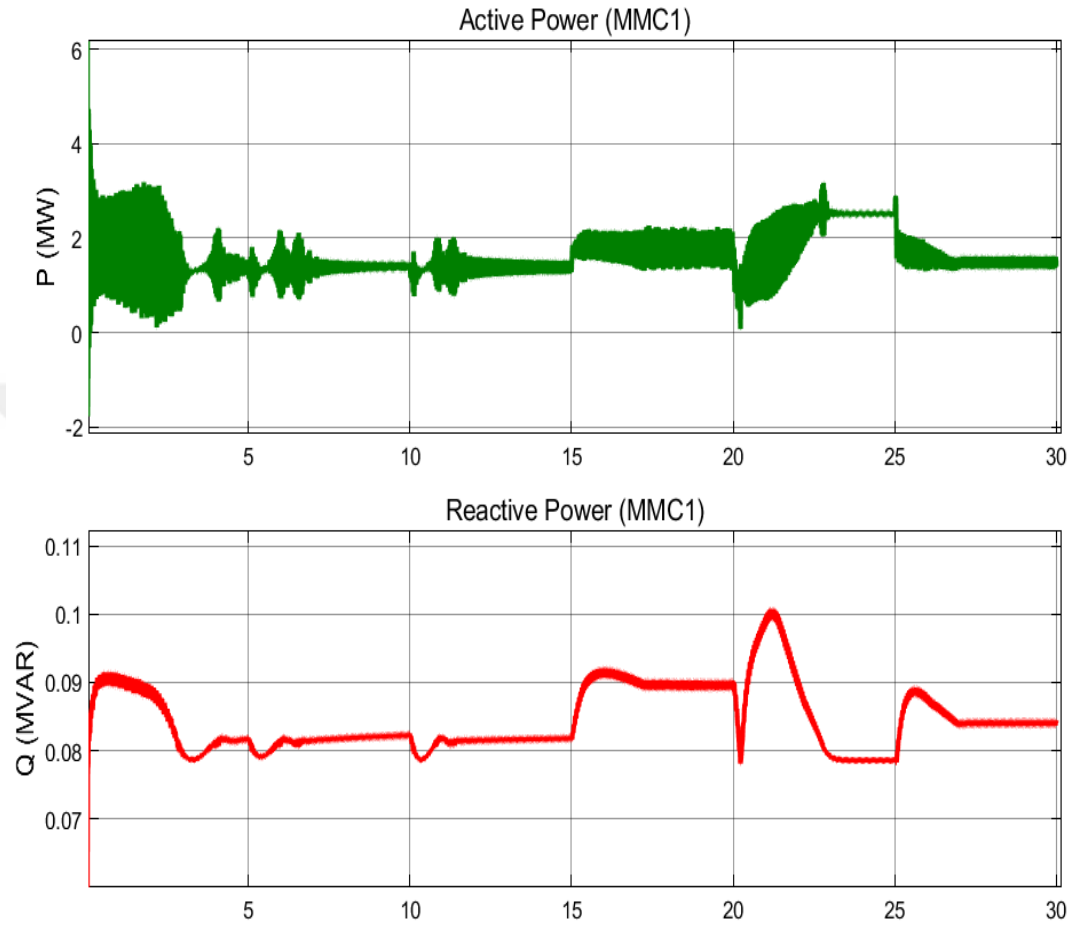

Figure 5.14 DFIG active and reactive power through 30 second time for different wind speed values (changed each 5 second)

As can noticed from previous results, when wind speed changed, the IG speed, torque mechanical active power and reactive power is changed too.

5.2.2.11 MMC Simulation Results

In this part we monitor the MMC aspects for both sides that includes voltage, current, apperent power and SM capactors voltage balance. The simulation results are in follows:

1- MMC1 (DFIG Side) Readings

The simulation results of MMC1 (in DFIG side) are shown in Figure 5.1

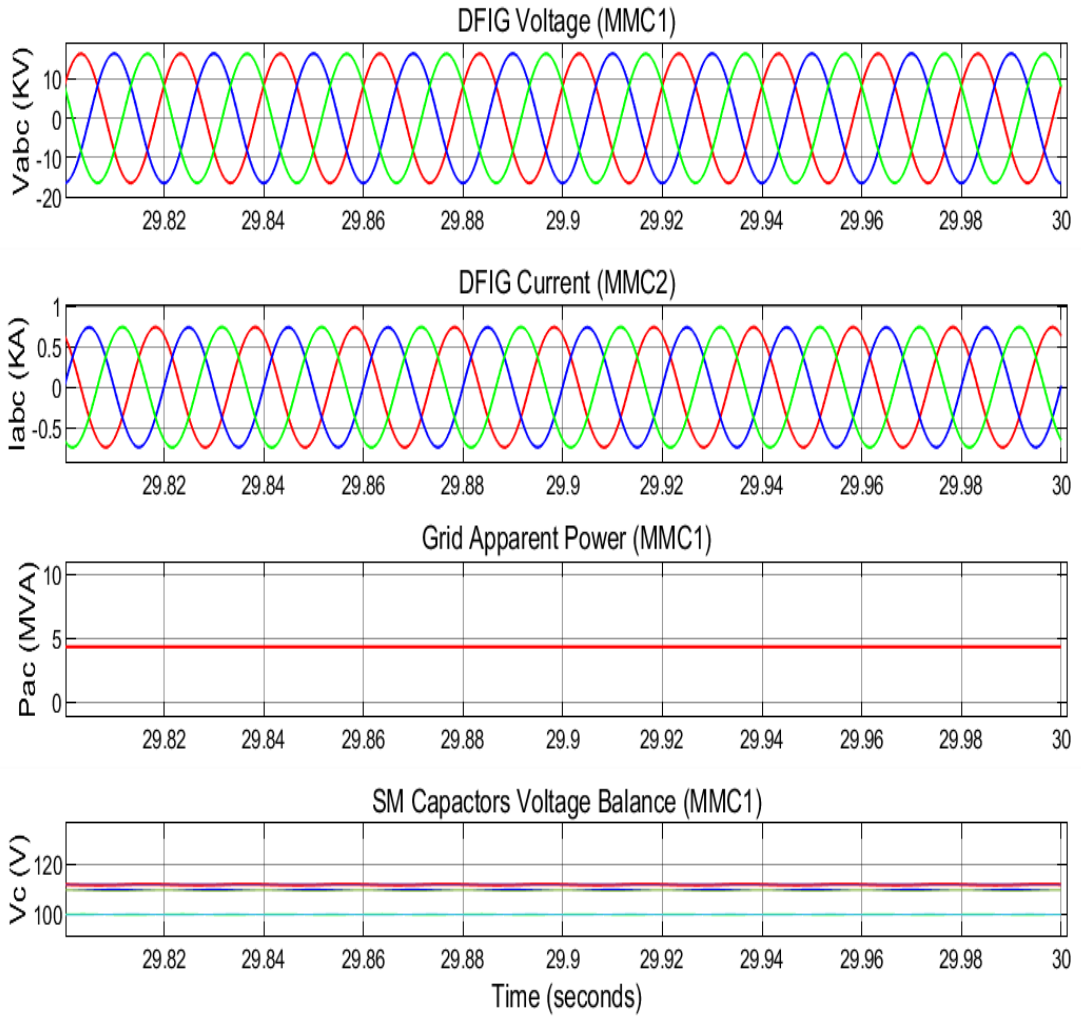

Figure 5.15 The MMC1 (DFIG side) voltage and current signals. From up to down, Vabc(Volt), Iabc(Volt), Active Power (watt), Capacitors Voltage-Vc (Volt).

2- MM2 (Grid Side) Readings

The simulation results of MMC2 (Grid Side) are shown in Figure 5.17

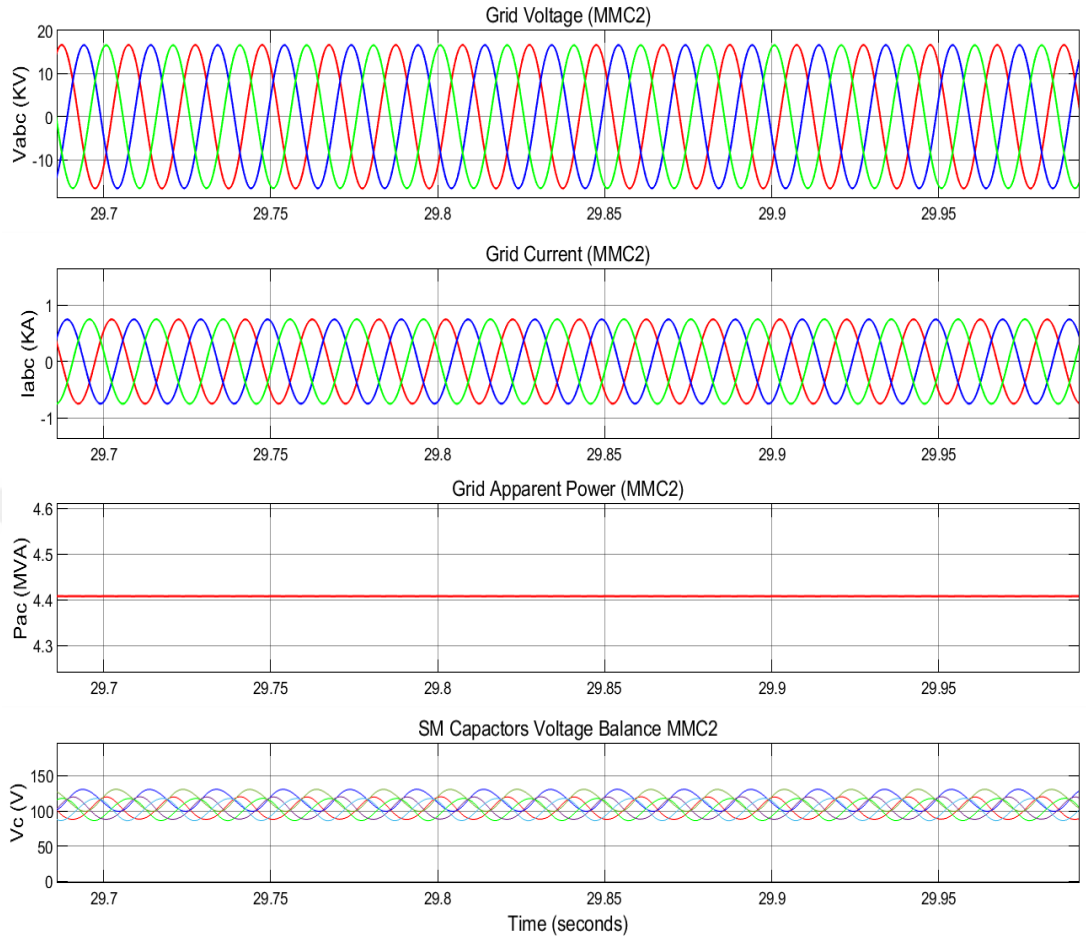

Figure 5.16 The MMC2 (Grid side) voltage and current signals. From up to down, Vabc(Volt), Iabc(Volt), Active Power (Watt), Capacitors Voltage-Vc (Volt).

The result shows that the voltage and current waveforms signals for both MMC1 and MMC2 are uniform and good and it is appearing that the waveforms of the regenerated signals are very close to the ideal sinusoidal signal waveforms of the transmitter power. The capacitor voltages (Vc) of the 5 submodules (shown in Figure 5.13), the DC voltage of submodules reaches to steady-state in about 1 seconds. It can notice that the capacitor voltages balance of submodules is very close to each other with a relatively uniform waveform shape. These results related to efficient (v, i) controller and to switching strategy that gives the suitable maximum peak to peak voltage deviation. Additionally, the MMC submodule waveforms are low ripples and it uniform. These results are also related to a good choice of submodules capacitor size.

5.2.2.12 DC link Readings

In this part we have been tested the DC Link voltage of MMC to investigate the DC link voltage that generated in the bidirectional way. The DC voltage pass from MMC1 to MMC2 and vise various through transmission line in which both MMC worked as rectification it converts AC to DC and transferring the DC voltage through transmission line to another MMC, the second MMC then works as inversion via convert the DC to AC again. The DFIG BTB MMC signal is shown in Figure

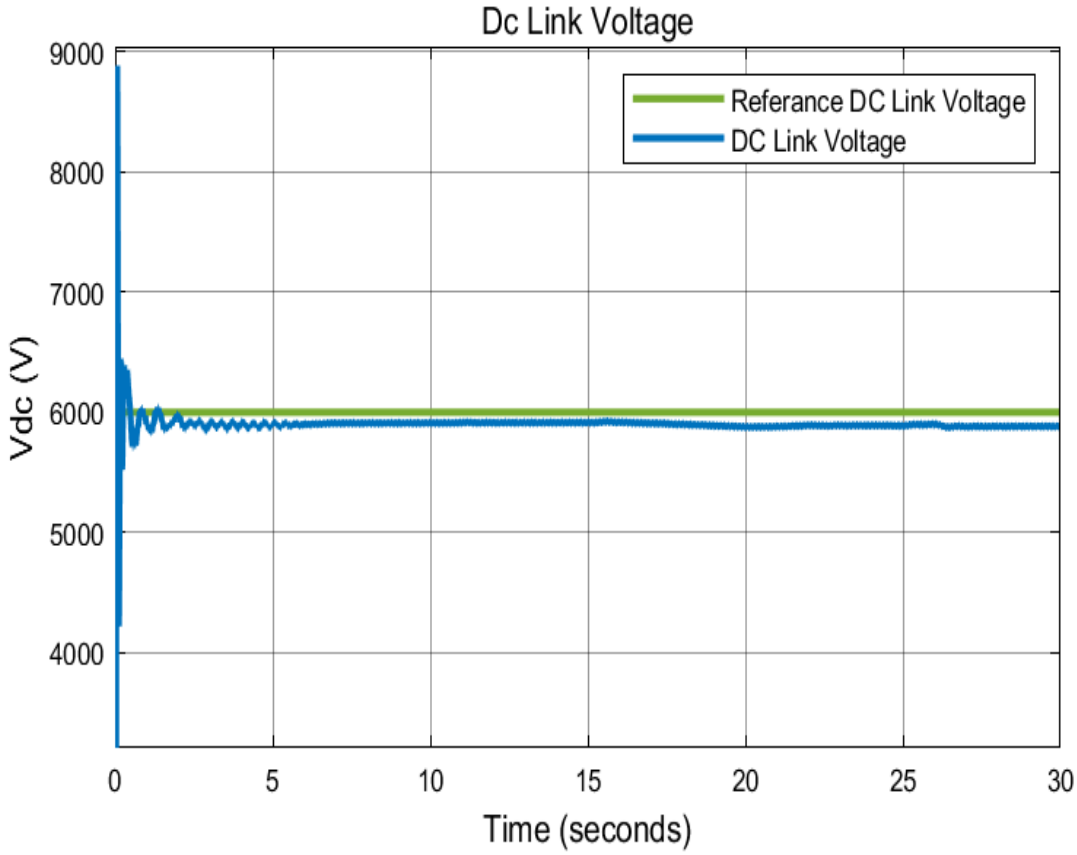

Figure 5.17 The Dc link voltage (Volt). Blue, represent the DC Link voltage of DFIG BTB MMC, Green, represent the referance DC Link Voltage.

CHAPTER 6
CONCLUSION

6.1 Summary

Wind energy systems plays an important role in various forms of human existence and has been used for irrigation and transport for centuries. However, the impact of large-scale electricity generation in the 21st century. has taken the application of wind power to a different level with global population growth and limited fossil fuel resources, In global warming, greenhouse gas emissions, and the sustainability of human comfort and land, global warming has become a very difficult issue for the 21st century and beyond. In the past two decades, global wind power production has been growing rapidly.

Although the actual output of electricity is very small (somewhere close to 1-5% in general, but for some countries more than 50%) of total electricity produced it is expected to grow steadily for the next 20-30yrs. In the United States, for example, the United States is the world's largest electricity user, its wind power production was about 10-35% of total electricity and other non-hydropower renewable sources. With great advances in electrical and electronic that provide faster response and smoother control, the integration of the wind farm system into the current network has become more manageable. However, when the wind and solar penetration increases at a level of 20-30%, there are many issues that need to be dealt with.

This is because the energy sources in nature are intermittent and energy is available when the demand is usually low. To control the network of non-aquatic renewable sources, storage must add.Recent progress of electrical power devices and digital control strategy available, however, Double feeding induction (DFIG) is more useful for large-scale wind farm. However, you must remember that the size of the individual DFIG unit is still Very small (2.00-5.00MW range) compared to large power units (500-1,200MW). In general the control case of a large unit is simp

than controlling a large number of small units. This thesis has mostly focused on the various aspects of the application of the DFIG design of the existing wind farm and the control suggested a number of new control strategy. After a brief overview of wind power growth and the basic principle of a typical wind conversion system, a detailed Dfig model in Matlab / Semolink was built from the basic principles. When we had designed the DFIG wind turbine, we connected it with a MMC-HVDC transmission system in order to control the changing of load conditions at the side of wind turbine. We used the d-q theory to design a 5 level MMC rectifier controller. The generated DC power is transmitted to the grid by converting it to a 3ph form again. 5 level MMC inverter ia used for this purpose with same type of controller. I had used the simulink of The MATLAB program to design and analyze the model. The designed model can be used in MMC based high power transmission systems to help in integrating the wind turbines with the grid satisfactorily and successfully.

The designed model was also used to perform the simulation of an MMC-based HVDC transmission system between two separate systems for power generation.

This MMC based HVDC transmission system can provide reactive power or voltage control and real power flow control at both converters AC terminals independently. Moreover, real power transfer can be reversed. From the simulation studies.

The simulation results presented the vector control strategy of the DFIG output active power vector based on stator flux oriented reference frames and confirmed the validity of the model. The thesis also presented the unique advantages of the variable pitch variable speed doubly fed induction generator based wind turbines such as providing energy transformation with fewest mechanical stresses and minimizing cost. Also the DFIG based turbines needs partial size rate rotor energy transformer to obtain the full control of the generator at variable wind speed. Typically, doubly fed induction generator based wind energy systems are built-up hundreds of miles far away from the load station and this causes several problems such as the weakness of electric power network, voltage regulation problems and network could distinctive by low short circuit proportion. Finite, reactive powercapability is another disadvantge of the doubly fed induction generator based wind energy systems when it is connected with a weak power network.

6.2 Suggestions for Future Work

This thesis has opened up many opportunities for applications of the wind turbine system using DFIG and Back to back work in the future and that is through the model of wind turbines can be developed in detail and added to the mathematical model of the proposed DVG in this work where more realistic wind speed profiles can be studied.

When using the MMC - based HVD.C is a promising technology in research and development studies in the field of electric power, such a system can be improved by developing dynamic controls that are able to provide a wide range of voltage conversion ratios.

the DFIG- based wind farm and back to back with more realistic power grid models, where other type of generators like synchronous generators are also present. Similar study can be done in those power grids .

REFERENCES

[1] L. Holdsworth, X. G. Wu, J. B. Ekanayake and N. Jenkins. (2003). Comparison of fixed speed and doubly-fed induction wind turbines during power system disturbances, *IEE Proc. Generation, Transmission and Distribution,* vol. 150. 3, p. 343–352,.

[2] T. M. Masaud, P. K. Sen. (2011). Modeling and Control of Doubly fed Induction Generator for Wind Power, in *North American Power Symposium (NAPS),*.

[3] G. Byeon, I. K. Park and G. Jang. (2010). Modeling and Control of a Doubly-Fed Induction Generator (DFIG) Wind Power Generation System for Real-time Simulations, *Journal of Electrical Engineering & Technology*, vol. 5. 61- 69.

[4] F. Wu, X.-P. Zhang, K. Godfrey and P. Ju. (2006). Modeling and Control of Wind Turbine with Doubly Fed Induction Generator, in *IEEE PES Power Systems Conference and Exposition (PSCE)*.

[5] M. Marinelli, A. Morini, A. Pitto and F. Silvestro. (2008). Modeling of double fed induction generator (DFIG) equipped wind turbine for dynamic studies, in 43rd International Universities Power Engineering Conference (UPEC), September 1-4.

[6] A. Junyent-Ferré, O. Gomis-Bellmunt, A. Sumper, M. Sala and M. Mata, "Modeling and control of the double fed induction generator wind turbine," *Simulation Modelling Practice and Theory,* vol. 18, pp. 1365-1381, 201

[7] A. P. Tennakoon, A. Arulampalam, J. B. Ekanayake and S. G. Abeyratne. (2006). "Modeling and Control of Doubly Fed Induction Generators (DFIGs) For Wind Energy Applications," in First International Conference on Industrial and Information Systems, ICIIS, Sri Lanka, 8 - 11 August.

[8] H. Li, Z. Chen and J. K. Pedersen. (2006). Optimal Power Control Strategy of Maximizing Wind Energy Tracking and Conversion for VSCF Doubly Fed Induction Generator System, in CES/IEEE 5th International Power Electronics and Motion Control Conference (IPEMC).

[9] P. B. Eriksen, T. Ackermann, H. Abildgaard, P. Smith, W. Winter and J. M. R. Garcia. (2005). System operation with high wind penetration, *IEEE Power & Energy Magazine,* vol. 3, pp. 65-74, Nov.

[10] S. Muller, M. Deicke, and R. W. D. Doncker. (2002). Doubly fed induction generator systems for wind turbine, *Industry Applications Magazine*, vol. 8, no. 3, p. 26–33.

[11] A. Petersson. (2010). Analysis, Modeling and Control of Doubly-Fed Induction Generators for Wind Turbines, in Energy and Environment, Goteborg: Chalmers University of Technology.
[12] M. Stiebler. (2008). Wind Energy Systems for Electric Power Generation, Springer, city.

[13] A. Ahlstrom. (2002). Simulating dynamical behavior of wind power structures, Technical Report, Royal Ins. of Tech., Sweden, August.

[14] S. Heier. (2006). Grid Integration of Wind Energy Conversion Systems, John Wiley & Sons.

[15] J. Walker, N. Jenkins. (1997). Wind energy technology, John Wiley & Sons, Chichester,
.
[16] I. Boldea. (2006). The electric generators handbook – variable speed generators, *Taylor &Francis*.

[17] F. Runcos, R. Carlson, A.M. Oliveira, et al. (2004). Performance analysis of a brushless double fed cage induction generator, *Nordic Wind Power Conf. (NWPC04) Chalmers University of Technology Göteborg, Sweden, Mar.*

[18] M.R. Dubois. (2004). Optimized permanent magnet generator topologies for direct-drive wind turbines, *PhD dissertation, Delft University Technology, Delft, Netherland.*

[19] A. Grauers. (1996). Design of direct-driven permanent-magnet generators for windturbines, *PhD dissertation, Chalmers University of Technology, Göteborg, Sweden.*

[20] D.A. Torrey. (2002). Switched reluctance generators and their control, *IEEE Tran. Indus.Electron., vol. 49, No. 1, pp. 3-14.*

[21] H. Li, Z. Chen. (2008). Overview of different wind generator systems and their comparisons, IET *Renew. Power Gener.vol. 2, No. 2, pp. 123-138.*

[22] M.R. Dubois, H. Polinder, J.A. Ferreira. (2000). Comparison of generator topologies for direct-drive wind turbines, Proc. Nordic Countries Power and Industrial Electronics Conf. (NORPIE), Aalborg, Denmar.

[23] S. Siegfriedsen, G. Bohmeke. (1998). Multibrid technology – a significant step to multimegawattwind turbines, Wind Energy, vol.

[24] H. Polinder, FFa. PIJL. Van Der, G.J. De Vilder, et al. (2006). Comparison of direct-drive and geared generator concepts for wind turbines, IEEE Tran. Energy Convers.

[25] L.H. Hansen, L. Helle, F. Blaabjerg, et al. (2001). Conceptual survey of generators and power electronics for wind turbines, *Riso National Laboratory Technical Report Riso-R-1205 (EN) Roskilde*, Denmark.

[26] H. Polinder, J. Morren. (2005). Developments in wind turbine generator systems ,*Electrimacs* , Hammamet, Tunisia.

[27] O. Carlson, A. Grauers, J. Svensson, et al. (1994). A comparison of electrical systems for variable speed operation of wind turbines, *Proc. European wind energy conf*.

[28] Francoise Mei. (2008). Small Signal Modeling and Analysis of Doubly Fed Induction Generator in Wind Power Applications, *Ph.D. dissertation*, Control and Power Group Department of Electrical and Electronic Engineering, Imperial College London University of London.

[29] Pao, Lucy Y, and Johnson, Kathryn E. (2011). Control of Wind Turbines, *IEEE Control SystemMagazine*, vol.

[30] Johnson, Kathryn E, Pao Lucy Y, Balas Mark J, Kulkami V, and Fingersh Lee J. (2004). "StabilityAnalysis of an Adaptive Torque Controller for Variable Speed Wind Turbines," 43rd IEEEConference on Decision and Control, Atlantis, Paradise Island, Bahamas, vol.

[31] P W Carlin, A. S. Laxson, and E.B. Muljadi. (2001). The History and State of the Art of Variable-Speed Wind Turbine Technology. *NREL Technical Report,* NREL/TP-500-28607, February.

[32] Quincy Wang, and Liuchen Chang. (2004). An Intelligent Maximum Power Extraction Algorithmfor Inverter-Based Variable Speed Wind Turbine Systems, *IEEE Transaction on Power Electronics*, vol.

[33] G. L. Johnsson. (1985). *Wind Energy Systems*. Englewood Cliffs, N.J., USA. Prentice-Hall.

[34] Magdi Ragheb, and Adam M. Ragheb. (2011). Fundamental and Advanced Topics in Wind Power.

[35] Andreas Petersson. (2005). Analysis, Modeling and Control of Doubly-Fed InductionGenerators for Wind Turbines , Chalmers University of Technology, Ph.D. dissertation, Sweden.

[36] Kostyantyn Protsenko and Dewei Xu. (2008). Modeling and Control of Brushless Doubly-Fed Induction Generators in Wind Energy Applications, IEEE Transactions on Power Electronics, Vol.

[37] Yongchang Zhang, Zhengxi Li, Jiefeng Hu, Wei Xu and Jianguo Zhu. (2011). A Cascaded Brushless Doubly Fed Induction Generator for Wind Energy Applications Based on Direct Power Control.

[38] I. Erlich and F. Shewarega. (2006). Modeling of Wind Turbines Equipped with Doubly-Fed Induction Machines for Power System Stability Studies, 2006 IEEE Power Systems Conference and Exposition, pp.

[39] Istvan Erlich, Jörg Kretschmann, Jens Fortmann, Stephan Mueller-Engelhardt and Holger Wrede. (2007).“Modeling of Wind Turbine Based on Doubly-Fed InductionGenerators for Power System Stability Studies”, IEEE Transactions on Power Systems.

[40] Alvaro Luna, Francisco Kleber de Araujo Lima, David Santos, Pedro Rodríguez, Edson H. Watanabe, and Santiago Arnaltes. (2011). Simplified Modeling of a DFIG for Transient Studies in Wind Power Applications, IEEE Transactions on Industrial Electronics.

[41] E. Muljadi, Fellow, M. Singh, Member, V. Gevorgian, Member. (2012). Doubly Fed Induction Generator in an Offshore Wind Power Plant Operated at Rated V/Hz

[42] Wenjin Li and Yong Kang, Guangfu Tang and Ming Kong. (2014). Start-up and Integration of DFIG-Based Wind Farm Using Modular Multilevel VSC-HVDC Transmission System IEEE Supported by the National Nature Science Fund of China.

[43] Yung-Tsai Weng , Yuan-Yih Hsu. (2016). Reactive power control strategy for a wind farm with DFIG ScienceDirect National Taiwan University, Department of Electrical Engineering, EE Building 2, No. 1, Sec. 4, Roosevelt Rd., Taipei, 10617, Taiwan, ROC .

[44] Divya Patel, Ritesh Diwan. (2016). Analysis and Modeling of Modular Multilevel Converter based Inverter for Grid Connected Wind Energy Conversion System International Journal of Innovative Research in Science, Engineering and Technology.

[45] Minyuan Guan, Zheng Xu, Member. (2010). Analysis of DC Voltage Ripples in ModularMultilevel Converters IEEE International Conference on Power System Tnology .

[46] Hagiwara, M., Akagi, H., (2009). Control and Experiment of Pulsewidth-Modulated Modular Multilevel Converters, Power Electronics, IEEE Transactions , 24, 7, pp.1737-1746.

[47] Ängquist, L., Antonopoulos, A., Siemaszko, D., Ilves, K., Vasiladiotis, M., Nee, H. P. (2010, June). Inner control of modular multilevel converters-an approach using open-loop estimation of stored energy. In Power Electronics Conference (IPEC), 2010 International (pp. 1579-1585). IEEE.

[48] Çiftçi, B. (2014). Selection Of Suitable Pwm Switching And Control Methods For Modular Multilevel Converter Drives, M.sc. Thesis, The Graduate School Of Natural And Applied Sciences, Middle East Technical University.

[49] Gayithri C1, R S Geetha2 (2014) ACTIVE POWER AND CURRENT CONTROL FOR A MODULAR MULTILEVEL CONVERTER (MMC) BASED SYSTEM IJRET: International Journal of Research in Engineering and Technology eISSN: 2319-1163 | pISSN: 2321-7308

[50] Haddioui, M. R. (2015). Control and Modulation Strategies for MMC - Based HVDC, Master's Thesis, Aalborg University.

[51] Eduard Muljadi, M. Singh, and V. Gevorgian. (2012). Doubly Fed Induction Generator in an Offshore Wind Power Plant Operated at Rated V/Hz, Energy Conversion Congress and Exposition (ECCE), Raleigh, NC, USA, pp. 779-786, 15-20 September.

[52] S. Muller, M. Deicke and RikW. De Doncker. (2002). Doubly fed induction generator systems for wind turbines, *IEEE, Industry Applications Magazine*.

[53] Paul C. Krause. (1986). Analysis of Electric Machinery, McGraw-Hill, Inc.City and State.

[54] M. Aktarujjaman, M.E. Haque, and K. M. Muttaqi. (2008). Control Dynamics of a Doubly Fed Induction Generator Under Sub- and Super-Synchronous Modes of Operation, IEEE PES General Meeting.

[55] M. Liserre, R. Cardenas, M. Molinas, and J. Rodriguez. (2011). Overview of multi-MW wind turbines and wind parks, IEEE Transactions on Industrial Electronics.

[56] S. Heier. (2014). "Grid integration of wind energy: Onshore and Offshore Conversion Systems.

[57] F. Blaabjerg, M.Liserre, and K. Ma. (2012). Power electronics converters for wind turbine systems, IEEE Transactions on Industry Applications, vol.

[58] R. Pena, J. C. Clare, and G. M. Asher. (1996). Doubly fed induction generator using back-to-back PWM converters and its application to variable-speed wind-energy generation, Proceedings Electric Power Applications.

[59] R. Cardenas, R. Pena, S. Alepuz, G. Asher. (2013). Overview of control systems for the operation of DFIGs in wind energy applications, IEEE Transactions on Industrial Electronics .

[60] M. Stiebler. (2008). Wind energy systems for electric power generation, Springer, Germany.

[61] I. Boldea. (2006). Variable Speed Generators (The Electric Generators Handbook), Taylorand Francis.

[62] P. Vas. (1990). Vector control of AC machines, Clarendon press Oxford.

[63] J. A. Santisteban and R. M. Stephan, Vector control methods for induction machines: An overview, IEEE Transactions Education., vol. 44, no. 2, pp. 170– 175, May 2001.

[64] L. Xu and P. Cartwright. (2006). Direct active and reactive power control of in DFIG for wind energy generation, IEEE Transactions on Energy Conversion.

[65] Wang Jialong; Hyun Seung Ho. (2011). ANN based pitch angle controller for variable speed variable pitch wind turbine generation system, In Strategic Technology (IFOST).

[66] I. Takahashi, and T. Noguchi. (1986). A new quick-response and high-efficiency control strategy of an induction motor, IEEE Transactions on Power Electronics.

[67] K. P. Gokhale. (1999). Controller for a wound rotor induction machine, U.S. Patent .

[68] M. Malinowski, M.P. Kazmierkowski, S. Hansen, F. Blaabjerg, G.D. Marques, Virtual-flux-based direct power control of three-phase PWM rectifiers, IEEE Transactions on Industry Applications, vol. 37, no. 4, pp.1019–1027, Jul/Aug 2001.

[69] A.L. Sergio, R. Angel, O. Estanis. (2007). Predictive control strategy for DC/AC converters based on direct power control, IEEE Transactions on Industrial Electronics.

[70] B. Hopfensperger, D. Atkinson, and R. A. Lakin. (1999). Stator-flux-oriented control of a doubly-fed induction machine with and without position encoder, IEE Proceedings Electric Power Applications.

[71] S. Pererada, A. Tilli, and A. Tonielli. (2003). Indirect stator flux-oriented output feedback control of a doubly fed induction machine, IEEE Transactions on Control System Technology.

[72] S. Wang, and Y. Ding. (1993). Stability analysis of field oriented doubly-fed induction machine drive based on computer simulation, Electric Machines and Power Systems.

[73] L. Congwei, W. Haiqing, S. Xudong, and L. Fahai. (2001). Research of stability of doubly fed induction motor vector control system, in Proceedings 5th International Conference on Electrical Machines and Systems, China.

[74] A. Pettersson, L. Harnefors, and T. Thiringer. (2004). Comparison between stator-flux and grid-flux-oriented rotor current control of doubly-fed induction generators, In Proceedings 35th Power Electronics Specialist Conference, vol. 1, Aachen, Germany.

[75] H. Akagi and H. Sato. (2002). Control and performance of a doubly-fed induction machine intended for a flywheel energy storage system, IEEE Transactions Power Electronics.

[76] Bimal K. Bose. (2002). Modern Power Electronics and AC Drives, Chapter 10, pp. 535-557, Prentice Hall PTR.

[77] Bose, B.K. (1994). Expert system, fuzzy logic, and neural network applications in power electronics and motion control, In Proceedings of the IEEE .

[78] Wang Jialong; Hyun Seung Ho. (2011). ANN based pitch angle controller for variable speed variable pitch wind turbine generation system, In Strategic Technology (IFOST).

[79] M. G. Simoes, B.K. Bose, Ronald J. Spiegel. (1997). Design and performance evaluation of a fuzzy logic-based variable-speed wind generation system, In IEEE Transactions on Industry Applications.

[80] S. Arnalte, J. C. Burgos, and J. L. Rodríguez-Amenedo. (2002). Direct torque control of a doubly-fed induction generator for variable speed wind turbines, Electric Power Components and Systems.

[81] I. Takahashi, and T. Noguchi. (1986). A new quick-response and high-efficiency control strategy of an induction motor, IEEE Transactions on Power Electronics.

[82] M. Depenbrock. (1988). Direct self-control (DSC) of inverter-fed induction motors, IEEE Transactions on Power Electronics.

[83] K. P. Gokhale. (1999). Controller for a wound rotor induction machine, U.S. Patent .

[84] M. Malinowski, M.P. Kazmierkowski, S. Hansen, F. Blaabjerg, G.D. Marques. (2001). Virtual-flux-based direct power control of three-phase PWM rectifiers, IEEE Transactions on Industry Applications.

[85] R. Datta, and V.T. Ranganathan. (2001). Direct power control of grid-connected wound rotor induction machine without rotor position sensors, IEEE Transactions on Power Electronics.

[86] L. Xu and P. Cartwright. (2006). Direct active and reactive power control of in DFIG for wind energy generation, IEEE Transactions on Energy Conversion.

[87] W. S. Kim, Su. Jou; K. Lee, and S. Watkins. (2008). Direct power control of a doubly fed induction generator with a fixed switching frequency, IEEE Industry Applications Society Annual Meeting.

[88] D. Zhi, L. Xu, and B.W. Williams. (2009). Improved direct power control of grid-connected dc/ac converters, IEEE Transactions on Power Electronics .

[89] P. Mutschler and R. Hoffmann. (2002). Comparison of wind turbines regarding their energy generation, In 33rd Annual IEEE Power Electronics Specialists Conference.

[90] M. Malinowski, M. Jasinski, and M.P. Kazmierkowski. (2004). Simple direct power control of three-Phase PWM rectifier using space-vector modulation (DPC-SVM), IEEE Transactions on Industrial Electronics.

[91] D. Casadei, G. Serra, A. Tani. (1998). Improvement of direct torque control performance by using a discrete SVM technique, Power Electronics Specialists Conference (PESC) 98 Record Annual IEEE 29th.

[92] M.V. Kazemi, A.S. Yazdankhah, H.M. Kojabadi. (2010). Direct power control of DFIG based on discrete space vector modulation, Journal of Renewable Energy.

[93] A.L. Sergio, R. Angel, O. Estanis.(2007). Predictive control strategy for DC/AC converters based on direct power control, IEEE Transactions on Industrial Electronics,.

[94] G. Abad, M. A. Rodrıguez, and J. Poza. (2007). Predictive direct power control of the doubly fed induction machine with reduced power ripple at low constant switching frequency, .

[95] M.V. Kazemi, M. Moradi, R.V. Kazemi.(2012). Minimization of powers ripple of direct power controlled DFIG by fuzzy controller and improved discrete space vector modulation, Electical Power System, .

[96] M. Pichan, H. Rastegar, M. Monfared.(2013). Two fuzzy-based direct power controlstrategies for doubly-fed induction generators in wind energy conversion systems,International Journal of Energy.

[97] L. Shang and J. Hu. (2012). Sliding-mode-based direct power control of grid-connected wind-turbine-driven doubly fed induction generators under unbalanced grid voltage conditions, IEEE Transactions on Energy Conversion, .

[98] A. Nabae, I. Takahashi, and H. Akagi. (1981). A New Neutral-Point-Clamped PWM Inverter, Industry Applications, IEEE Transactions on.

[99] Asplund, G., Eriksson, K., Jiang, H., Lindberg, J., Pålsson, R., Svensson, K., Dc Transmission Based on Voltage Source Converters, ABB Power Systems AB, Sweden.

[100] Bonilla, C. C., Tigga, S. M. (2011). Design and performance comparison of Two-level and Multilevel Converters for HVDC Applications, Master's Thesis in Electric Power Engineering, Department of Energy and Environment, Division of Electric Power Engineering, Chalmers University of Technology, Sweden.

[101] ABB, The Eagle Pass 36 MW back-to-back HVDC Light installation is a voltage source converter (VSC) supported tie interconnecting transmission grids in TexasandMexico,ABBCompany,link:http://new.abb.com/systems/hvdc/references/eagle-pass.

[102] T. A. Meynard, and H. Foch. (1990). Multi-level conversion: high voltage choppers and voltage-source inverters, Power Electronics Specialists Conference.

[103] Iversen, T. M., Gjerde, S. S., Undeland, T. (2013, September). Multilevel converters for a 10 MW, 100 kV transformer-less offshore wind generator system. In Power Electronics and Applications (EPE), 2013 15th European Conference on (pp. 1-10). IEEE.

[104] Meier, S. (2009). System Aspects and Modulation Strategies of an HVDC-based Converter System for Wind Farms, Phd. Thesis, Royal Institute of Technology, School of Electrical Engineering, Stephan Meier, Sweden, ISSN: 1653–5146.

[105] A. Lesnicar, and R. Marquardt, An innovative modular multilevel converter topology suitable for a wide power range, Power Tech Conf. Proc., 2003 IEEE

[106] Timofejevs, A., Gamboa, D. (2013). Control of MMC in HVDC Applications, Master's Thesis, Department of Energy Technology, Aalborg University, Denmark.

[107] Shukla, A., Nami, A. (2015). Multilevel Converter Topologiesfor STATCOMs, Springer Science + Business Media Singapore, DOI 10.1007/ 978-981-287-281-4_2.

[108] Nicholls, J. C. (2009). Soft-switching performance analysis of the clustered insulated gate bipolar transistor (CIGBT), PHD thesis, Emerging Technologies Research Centre, De Montfort University.

[109] Ilves, K., Taffner, F., Norrga, S., Antonopoulos, A. (2013 September). A Submodule Implementation for Parallel Connection of Capacitors in Modular Multilevel Converters, Conference Paper in IEEE Transactions on Power Electronics, DOI: 10.1109/EPE.2013.6634325.

[110] Georgios, S. K., Mihai, C., Vassilios, G. A. (2011). Analysis of Multi-carrier PWM Methods for Back-to-back HVDC Systems based on Modular Multilevel Converters, IEEE,1-61284-972-978/11/$26.00.

[112] Abun, A. (2016). Modelling of Modular Multilevel Converter Using Input Admittance Approach, Master's Thesis in Electric Power Engineering, Chalmers University of Technology, Sweden.

[113] Rudervall, R., Charpentier, J.P., Sharma, R. (2000). High Voltage Direct Current (HVDC)Transmission Systems Technology Review Paper, Energy Week 2000, Washington, D.C, USA.

[114] Deng, Y., Teo, K. H., Duan, C. T., Habetler, G., Harley, G. R. (2013). A Fast and Generalized Space Vector, Modulation Scheme for Multilevel Inverters, IEEE Transactions on Power Electronics.

[115] Çiftçi, B. (2014). Selection Of Suitable Pwm Switching And Control Methods For Modular Multilevel Converter Drives, M.sc. Thesis, The Graduate School Of Natural And Applied Sciences, Middle East Technical University

[116] Yu Zou (August, 2012) Modeling, Control And Maximum Power Point Tracking (Mppt) Of Doubly-Fed Induction Generator (Dfig) Wind Power System, Phd Thesis, University of Akron.

[117] Tarek Masaud (2013) Modeling, Analysis, Control And Design Application Guide lines Of Doubly Fed Induction Generator (Dfig) For Wind Power Applications.

[118] Sam Mahmodicherati (2016) Direct Power Control Of A Doubly Fed Induction Generator In Wind Power Systems Phd Thesis, University of Akron.